



UNIVERSIDAD NACIONAL AUTÓNOMA DE MÉXICO
DOCTORADO EN CIENCIAS DE LA PRODUCCIÓN Y DE LA SALUD ANIMAL
FACULTAD DE MEDICINA VETERINARIA Y ZOOTECNIA

**AISLAMIENTO E IDENTIFICACIÓN DE *OVINE GAMMAHERPESVIRUS* TIPO 2 EN
ARTIODÁCTILOS Y EQUINOS, A PARTIR DE UN BROTE DE FIEBRE CATARRAL
MALIGNA EN MÉXICO.**

T E S I S

**QUE PARA OPTAR POR EL GRADO DE:
DOCTOR EN CIENCIAS DE LA PRODUCCIÓN Y DE LA SALUD ANIMAL**

PRESENTA:

TANIA LUCIA MADRIGAL VALENCIA

**TUTOR PRINCIPAL:
DR. HUMBERTO RAMÍREZ MENDOZA
FACULTAD DE MEDICINA VETERINARIA Y ZOOTECNIA**

**MIEMBROS DEL COMITÉ TUTORAL:
DR. JESÚS HERNÁNDEZ LÓPEZ
DOCTORADO EN CIENCIAS DE LA PRODUCCIÓN Y DE LA SALUD ANIMAL
DR. JOAQUIM SEGALÉS COMA
DOCTORADO EN CIENCIAS DE LA PRODUCCIÓN Y DE LA SALUD ANIMAL
DR. ARMANDO PÉREZ TORRES
FACULTAD DE MEDICINA, UNAM**



Universidad Nacional
Autónoma de México

Dirección General de Bibliotecas de la UNAM

Biblioteca Central



UNAM – Dirección General de Bibliotecas
Tesis Digitales
Restricciones de uso

DERECHOS RESERVADOS ©
PROHIBIDA SU REPRODUCCIÓN TOTAL O PARCIAL

Todo el material contenido en esta tesis esta protegido por la Ley Federal del Derecho de Autor (LFDA) de los Estados Unidos Mexicanos (México).

El uso de imágenes, fragmentos de videos, y demás material que sea objeto de protección de los derechos de autor, será exclusivamente para fines educativos e informativos y deberá citar la fuente donde la obtuvo mencionando el autor o autores. Cualquier uso distinto como el lucro, reproducción, edición o modificación, será perseguido y sancionado por el respectivo titular de los Derechos de Autor.

Dedicatorias

A Dios, por su apoyo, guía y fortaleza espiritual que me da en cada momento de mi vida.

A mi madre, hermano y a mi querida tía, por su sacrificio y apoyo incondicional.

A mi novio, por su apoyo y por estar conmigo en esta etapa tan difícil. Eres el amor de mi vida.

A la memoria de mi abuelita, por ser mi motivo de superación y el bastón que guío mi vida por el camino correcto.

Agradecimientos

A mi tutor Dr. Humberto Ramírez Mendoza, por creer en mí y apoyarme en mi formación como una investigadora de excelencia. Gracias de todo corazón.

A mi comité tutorial: Dr. Jesús Hernández, por su apoyo y paciencia en la realización de este trabajo. Dr. Joaquim Segalés, por sus comentarios asertivos que me hicieron crecer profesionalmente, su ayuda fue muy valiosa. Dr. Armando Pérez, infinitas gracias por su experiencia, apoyo incondicional, y por su valiosa amistad.

A los miembros del jurado: Dra. Susana Elisa Mendoza Elvira, Dr. José Iván Sánchez Betancourt y Dr. Rene Álvaro Segura Velázquez, por sus valiosas aportaciones en la revisión de la tesis.

A la Dra. en C. Marcela Villarreal Silva, subdirectora de diagnóstico especializado de alta responsabilidad de CPA y a su grupo de trabajo, por su apoyo brindado durante mi estancia en sus instalaciones. Gracias por su capacitación y comentarios que me hicieron crecer como investigadora.

A mi asesor y amigo: Dr. Manuel Saavedra, gracias por todo el apoyo técnico y tu gran disponibilidad para ayudarme en todo momento.

A la histotecnóloga: Verónica Rodríguez Mata, por su capacitación y apoyo técnico en la estandarización de la técnica de inmunohistoquímica, gracias por la paciencia y consejos que me brindo fueron cruciales para mi formación.

A la M. en C. Elba Carrasco Ramírez, de la Unidad de Microscopia de la Facultad de Medicina por el apoyo en la microscopía electrónica.

Agradecimientos Institucionales

Al Consejo Nacional de Ciencia y Tecnología (CONACYT) por la beca que me fue otorgada para la realización de mis estudios, ID 968751.

El presente trabajo fue financiado por los siguientes proyectos: PAPIIT IN213321, PAPIIT IT201918 y PAPIIT IT201821.

A la Comisión México-Estados Unidos para la Prevención de la Fiebre Aftosa y otras Enfermedades Exóticas de los Animales (CPA), por su financiamiento en la estandarización de una prueba de PCR para el diagnóstico del OvHV-2.

Al laboratorio de filogenia del sistema inmune de piel y mucosas de la facultad de medicina, por el procesamiento de muestras para la técnica histológica y por la capacitación brindada durante la estandarización de la técnica de inmunohistoquímica.

A la Unidad de Microscopia de la Facultad de Medicina, por el apoyo técnico brindado para el procesamiento de muestras para microscopia electrónica

Al Departamento de Microbiología e Inmunología de la Facultad de Medicina Veterinaria y Zootecnia de la Universidad Nacional Autónoma de México por las facilidades brindadas durante la realización de esta tesis.

Datos Bibliográficos

Artículos científicos generados durante el desarrollo de los estudios de doctorado.

- Albarrán-Rodríguez RR, Castillo-Juárez H, Rivera-Benítez F, Campos-Montes GR, Espinosa B, **Madrigal-Valencia TL**, Jiménez ENS, Ramírez-Mendoza H (2022). Assessment of the hemagglutinating activity of the Porcine orthorubulavirus. **Comparative Immunology, Microbiology, and Infectious Diseases.**
- Hidalgo-Lara DR, De la Luz-Armendáriz J, Rivera-Benítez JF, Gómez-Núñez L, Salazar-Jiménez EN, **Madrigal-Valencia TL**, Ramírez-Mendoza H (2021). Comparison of hemagglutination inhibition tests, immunoperoxidase monolayer assays, and serum neutralizing tests in detecting antibodies against blue eye disease in pigs. **Journal of Immunological Methods.**

Artículo enviado

- **Madrigal-Valencia TL**, Saavedra-Montañez M, Pérez-Torres A, Hernández J, Segalés J, Domínguez Hernández Y, Cancanosa-Aranda IE, Pérez-Guiot A, Ramírez-Mendoza H (2023). Identification and characterization of Ovine gammaherpesvirus type 2 in Artiodactyla and its isolation in horses from an outbreak of malignant catarrhal fever in Mexico. Enviado a Plos One.

Ponencias en congresos y seminarios

- 2023. Ponente en los seminarios mensuales del Departamento de Medicina y Zootecnia de cerdos, con el tema “Aislamiento e identificación del Ovine gammaherpesvirus tipo 2, a partir de un brote de fiebre catarral maligna en Mexico”. Impartido el día 11 de abril.

- 2022. **Ponente en los seminarios de Microbiología e Inmunología de la FMVZ UNAM**, con el tema “Aislamiento e identificación del Ovine gammaherpesvirus tipo 2, a partir de un brote de fiebre catarral maligna en Mexico”. Impartido el día 6 de octubre.
- 2022. **Ponente en el primer congreso internacional de la AMMVECA**, con el tema “Aislamiento e identificación del Ovine gammaherpesvirus tipo 2, a partir de un brote de fiebre catarral maligna en Mexico”. Impartido el día 9 de septiembre.
- 2020. **Ponente en los seminarios de Microbiología e Inmunología de la FMVZ UNAM**, con el tema “Aislamiento e identificación del Ovine gammaherpesvirus tipo 2, a partir de un brote de fiebre catarral maligna en Mexico”. Impartido el día 9 de septiembre.

Resumen

El gammaherpesvirus ovino 2 (OvHV-2), miembro del género *Macavirus*, es el causante de la Fiebre Catarral Maligna asociada a las ovejas (SA-MCF, por sus siglas en inglés), una enfermedad linfoproliferativa mortal que afecta a una amplia variedad de ungulados, incluidos los caballos (orden *Perissodactyla*). En este estudio se describió un brote de SA-MCF que ocurrió en el Centro de Enseñanza, Investigación y Extensión en Producción Animal en Altiplano (CEIEPAA) en Tequisquiapan (Querétaro). La identificación del agente viral se realizó mediante el aislamiento, inmunofluorescencia (IF), inmunocitoquímica (ICC), inmunohistoquímica (IHQ), reacción en cadena de la polimerasa (PCR) punto final y secuenciación parcial del gen ORF75, también se realizó una inoculación experimental en conejos. Los animales involucrados en este brote (caballos, ganado de engorda, ganado lechero, cabras, ovejas y ciervos), mostraron signos clínicos y lesiones compatibles con la presentación de cabeza y ocular de la SA-MCF. Se tomaron muestras de leucocitos de los animales afectados durante el brote de SA-MCF y se intentó el aislamiento en cultivos primarios de testículo de conejo. Pequeños grupos de células citomegálicas refráctiles caracterizaron el efecto citopático entre las 48 y 72 horas post-infección. Además, se identificaron cuerpos de inclusión intranucleares e inmunorreactividad intracitoplasmática en las células infectadas. Las secuencias parciales del gen *ORF75* obtenidas a partir de seis aislamientos, se alinearon con otras secuencias del OvHV-2 reportadas en el GenBank y revelaron una identidad de nucleótidos superior al 98%. Los tres conejos que se inocularon desarrollaron lesiones histológicas compatibles con SA-MCF, incluyendo infiltrado linfoide perivascular multisistémico, acumulación linfoide perivascular e hiperplasia linfoide en bazo. Además, se identificaron morfológicamente las partículas herpesvirales en células epiteliales bronquiolares y del intersticio pulmonar, mediante microscopía electrónica de transmisión (MET). Los resultados indican que el brote que se presentó en el CEIEPAA fue causado por el virus OvHV-2, siendo los cultivos primarios de testículo de conejo susceptibles y permisibles para su replicación. Por otra parte, los caballos fueron susceptibles a la infección por OvHV-2 y pueden desarrollar la enfermedad clínica. Por último, los conejos son un modelo útil para el estudio de la infección por este virus.

Palabras clave: Caballos, fiebre catarral maligna, OvHV-2, conejos, cultivos primarios

Abstract

Ovine gammaherpesvirus 2 (OvHV-2), a member of the genus *Macavirus*, causes Sheep-Associated Catarrhal Fever (SA-MCF), a fatal lymphoproliferative disease that affecting a wide variety of ungulate animals including horses (order perissodactyls). This study described an outbreak of SA-MCF in the Centro de Enseñanza, Investigación y Extensión en Producción Animal en Altiplano (CIEEPAA) ranch in Tequisquiapan, Querétaro. The identification of the viral agent was carried out through isolation, immunofluorescence (IF), immunocytochemistry (ICC), immunohistochemistry (IHC), polymerase chain reaction (PCR) endpoint and partial sequencing of the ORF75 gene, an experimental inoculation was also performed. in rabbits. The animals involved in this outbreak showed mucogingival ulcers in the vestibule of the mouth and tongue, hypersalivation, corneal opacity, reduced food consumption, and weight loss of variable severity. These clinical signs and the histopathological findings suggested the diagnosis of SA-MCF. Buffy coat fractions from anticoagulated blood samples of ill animals were collected and analyzed by PCR. Positive buffy coats were used to inoculate the primary cell cultures of rabbit testes to isolate the virus. Small clusters of refractile cytomegalic cells, characteristic of viral cytopathic effects, were observed between 48 and 72 h post-inoculation. Furthermore, cytoplasmic acidophilic inclusion bodies were identified in the infected primary culture cells. These structures and the cytoplasm showed immunoreactivity with hyperimmune rabbit serum against OvHV-2. Moreover, in the liver histological sections from sick deer, immunoreactive juxtannuclear inclusion bodies were identified in the same rabbit hyperimmune serum. The obtained sequences were aligned with the OvHV-2 sequences reported in GenBank and revealed a nucleotide identity higher than 98%. Based on the evidence provided in this study, we conclude that the outbreak of SA-MCF in the municipality of Tequisquiapan in the state of Queretaro, Mexico, was caused by OvHV-2. To the best of our knowledge, this is the second study reporting that horses are susceptible to OvHV-2 infection and can develop SA-MCF. Finally, rabbits represent a useful model for the study of infection by this virus.

Keywords: Horses, malignant catarrhal fever, OvHV-2, rabbits, primary cultures.

Declaración

El autor de esta tesis otorga el consentimiento al Posgrado en Ciencias de la Producción y de la Salud Animal, de la Universidad Nacional Autónoma de México, para que esta tesis se encuentre disponible para cualquier tipo de intercambio bibliotecario.

Tania Lucia Madrigal Valencia

Lista de cuadros y figuras

	Página
Figura 1 Estructura del virus herpes.....	2
Figura 2 Organización del genoma de AIHV-1 y OvHV-2.....	3
Cuadro 1 Susceptibilidad de ovejas, vacas, cerdos, conejos y bisontes a la infección por OvHV-2.....	4
Figura 3 Ilustración de la transmisión del OvHV-2 en el reservorio (oveja) y en el hospedador clínicamente susceptible (bisonte).....	7
Figura 4 Presentación clínica de cabeza y ocular.....	8
Figura 5 1-Pulmón; áreas multifocales de consolidación (flecha).....	10
Figura 6 Distribución de animales en el CEIEPAA, UNAM.....	19
Figura 7 Lesiones ulcerativas en la mucosa oral de animales afectados con SA-FCM.....	35
Figura 8 Lesiones post mortem observadas en ciervos afectados durante el brote SA-MCF en Querétaro, México.....	35
Cuadro 2 Especies afectadas, diagnósticos previos y porcentaje de animales positivos para OvHV-2.....	36
Figura 9 ECP en cultivos primarios de testículo de conejo inoculados con el lisado de capa leucocítica de las diferentes especies animales afectadas durante el brote de SA-MCF a las 72 horas post-infección.	37
Cuadro 3 Efecto citopático en cultivos primarios de testículo de conejo.....	38
Figura 10 Titulación viral de los sobrenadantes de los pases 3 a 14 de los caballos.....	39
Figura 11 CI acidófilos intranucleares a las 24 h después de la infección.....	40
Figura 12 Gel de agarosa (1,5 %) corrido en tampón TAE 1X.....	41
Figura 13 Cinética de replicación de los sobrenadantes libres de células de los pases 4, 5 y 14 del lisado de capa leucocítica de los caballos.....	43
Figura 14 Análisis filogenético de las secuencias parciales del gen <i>ORF75</i>	44
Cuadro 4 Diversidad genética de secuencias <i>ORF75</i> mexicanas en comparación con el gen de referencia BJ1035.....	45

Figura 15	Inmunorreactividad citoplasmática con las técnicas de ICC e IF en cultivos celulares primarios de testículo de conejo.....	46
Figura 16	Inmunohistoquímica de hígado de ciervo.....	47
Figura 17	Características tintoriales y morfológicas de los cuerpos de inclusión citoplasmáticos (CI) yuxt nucleares en hepatocitos de un ciervo que murió por SA-MCF secundaria a infección natural por OvHV-2.....	48
Figura 18	Lesiones microscópicas de los conejos desafiados con el aislamiento de los caballos.....	50
Figura 19	Micrografías electrónicas de pulmón de conejo inoculado por vía intranasal con el aislamiento viral del OvHV-2 a partir de leucocitos de caballo.....	51
Figura 20	Micrografías electrónicas de pulmón de conejo inoculado por vía intranasal con el aislamiento viral del OvHV-2 a partir de leucocitos de caballo.....	52
Figura 21	Micrografías electrónicas de pulmón de conejo inoculado por vía intranasal con el aislamiento viral del OvHV-2 a partir de leucocitos de caballo.....	52
Figura 22	Micrografías electrónicas de pulmón de conejo inoculado por vía intranasal con el aislamiento viral del OvHV-2 a partir de leucocitos de caballo.....	53
Figura 23	Reaislamiento del virus OvHV-2, en cultivos primarios de testículo de conejo.....	54
Figura 24	Prueba de PCR punto final anidada en órganos de conejos inoculados experimentalmente con OvHV-2.....	55

Abreviaturas o siglas utilizadas

FCM	Fiebre catarral maligna
AIHV-1	<i>Alcelaphine Gammaherpesvirus</i> tipo 1
AIHV-2	<i>Alcelaphine Gammaherpesvirus</i> tipo 2
CpHV-2	<i>Caprine Gammaherpesvirus</i> tipo 2
OvHV-2	<i>Ovine Gammaherpesvirus</i> tipo 2
ICTV	Comité internacional en taxonomía de virus
ADN	Ácido desoxirribonucleico
mAb	Anticuerpo monoclonal
ORF	Marco de lectura abierto
SA-MCF	Fiebre catarral maligna asociada a ovinos
DPI	Dosis post-infección
HE	Hematoxilina-eosina
BTh	Células tiroideas de bovino
BK	Células de riñón bovino
BEK	Células de riñón embrionario bovino
CT	Células de testículo de ternera
MDBK	Células de riñón de bovino
ECP	Efecto citopático
CI	Cuerpos de inclusión
ELISA	Ensayo inmunoabsorbente ligado a enzimas
ELISA c	Ensayo inmunoabsorbente ligado a enzimas competitivo
IF	Inmunofluorescencia
ICC	Inmunocitoquímica
PCR	Reacción en cadena de la polimerasa
BALT	Tejido linfoide asociado a bronquios
MET	Microscopía electrónica de transmisión
KV	Kilovolts
PR	Paramixovirus

CE	Ectima contagioso
BVD	Diarrea viral bovina
LA	Lengua azul
IBR	Rinotraqueitis infecciosa bovina
FA	Fiebre aftosa
VS	Estomatitis vesicular
CEIEPAA	Centro de Enseñanza, Investigación y Extensión en Producción Animal en Altiplano
GenBank	Banco de genes
RT-PCR	Transcripción reversa-PCR
FGARAT	Enzima fosforibosilformilglicinamidina sintasa
CPA	Comisión México-Estados Unidos para la Prevención de la Fiebre Aftosa y otras Enfermedades Exóticas de los Animales
DMEM	Medio Eagle modificado por Dulbeccos
PBS	Solución salina fosfatada
IHQ	Inmunohistoquímica
FITC	Isotiocianato de fluoresceína
BSA	Albumina sérica bovina
PAS	Tinción de ácido periódico de Schiff
BLAST	Herramienta básica de búsqueda de alineación local
TCID	Dosis infectante en cultivo celular 50%
CNA	Control negativo de amplificación
CNCP	Cultivos primarios no infectados
CNE	Control negativo de extracción

CONTENIDO

Dedicatorias	II
Agradecimientos	III
Agradecimientos Institucionales	V
Datos Bibliográficos	VI
Resumen	VIII
Abstract	IX
Declaración	X
Lista de cuadros y figuras	XI
Abreviaturas o siglas utilizadas	XIII
1. INTRODUCCIÓN	1
1.1 Agente causal	1
1.2 Estructura viral	1
1.4 Hospedadores y reservorio del OvHV-2	3
1.4 Transmisión del virus OvHV-2	4
1.5 Replicación del virus OvHV-2	5
1.6 Presentación clínica del OvHV-2	8
1.7 Lesiones histopatológicas del OvHV-2	9
1.8 Distribución geográfica del virus OvHV-2	10
1.9 Impacto económico de la FCM	11
1.10 Diagnóstico de SA-FCM	12
1.11 Aislamiento de los virus causantes de la FCM	12
1.12 Diagnóstico diferencial	14
2. JUSTIFICACIÓN	15
3. HIPÓTESIS	16
4. OBJETIVO GENERAL	17
4.1 Objetivos específicos	17
5. MATERIAL Y MÉTODOS	18
5.1 Lugar de muestreo	18
5.2 Cronología del brote	19
5.3 Pruebas complementarias	19

5.4 Evaluación <i>post-mortem</i>	20
5.5 Recolección y preparación de muestras clínicas	20
5.6 Reacción en cadena de la polimerasa (PCR) punto final anidada para la detección del virus OvHV-2.....	20
5.7 Cultivo primario de testículo de conejo	22
5.8 Aislamiento viral del OvHV-2.....	22
5.9 Cinética de replicación viral.....	24
5.10 Secuenciación parcial del gen <i>ORF75</i>	24
5.11 Análisis Filogenético	25
5.12 Elaboración de un suero hiperinmune anti-OvHV-2	25
5.13 Inmunocitoquímica (ICC) e inmunofluorescencia (IF) indirecta.....	26
5.14 Inmunohistoquímica	27
5.15 Tinción de hígado con Ácido Peryódico de Schiff (PAS).....	28
5.16 Tinción de hígado con Feulgen	29
5.17 Animales para desafío.....	29
5.18 Inoculación experimental de conejos con el virus OvHV-2.....	30
5.19 Microscopia Electrónica de Transmisión (MET)	30
5.20 Reaislamiento del OvHV-2	31
6. RESULTADOS.....	33
6.1 Cronología del brote	33
6.2 Evaluación <i>post-mortem</i>	34
6.3 Muestras de leucocitos.....	36
6.4 Aislamiento del virus OvHV-2 en cultivos primarios de testículo de conejo.....	37
6.5 PCR punto final anidada para la detección de OvHV-2	40
6.6 Cinética de replicación viral.....	42
6.7 Análisis Filogenético	43
6.8 Inmunocitoquímica (ICC) e inmunofluorescencia (IF) indirecta	45
6.9 Inmunohistoquímica enzimática de hígado	47
6.10 Identificación del contenido de los CI en hígado	47
6.11 Signos clínicos en conejos inoculados con el virus OvHV-2	48
6.12 Lesiones macroscópicas e histológicas en conejos.....	49
6.13 Microscopia electrónica de transmisión (MET).....	51
6.14 Reaislamiento del virus OvHV-2.....	53

6.15 Detección del OvHV-2 mediante PCR punto final anidada en reaislamientos	54
7. DISCUSIÓN	56
8. CONCLUSIONES	60
9. REFERENCIAS	61
10. Artículos científicos generados durante el desarrollo de los estudios de doctorado	73

1. INTRODUCCIÓN

La fiebre catarral maligna (FCM), es una enfermedad linfoproliferativa grave, frecuentemente mortal, de muchas especies unguladas del orden *Artiodactyla* (1).

1.1 Agente causal

La FCM es causada por varios Gammaherpesvirus pertenecientes al género *Macavirus* (subfamilia *Gammaherpesvirinae*; familia *Herpesviridae*; orden *herpesvirales*) (2). Dentro del género *Macavirus* se han identificado nueve especies virales: *Alcelaphine Gammaherpesvirus* tipo 1 (AIHV-1), *Ovine Gammaherpesvirus* tipo 2 (OvHV-2), *Alcelaphine Gammaherpesvirus* tipo 2 (AIHV-2), *Caprine Gammaherpesvirus* tipo 2 (CpHV-2), *Hippotragine Gammaherpesvirus* tipo 1, *Bovine Gammaherpesvirus* tipo 6 y *Suid Gammaherpesvirus* de los tipos 3, 4 y 5, de acuerdo con la última nomenclatura oficial publicada por el “International Committee on Taxonomy of Viruses” (“ICTV” 2023) (3). Los dos virus más estudiados son OvHV-2 y AIHV-1, que se mantienen de forma asintomática en las poblaciones de reservorio de ovejas y ñus, respectivamente (1).

1.2 Estructura viral

Todos los herpesvirus comparten una estructura que consiste en un núcleo de ADN, rodeado por una cápside icosaédrica. La cápside está incrustada en una matriz proteica llamada tegumento, además de contener una envoltura lipídica (Figura 1) (4).

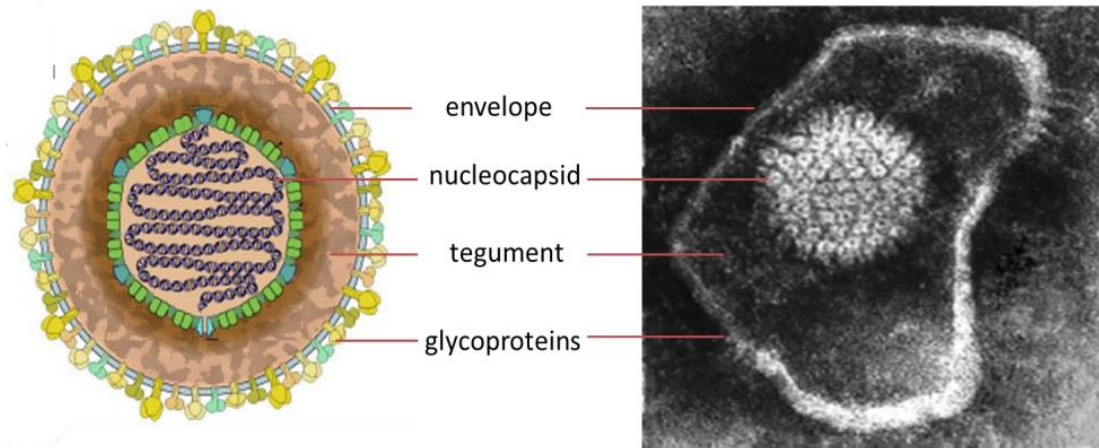


Figura 1. Estructura del virus herpes. Ayesha Riaz *et al.* Herpesvirus. Revisión de Letras Científicas. 2017.

AIHV-1 y OvHV-2, son los únicos virus cuyo genoma completo ha sido caracterizado (5,6). Se han identificado setenta marcos de lectura abiertos (ORF, *Open Reading Frame*) en AIHV-1; mientras que en OvHV-2 se han identificado setenta y tres marcos ORFs, de los cuales sesenta y uno son similares a otros *Gammaherpesvirus*, ocho son homólogos en AIHV-1 y cuatro genes únicos adicionales designados como Ov2.5, Ov3.5, Ov4.5 y Ov8.5 (Figura 2) (6). El genoma completo del *Ovine Gammaherpesvirus* tipo 2 consta de 130 930 pb (7).

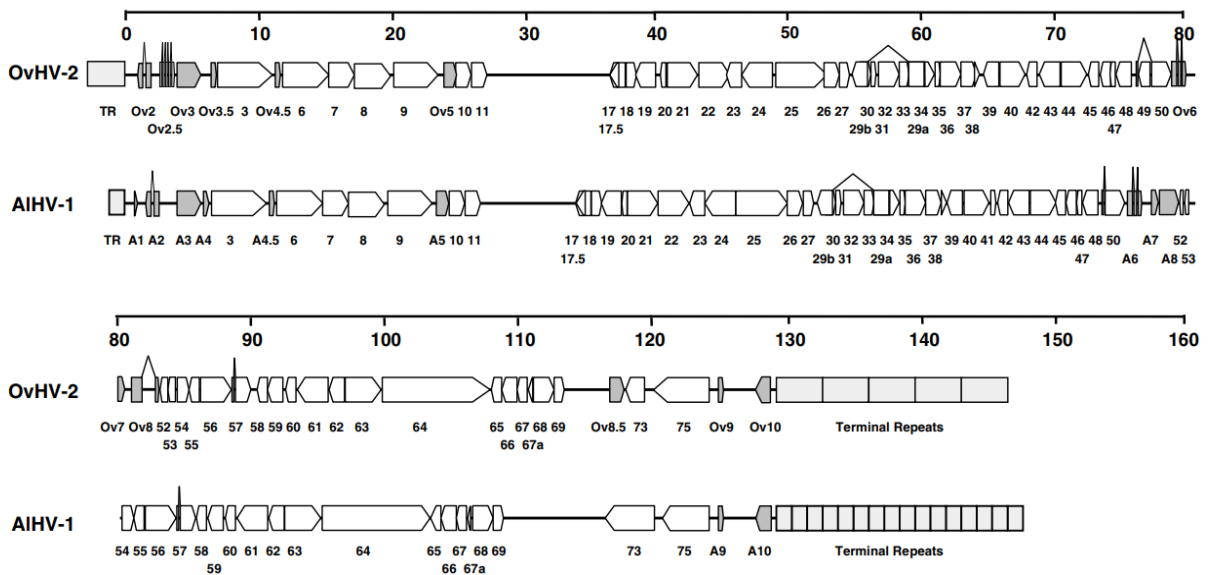


Figura 2. Organización del genoma de AIHV-1 y OvHV-2. George C. Russell *et al.* Fiebre Catarral Maligna: Revisión. Revista Veterinaria. 2009.

1.3 Hospedadores y reservorio del OvHV-2

Las ovejas son el reservorio de la FCM asociada a ovejas (SA-MCF, Sheep associated malignant catarrhal fever, por sus siglas en inglés). Se infectan con dosis de OvHV-2 bajas (10^4 copias de ADN), pero pueden desarrollar la enfermedad sólo cuando se exponen experimentalmente a una dosis extremadamente alta de virus (10^9 copias de ADN) lo que es poco probable que ocurra de forma natural (Cuadro 1) (8).

Cuando OvHV-2 se transmite a especies susceptibles puede desarrollarse la SA-MCF (9). Entre los hospedadores más susceptibles se encuentran los bovinos Bali, los bisontes americanos, los búfalos de agua y ciertas especies de ciervos, como el ciervo de Pere David (10,11). Los bisontes americanos son aproximadamente 100 veces más susceptibles a la infección y 10,000 veces más susceptibles a desarrollar la enfermedad en comparación con los bovinos (12,13). OvHV-2, también puede afectar a cerdos, jirafas y, recientemente, fue reportado en caballos (orden *Perissodactyla*) pertenecientes a una granja en Brasil en la cual estos animales compartían su alimentación con las cabras (14). Por otro lado, se ha demostrado experimentalmente que los conejos y hámsteres pueden infectarse con AIHV-1 o con OvHV-2 y desarrollar signos clínicos y lesiones de SA-MCF similar a los bisontes (15–19).

Cuadro 1. Susceptibilidad de ovejas, vacas, cerdos, conejos y bisontes a la infección por OvHV-2. Hong Li *et al.* Avance lento hacia la comprensión de la Fiebre Catarral Maligna. Revisión anual de biociencias animales. 2014.

Species	OvHV-2 inoculum (DNA copies) ^b							
	10 ²	10 ³	10 ⁴	10 ⁵	10 ⁶	10 ⁷	10 ⁸	>10 ⁹
Sheep	Neg	Pos	Pos	Pos	Pos	Pos	Pos	MCF
Cattle				Neg	Pos	Pos	Pos/MCF	
Pigs			Neg	Neg	MCF	MCF	MCF	
Rabbits			Neg	Pos/MCF	MCF	MCF		
Bison		Neg	Pos/MCF	MCF	MCF	MCF	MCF	

^aData reported by Li et al. (48, 52, 149), O'Toole et al. (50), and Taus et al. (47, 51) for OvHV-2 dose-response studies.

^bThe animals were infected by intranasal nebulization with 2 ml of OvHV-2 inoculum.

Abbreviations: Neg, no infection; Pos, subclinical infection. Grey shaded blocks indicate a minimal dose required for induction of disease.

1.4 Transmisión del virus OvHV-2

El virus OvHV-2 se transmite a través de las secreciones nasales y oculares de un reservorio infectado a un hospedador clínicamente susceptible. La transmisión es favorecida por contacto cercano y por un medio ambiente fresco y húmedo. Al igual que otros herpesvirus, OvHV-2 es relativamente inestable en el medio ambiente. Las especies clínicamente susceptibles adquieren los virus por inhalación o ingestión de alimentos o agua contaminados (20).

La transmisión placentaria rara vez ocurre en ovinos, aunque no se pueden descartar otras vías, incluida la transmisión sexual con semen (21,22). El ácido desoxirribonucleico (ADN) de OvHV-2 se puede detectar continuamente en las secreciones nasales de la mayoría de las ovejas infectadas, pero los niveles altos de ADN viral se encuentran, predominantemente, en ovejas entre los seis y nueve meses de edad (23,24). Además, los corderos recién nacidos no están infectados con el virus y no hay evidencia de que las ovejas que paren excreten más virus que otras ovejas adultas en cualquier época del año (21). La transmisión experimental de OvHV-2 desde un animal enfermo a otro susceptible suele ser difícil, dado que requiere la transferencia de grandes volúmenes de sangre fresca vía intravenosa o la inoculación de una suspensión de órgano infectado. La transmisión natural de OvHV-2 entre animales susceptibles es muy difícil debido a

que la cantidad de virus que se elimina por secreciones nasales es muy baja, y se requieren grandes cantidades de partículas virales para generar la enfermedad (25,26).

1.5 Replicación del virus OvHV-2

En ovejas infectadas experimentalmente con OvHV-2, se puede detectar el gen *ORF25* que codifica para la proteína principal de la cápside viral en pulmón al día después de la infección (DI) (27). Se alcanza su punto máximo de detección el día 7 DI y desciende alrededor del día 9 DI, lo que demuestra que se produce un periodo transitorio inicial de replicación lítica de OvHV-2 en pulmones. La diseminación del virus principalmente latente en leucocitos infectados ocurre después de esta replicación lítica inicial y el ADN de OvHV-2 se detecta fácilmente en prácticamente todos los órganos (27). En esta etapa, las transcripciones del gen *ORF25* rara vez se detectan, lo que indica el predominio de virus latente. Un estudio reciente de ovejas infectadas de forma natural con OvHV-2 documentó que el virus se mantiene predominantemente en los linfocitos T CD2+ y asesinas naturales NK CD2+ (28). El hecho de que OvHV-2 se mantenga en poblaciones de ovejas sin enfermedad clínica indica un control equilibrado entre latencia y reactivación, aunque el factor clave que desencadena la reactivación en linfocitos infectados es desconocido. La presencia de transcritos de *ORF25* y la proteína de la cápside en células epiteliales de secreciones nasales, indica que las células epiteliales de cornete nasal permiten la replicación lítica de OvHV-2 y acaban desprendiéndose del epitelio (29,30). A diferencia de otros herpesvirus, la excreción de OvHV-2 en ovejas ocurre como un patrón único con un episodio intenso, pero de corta duración, lo que implica un solo ciclo de replicación viral (24).

Tomando en conjunto, el ciclo de replicación de OvHV-2 en ovejas parece estar asociado con tres etapas distintas: entrada (replicación en pulmón), mantenimiento (latencia en linfocitos) y salida (replicación epitelial en cornetes nasales), con posibles cambios en el tropismo celular al menos a la entrada y salida (27).

En hospedadores clínicamente susceptibles (bovinos, ciervos, búfalos, bisontes, cabras, cerdos, conejos etc.) infectados experimentalmente con OvHV-2 ocurre una replicación viral inicial en pulmón similar a la de las ovejas (reservorio) (18,31). Una marcada diferencia es que la diseminación del virus por todo el cuerpo en bisontes y conejos está asociada con un patrón de transcripción de genes (*ORF25*, *ORF50* y *ORF73*), en la mayoría de los órganos examinados

durante la enfermedad clínica (18,31). También se ha confirmado la replicación viral lítica en órganos de animales clínicamente afectados, principalmente en células epiteliales y células M del apéndice vermiforme de conejos con FCM inducida por inoculación intravenosa de células linfoblastoides infectadas con OvHV-2 (32). Esto también está respaldado por un estudio reciente que demuestra que la proteína de la cápside codificada por el gen *ORF25* esta predominantemente presente en los fibroblastos perivasculares en varios órganos de bisontes con SA-MCF inducido experimentalmente. Sin embargo, la distribución citoplasmática de la proteína principal de la cápside viral (codificada por el gen *ORF25*), sugiere que la replicación viral en los fibroblastos perivasculares puede ser abortiva (33).

En general, el ciclo viral de replicación de OvHV-2 en bisontes, un hospedador clínicamente susceptible terminal, parece tener sólo dos etapas: entrada (replicación en pulmón) y mantenimiento (en linfocitos y órganos asociados con un perfil de expresión genética latente y lítica; como el riñón, hígado, bazo, encéfalo, linfonodos, vejiga, intestino, rumen, etc.), sin salida del virus (Figura 3).

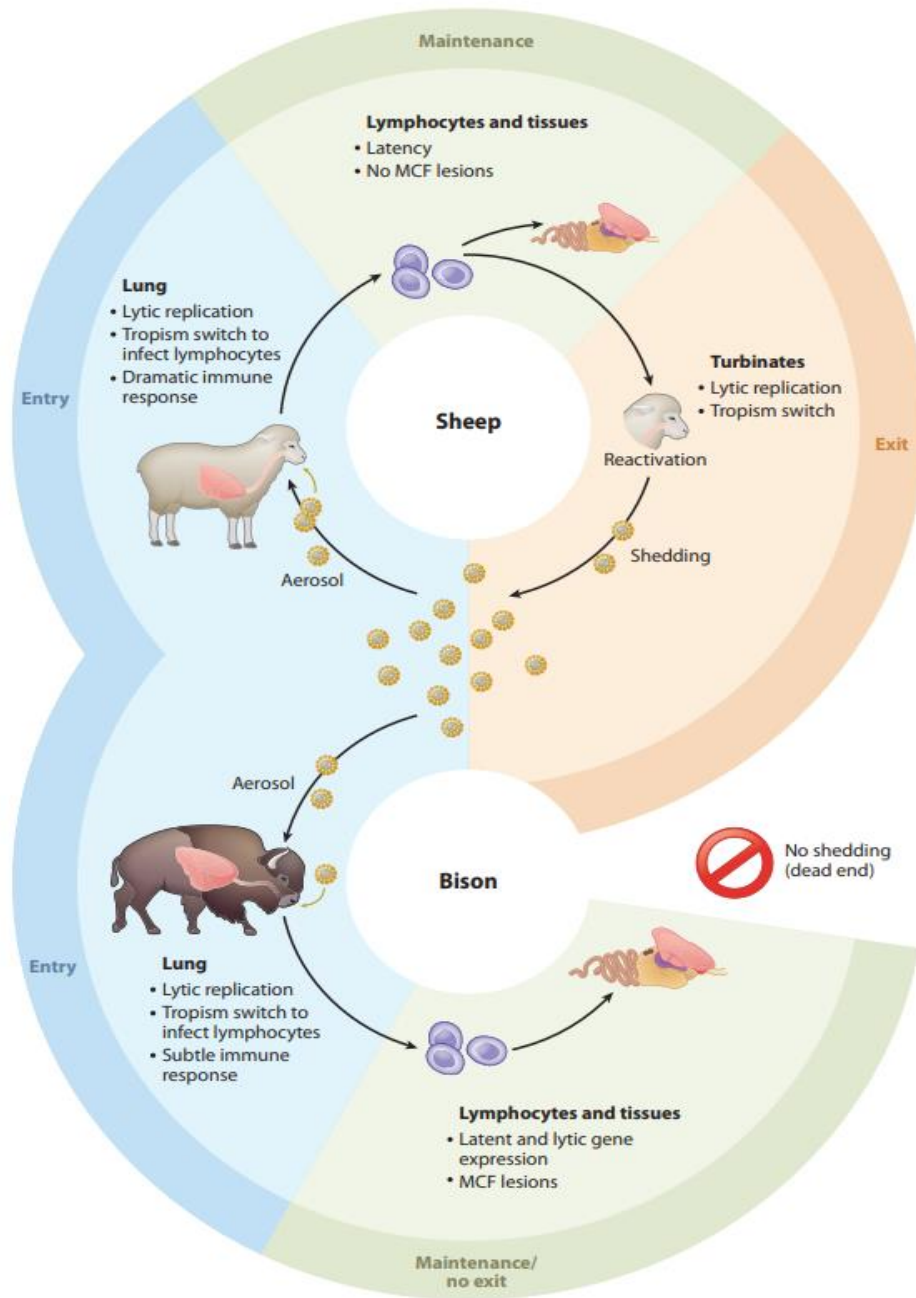


Figura 3. Ilustración de la transmisión del OvHV-2 en el reservorio (oveja) y en el hospedador clínicamente susceptible (bisonte). Hong Li *et al.* Avance lento hacia la comprensión de la Fiebre Catarral Maligna. Revisión anual de biociencias animales. 2014.

1.6 Presentación clínica del OvHV-2

Se han descrito cinco presentaciones clínicas de FCM: hiperaguda, de cabeza y ocular, alimentaria, neurológica y cutánea (34). La forma de presentación hiperaguda se caracteriza por una muerte súbita y fiebre elevada de hasta 41°C. La presentación de cabeza y ocular es la expresión más común de la enfermedad, y los signos típicos incluyen pirexia de 40.5 °C a 41°C al tercer o cuarto día de inicio de la enfermedad, inapetencia, secreción mucopurulenta ocular y nasal, además de congestión, necrosis y erosión de las mucosas superficiales en encías y paladar. También los animales pueden presentar opacidad corneal, salivación excesiva y diarrea (Figura 4). Los signos clínicos dependen en cierta medida de la especie infectada, dosis infecciosa y cuánto tiempo sobrevive el animal después del inicio de los signos clínicos. Muchos ciervos mueren dentro de las 48 horas después de los primeros signos clínicos y los bisontes afectados generalmente mueren dentro de los 3 primeros días, por el contrario, los bovinos pueden sobrevivir durante una semana o más (35).

La presentación nerviosa se caracteriza por temblores musculares, incoordinación, nistagmos, contracciones de las orejas, torticolis e incluso, un comportamiento agresivo. La presentación digestiva se caracteriza por diarrea o disentería en el ganado vacuno. En el caso de los ciervos y los conejos infectados, la evolución hacia la muerte es rápida (1). La presentación cutánea es rara y se caracteriza por exudación y formación de escaras en la piel de la ubre (36).



Figura 4. Presentación clínica de cabeza y ocular. D. O'Toole and Hong Li *et al.* La patología de la fiebre catarral maligna, con énfasis en el herpesvirus ovino 2. Patología Veterinaria en línea. 2014.

1.7 Lesiones histopatológicas del OvHV-2

Los hallazgos macroscópicos en el examen *post-mortem*, incluyen hemorragias petequiales en lengua, mucosa oral, tracto gastrointestinal, tracto respiratorio y vejiga urinaria (Figura 5). Comúnmente hay focos pálidos elevados en la superficie de los riñones y agrandamiento general de los ganglios linfáticos. Histopatológicamente, la FCM se caracteriza por la acumulación de linfocitos en múltiples órganos, algunos de los cuales están asociados con vasculitis y lesiones necróticas (1). Además, en pulmón se observan focos de neumonía intersticial que afectan a todos los lóbulos pulmonares e involucra del 1% al 2% del parénquima (Figura 5). La enfermedad presenta una miscelánea de procesos inflamatorios: cistitis hemorrágica, tiflocolitis necrohemorrágica, rinitis ulcerosa erosiva, estomatitis, faringitis, laringitis, esofagitis, arteritis-flebitis en vasos de calibre medio y linfadenitis generalizada de ganglios linfáticos con hiperplasia paracortical.

Algunos bisontes abortan durante el curso clínico, presumiblemente debido a fiebre y toxemia. Además, se presentan zonas de apoptosis y / o necrosis en la piel, en tracto digestivo, y en vías urinarias. También causa degeneración del urotelio de los cálices renales, los uréteres, la vejiga y la uretra. Se puede observar en algunos casos meningoencefalitis no supurativa con leve gliosis multifocal. Las lesiones oculares se observan como congestión de la conjuntiva y de la esclerótica, acompañada por una opacidad centripeta progresiva de la córnea. La queratitis se acompaña con exudados celulares y fibrinosos en la cámara anterior, lo que resulta en fotofobia y ceguera parcial. También es común observar el miocardio con necrosis multifocal, probablemente debido a miopatía por esfuerzo (35).

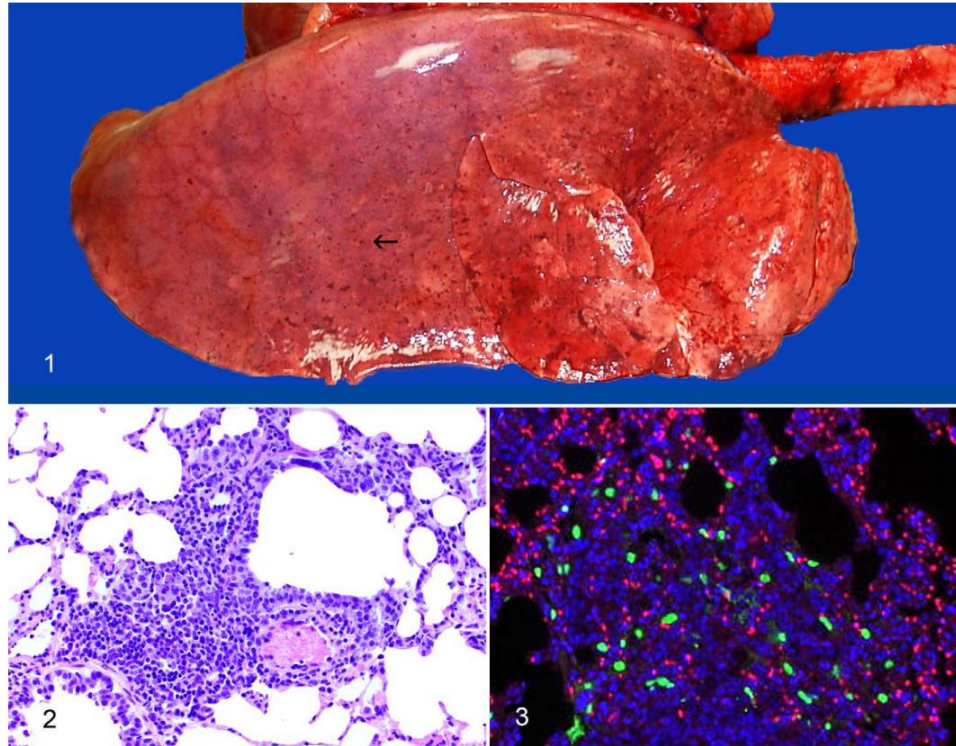


Figura 5. 1-Pulmón; áreas multifocales de consolidación (flecha), 2- Pulmón; neumonía broncointersticial en un cordero, hematoxilina y eosina (HE), 3- Pulmón; Inmunorreactividad anti-ORF25 (verde) en un cordero después del desafío con OvHV-2. D. O'Toole and Hong Li *et al.* La patología de la fiebre catarral maligna, con énfasis en el herpesvirus ovino 2. Patología Veterinaria en línea. 2014.

1.8 Distribución geográfica del virus OvHV-2

La FCM causada por el virus OvHV-2, puede observarse en todo el mundo, pero la manifestación de la enfermedad depende de la presencia del reservorio y de un huésped susceptible. La SA-MCF actualmente representa un problema económico en Indonesia y en Estados Unidos porque afecta al ganado Bali (banteng; *Bos javanicus*) y a bisontes, respectivamente. La enfermedad ha sido reportada en diferentes hospedadores susceptibles (bovinos, bisontes, búfalos, ciervos, etc.) de América del norte y del sur (37–39), Europa (40–43), Asia (44), África (45) y Nueva Zelanda (46).

El primer caso de SA-MCF en México se documentó en 1969, en la Ciudad de México, en una vaca Holstein de 6 años, la cual manifestó la presentación clínica cefálica y ocular, además de infiltrados linfoides perivasculares en diversos órganos. Sin embargo, el diagnóstico solo se basó

en un estudio clínico-patológico (47). Más recientemente, ocurrió un brote de SA-MCF en el municipio de Tequisquiapan en el estado de Querétaro, México, afectando a varias especies de animales (ovejas, cabras, ciervos, ganado lechero, ganado de engorda y caballos) con una presentación clínica cefálica y ocular. Debido a que es una enfermedad exótica para el país se desconoce el impacto económico y epidemiológico de la enfermedad, así como la distribución y caracterización molecular del virus OvHV-2.

1.9 Impacto económico de la FCM

El impacto económico de la FCM varía ampliamente y las pérdidas asociadas nunca se han calculado sistemáticamente, en parte porque no existe un sistema de notificación organizado y obligatorio para esta enfermedad (48). Además, hasta hace poco, la imprecisión de las pruebas diagnósticas ocasionó un número significativo de diagnósticos erróneos, particularmente en casos leves o atípicos. Por lo tanto, la verdadera incidencia es probablemente más alta de lo estimado (25). En ganado europeo, la enfermedad es generalmente esporádica y con baja mortalidad, siendo mayoritariamente casos aislados (40,49). En África, la FCM causada por AIHV-1, provoca una pérdida media anual estimada del 7% en la población bovina, asociada con los ñus (reservorio). Esta enfermedad se ha clasificado entre las cinco enfermedades bovinas más importantes, ubicándose solo detrás de la fiebre de la costa del Este o teileriosis, en áreas de alto riesgo (50). La FCM es a menudo devastadora para granjas que tengan especies altamente susceptibles como bisontes, ciervos, así como en zoológicos (51).

En América del Norte, las pérdidas debidas a la SA-MCF causada por el virus OvHV-2 han forzado a productores de bisontes a salir del negocio (52); en 2003, se perdieron más de 800 cabezas, con pérdidas financieras de aproximadamente un millón de dólares (10). En Brasil, las pérdidas económicas directas asociadas con la morbilidad y mortalidad de SA-MCF se estimaron en US\$215.592 y US\$214.368, respectivamente. Si los datos se proyectaran a nivel nacional, daría como resultado una pérdida económica proyectada de US\$ 3,5 a US\$ 4,8 mil millones para la industria ganadera en Brasil (53).

1.10 Diagnóstico de SA-FCM

El diagnóstico presuntivo de SA-MCF se realiza con criterios clínico-patológicos, combinados con una historia reciente de exposición con un reservorio (16). El diagnóstico serológico para la detección de anticuerpos contra OvHV-2 se ha realizado utilizando el ensayo inmunoabsorbente ligado a enzimas (ELISA) y ELISA de inhibición competitiva (cELISA) (54,55).

La reacción en cadena de la polimerasa (PCR) es una prueba sensible y específica que puede apoyar en el diagnóstico de SA-MCF (56). Los cebadores de la prueba de PCR punto final anidada desarrollada por Baxter *et al.* (57) están dirigidos a un fragmento del gen *ORF75* de OvHV-2, un gen que codifica para una proteína de tegumento viral (57). Además, existe una prueba de PCR cuantitativa (qPCR) en tiempo real, la cual mostró una sensibilidad adecuada para muestras clínicas (56). El conjunto cebador-sonda es específico para el gen *ORF75* similar a la PCR anidada. Para granjas con especies mixtas y zoológicos, se recomienda el uso de una PCR multiplex para la detección y diferenciación de los virus causantes de FCM que se sabe que causan enfermedades (58). La PCR multiplex es una prueba de tiempo real basada en sondas específicas para cada virus, con un único par de cebadores que se dirigen a una región polimórfica en el gen de la ADN polimerasa viral. Esta representa un método rápido, confiable y diferencial para la identificación de virus causantes de FCM en muestras clínicas. Para el diagnóstico de animales libres de SA-MCF y su separación temprana del rebaño positivo (59), es necesario utilizar una PCR anidada para maximizar la sensibilidad, ya que la PCR anidada es más sensible que la qPCR (60). Los leucocitos y el tejido linfoide son fuentes ideales para aislar el virus OvHV-2 y realizar pruebas de PCR (61).

1.11 Aislamiento de los virus causantes de la FCM

Para el aislamiento *in vitro* de virus causantes de FCM, se pueden utilizar cultivos celulares primarios de células tiroideas bovinas (BTh), células de riñón bovino (BK), células de riñón embrionario bovino (BEK) y células de testículo de ternera (CT) (62–64). Los leucocitos de sangre periférica y los órganos linfoides secundarios son la fuente más común de muestras para intentar

el aislamiento. El aislamiento de AIHV-1 en cultivos celulares se asocia con la formación de sincitios transitorios de los 3 a 21 días post-infección (20).

En un estudio previo se reveló que AIHV-1 pierde la capacidad de inducir FCM en el ganado y los conejos después de cinco pases en cultivo celular; debido a varios reordenamientos del genoma que ocasionan la atenuación del virus. Esto sugiere que los genes contenidos dentro de los fragmentos reordenados podrían ser necesarios para la inducción de enfermedad clínica (65,66). Estos reordenamientos involucran deleciones de genes y translocaciones desde la región central del genoma a la región de repetición terminal (66). Los receptores utilizados por el virus para entrar en las células (epiteliales o linfocitos) y establecer una infección latente o lítica son desconocidos.

Por otro lado, Hristov *et al.* (2016) describieron el uso de cultivos celulares primarios de riñón de conejo (RK) y cultivos celulares permanentes (línea celular de riñón bovino Madin Darby (MDBK), línea celular embrionaria traqueal bovina (EBTR), línea celular de riñón de mono verde (VERO) y línea celular de mono (MA-104)) para el aislamiento del virus OvHV-2. Sin embargo, mencionan que se necesitan investigaciones adicionales para confirmar qué tipo de aislamiento viral OvHV-2 o AIHV-1 realizaron (61). Durante los pases iniciales del virus, el efecto citopático (ECP) aparece tardíamente, muy probablemente debido a la gran cantidad de virus asociado a las células. Después del pase 19 la cantidad de virus libre en el medio de cultivo fue suficiente para observar un ECP temprano a las 24 horas. La monocapa se destruyó completamente entre las 48 y 72 horas post-infección. Esto se debe a la adaptación del virus al cultivo celular, como resultado de la interacción de los receptores virales y celulares (61).

Los cuerpos de inclusión (CI) intranucleares herpesvirales se forman en cultivos celulares y en pulmones de ovejas infectadas experimentalmente (61,64). Sin embargo, en hospedadores susceptibles terminales se han encontrado CI acidófilos citoplasmáticos en algunas neuronas a nivel del cuerpo estriado y de la médula oblonga y en células epiteliales de mucosas (47,67). También en hospederos susceptibles terminales como los bovinos y bisontes, se demostró una distribución citoplasmática de la proteína de la cápside lo que sugiere una posible replicación abortiva en estos hospederos (33). Además, la acumulación de proteínas virales y celulares en citoplasma se han demostrado en citomegalovirus. Estos sitios de acumulación y retención de proteínas se conocen como “Cuerpos Densos”, localizados cerca de la cubierta nuclear. Estas proteínas pueden ser importadas al núcleo para llevar a cabo el correcto ensamblado viral (68)

1.11 Diagnóstico diferencial

Es necesario utilizar herramientas de diagnóstico diferencial debido a que las lesiones vesiculares en mucosas provocadas por la FCM son similares a aquellas que aparecen en enfermedades como la diarrea viral bovina (BVD), lengua azul (BT), rinotraqueitis infecciosa bovina (IBR), fiebre aftosa (FMD), estomatitis vesicular (VS), ingestión de materiales cáusticos, plantas tóxicas, y micotoxinas (69). El uso de las diferentes herramientas de diagnóstico mencionadas anteriormente permite identificar de forma específica y confiable el antígeno OvHV-2 y descartar cualquier otro patógeno.

2. JUSTIFICACIÓN

Durante el brote de SA-MCF que se presentó en 2018 en CEIEPAA, murieron 14 ciervos que representa el 18% del hato, además de identificarse el primer caso de SA-MCF en caballos en México, una especie considerada no susceptible hasta 2009 cuando se presentó el primer caso de esta enfermedad en Brasil. El virus OvHV-2 se encuentra clasificado en el grupo 1 del listado de enfermedades y plagas exóticas de notificación obligatoria inmediata. Debido a lo anterior, en nuestro país se desconoce el impacto económico y epidemiológico, así como la distribución y caracterización molecular del virus OvHV-2.

Es de interés aislar y caracterizar al virus OvHV-2 causante del brote de SA-MCF de 2018 en CEIEPAA, y es necesario desarrollar técnicas de diagnóstico accesibles, específicas, sensibles y rápidas, que motiven la implementación de políticas de prevención y control de la diseminación epidémica de este virus y de la SA-MCF a otros estados de la República Mexicana, afectando a especies altamente susceptibles y a caballos.

3. HIPÓTESIS

La enfermedad vesicular que afectó a las diferentes especies de ungulados y a los caballos del CEIEPAA en agosto del 2018, fue causada por el virus OvHV-2.

4. OBJETIVO GENERAL

- Identificar y caracterizar al virus OvHV-2 causante del brote de SA-MCF en artiodáctilos y caballos mantenidos en el rancho CEIEPAA, Tequisquiapan, Querétaro.

4.1 Objetivos específicos

1. Demostrar que los leucocitos de los ovinos, caprinos, bovinos, ciervos y caballos del CEIEPAA están infectados por el virus OvHV-2.
2. Probar que la replicación viral de OvHV-2 ocurre en cultivos primarios de testículo de conejo.
3. Conocer los posibles cambios genéticos de las secuencias parciales del gen *ORF75*.
4. Demostrar que la inoculación experimental de conejos con OvHV-2 provoca lesiones histopatológicas compatibles con SA-MCF.

5. MATERIAL Y MÉTODOS

5.1 Lugar de muestreo

El muestreo se realizó en el Centro de Enseñanza, Investigación y Extensión en Producción Animal en Atilplano (CEIEPAA), perteneciente a la Universidad Nacional Autónoma de México (UNAM), ubicado en Tequisquiapan, estado de Querétaro, México. Esta finca tiene una superficie de 186 ha. Se basa en un sistema de producción semi-intensivo con múltiples especies: ciervos (rojo europeo), ganado lechero (Holstein, Jersey y cruces), ganado de engorda (Limousin), ovejas (Suffolk, Katahdin y cruces), cabras (Alpine Frances, Saanen, Toggenburg y Boer) y caballos (pura sangre inglés, cuarto de milla, apéndice, portugués, Santa Gertrudis y criollo) (Figura 6). Las especies se separaron entre 1.14 y 2.8 km (70).

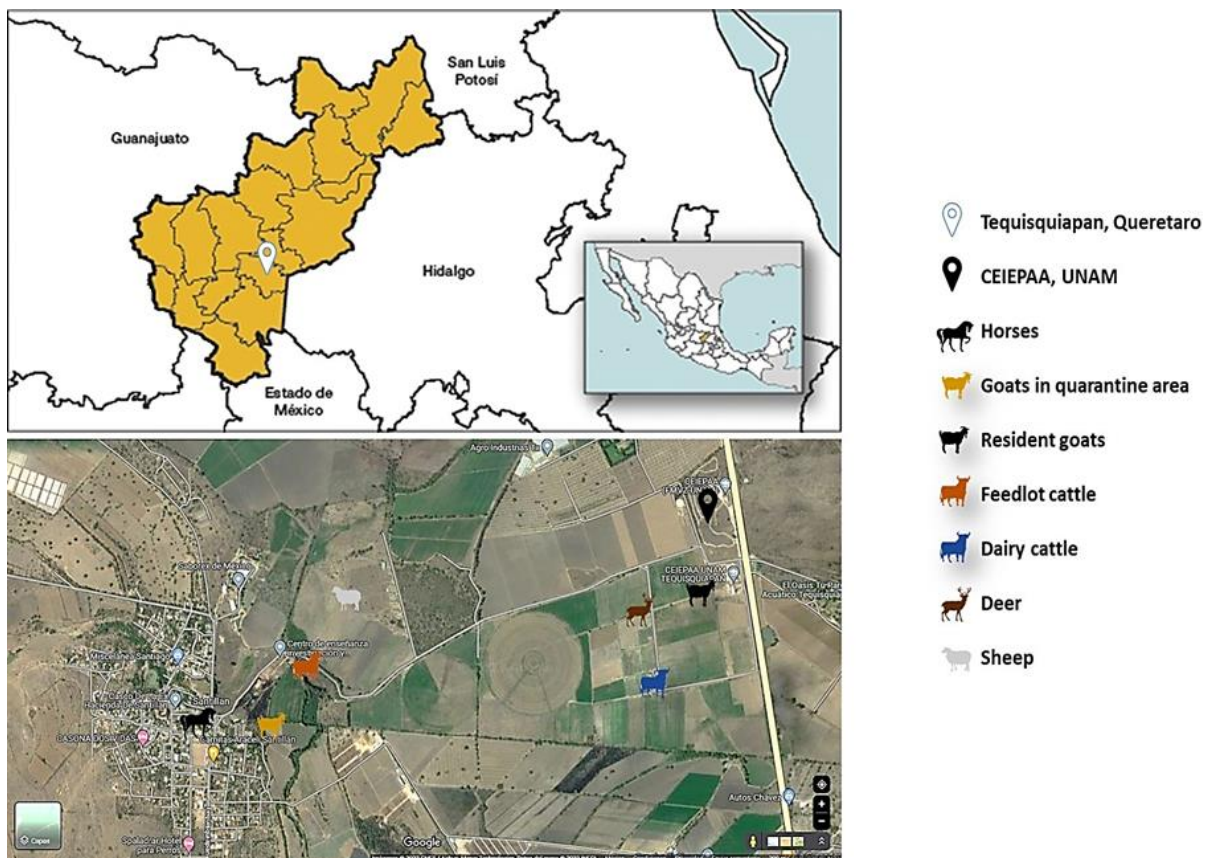


Figura 6. Distribución de animales en el CEIEPAA, UNAM. En la parte superior izquierda se indica la ubicación geográfica de Tequisquiapan (10°36'13.88" latitud norte, 99°55'02.91" longitud Oeste, y una altitud de 1913 metros sobre el nivel del mar (msnm)), estado de Querétaro, México. La distribución de especies en el área se representa en la sección inferior izquierda.

5.2 Cronología del brote

De agosto a diciembre de 2018 se presentó una enfermedad vesicular que afectó a todas las especies de animales pertenecientes al rancho CEIEPAA. La Comisión México-Estados Unidos para la Prevención de la Fiebre Aftosa y otras Enfermedades de los Animales Exóticos (CPA) tomó muestras de suero, sangre, epitelio de lesiones ulcerativas de la mucosa oral, órganos de los ciervos (lengua, cerebro, ganglios linfáticos submandibulares, riñón y bazo) e hisopos nasales para realizar diagnósticos diferenciales de enfermedades vesiculares (70). En enero de 2019, la UNAM realizó un muestreo dirigido para aislar el virus OvHV-2 (Cuadro 2).

5.3 Pruebas complementarias

Las muestras de suero se analizaron con pruebas ELISA para diagnosticar el virus de la fiebre aftosa (FMDV) y el virus de la estomatitis vesicular (VSV). Por otro lado, se utilizaron muestras de epitelio, sangre, órganos de los ciervos (lengua, cerebro, ganglios linfáticos submandibulares, riñón y bazo) e hisopados nasales para realizar diferentes diagnósticos moleculares: PCR o reacción en cadena de la polimerasa con transcriptasa inversa (RT-PCR) para el FMDV, el virus de la rinotraqueítis bovina infecciosa (IBRV), el VSV de Indiana y Nueva Jersey, el virus de la parapoxvirus (PRV), el virus de la lengua azul (BTV) y el virus del ectima contagioso (CEV). Además del aislamiento de VSV (Cuadro 2).

5.4 Evaluación *post-mortem*

De los 14 ciervos que murieron durante el brote de SA-MCF de 2018, 9 ciervos fueron evaluados *post-mortem* porque 5 estaban en un estado avanzado de descomposición. Los resultados de la evaluación *post-mortem* fueron publicados por Pérez *et al.* (2022) (70). Nuestra investigación actual presenta los resultados de estos dos ciervos (#172 y #174), que fueron elegidos debido a la gravedad de sus signos clínicos y lesiones. Se tomaron muestras de córnea, ganglios linfáticos, lengua, rumen, hígado, pulmón y riñón y se fijaron por inmersión en solución de formalina tamponada al 10 % y se procesaron de forma rutinaria para inclusión y corte en parafina y mediante la tinción con hematoxilina y eosina (H&E) para observación y análisis histopatológico.

5.5 Recolección y preparación de muestras clínicas

En enero de 2019 se realizó un nuevo muestreo. No obstante, esta vez estuvo dirigido a los animales que previamente habían sido positivos por PCR para OvHV-2 por parte de la CPA, incluidos aquellos que aún presentaban lesiones ulcerativas (11 caballos) y algunos animales sanos. El propósito de este muestreo fue aislar el virus OvHV-2. Se obtuvieron aproximadamente 30 muestras de sangre de cada especie animal (ciervos, ganado de engorda, ganado lechero, ovejas, cabras y caballos) en tubos Vacutainer®. Posteriormente, las capas leucocíticas se separaron según la metodología descrita por English & Andersen (1974) (71), y luego de su identificación, se almacenaron a -196°C hasta su procesamiento para aislamiento viral y PCR.

5.6 Reacción en cadena de la polimerasa (PCR) punto final anidada para la detección del virus OvHV-2

La prueba de PCR punto final anidada es específica para el gen *ORF75* del OvHV-2, que codifica para la enzima fosforibosilformilglicinamida sintasa (FGARAT) que participa en el

metabolismo de las purinas y la síntesis de proteínas del tegumento viral (72). La extracción del material genético se hizo siguiendo las instrucciones del fabricante del kit High Pure PCR de Roche® (*Roche Diagnostics GmbH. High Pure PCR Template Preparation Kit, 2008*) (73).

Los pares de cebadores fueron diseñados por Baxter *et al.* (1993), y se realizó una PCR anidada siguiendo el método de Li *et al.* (1995), con algunas modificaciones (57,74). Se realizaron dos amplificaciones; en la primera se utilizaron los iniciadores MCF 556 (5' GTC TGG GGT ATA TGA ATCCAG ATG GCT CTC 3') y MCF 755 (5' AAG ATA AGC ACC AGTTAT GCA TCT GAT AAA 3'), para amplificar un segmento de 422 pares de bases (pb). Las condiciones de reacción se ajustaron a 25 µL y se utilizó una PCR Máster Mix 5X (Taq-Load). En la segunda amplificación se utilizaron los iniciadores MCF 555 (5' TTC TGG GGT AGTGGC GAG CGA AGG CTT C 3') y MCF 556 (5' GTC TGG GGT ATA TGA ATCCAG ATG GCT CTC 3') para amplificar un segmento de 238 pares de bases (74). La concentración de cebadores externos e internos fue de 10 µM. Todas las reacciones se realizaron en un GeneAmp® PCR System 9700 (Applied Biosystems, Waltham, MA, EE. UU).

Los parámetros para la amplificación de la PCR fueron los siguientes: pre-desnaturalización a 95°C por 10 min, 35 ciclos de desnaturalización a 94°C por 35 s, una alineación a 55°C por un min, una extensión a 72°C por 45 s y una extensión final a 72°C durante 10 min. En la segunda amplificación se tomó 1 µl de la primera reacción como plantilla para la segunda ronda de PCR con los mismos parámetros de la primera ronda de amplificación, con la excepción en la temperatura de alineamiento que fue a 60°C por 35 s. Para la visualización de la reacción, se utilizaron 5 µl del producto amplificado y 2 µl del buffer de carga con GelRed® (Biotium, cat.41003). Al producto de amplificación se le realizó una electroforesis durante 35 min a 120 V, en un gel de agarosa al 1.5%. Un resultado positivo genera una banda de 238 pb en la segunda amplificación. Se utilizó como control positivo una muestra de sangre de bovino donada por la CPA. Como control negativo se utilizó agua libre de nucleasas.

5.7 Cultivo primario de testículo de conejo

El cultivo celular primario se preparó utilizando testículos de conejos machos de 2 meses de edad, que fueron sacrificados humanitariamente (SICUAE.DC-2020/3-5)]. Los testículos se lavaron cinco veces con solución salina balanceada de Hanks (HBSS, Gibco, Life Technologies) suplementada con penicilina (100 U/mL, Gibco, Life Technologies), estreptomicina (100 g/mL, Gibco, Life Technologies) y fungizona (2,5 g/ml, Gibco, Life Technologies). Luego se colocaron en una placa de Petri estéril donde se diseccionaron la túnica albugínea y las capas de tejido conjuntivo de cada testículo con tijeras estériles. Con ayuda de unas tijeras estériles se realizaron cortes manuales para obtener fragmentos menores de 0.5 cm² de ambos testículos. Los fragmentos de testículos se tripsinizaron durante 1 h a 37 °C en agitación constante utilizando 0.25% de tripsina-EDTA con rojo fenol (Gibco, Cat: 25200056) en una proporción de 1:5.

Después de la incubación, las células desprendidas se filtraron a través de un embudo con gasa estéril y el filtrado se recogió en un tubo de centrifuga y se centrifugó a 800 × g durante 10 min. Se descartó el sobrenadante y el sedimento de células se resuspendió en medio de Eagle modificado por Dulbecco (DMEM, Gibco™, cat. 11574486) suplementado con suero de ternera fetal al 10%. Se sembraron aproximadamente 0.5 × 10⁶ células/mL por botella. Los cultivos se mantuvieron en botellas de cultivo de 25 cm² (Nunc, Roskilde, Dinamarca) a 37°C con una atmósfera de CO₂ al 5%. Las células se monitorearon diariamente bajo un microscopio Olympus invertido (IX71) con un objetivo de 10x (Olympus Corporation, Shinjuku City, Tokio, Japón), y después de 2 días, el DMEM suplementado con suero fetal bovino al 10% se cambió a un medio fresco similar.

5.8 Aislamiento viral del OvHV-2

Para el aislamiento del OvHV-2 se utilizaron botellas de cultivo de 25 cm² con un 80% de confluencia celular. Cada botella se inoculó con 200 µL de lisado de capa leucocítica (PCR positiva para OvHV-2). Los lisados se obtuvieron congelando y descongelando las capas leucocíticas de cada una de las seis especies naturalmente infectadas con OvHV-2 (ciervos, ganado

lechero, ganado de engorda, ovejas, cabras y caballos). Las células inoculadas se propagaron en DMEM suplementado con suero fetal bovino al 5 % y se incubaron a 37 °C con una atmósfera de CO₂ al 5 %. Las botellas de cultivo con las células inoculadas se observaron cada 24 h durante 7 días utilizando un microscopio invertido Olympus (IX71) con un objetivo de 10x (Olympus Corporation) para identificar el efecto citopático específico del OvHV-2 (61).

Se realizaron al menos cuatro pases ciegos en todas las especies excepto en los caballos, en los que se necesitaron catorce pases ciegos para la adaptación del virus al cultivo celular y la producción de virus libre de células. Las botellas de cultivo con las células inoculadas se congelaron y descongelaron cuando se observaron cambios citopáticos en las monocapas (focos de células citomegálicas refráctiles, sincitios o destrucción del 50% de la monocapa). Luego, el sobrenadante del cultivo se centrifugó a 1200 × g durante 10 min, y el sobrenadante final se dividió en pequeñas alícuotas y se almacenó a -80 °C hasta su uso. Para pases consecutivos, se prepararon monocapas frescas y se inocularon con el sobrenadante de virus mencionado anteriormente. Cuando se observaron cambios citopáticos en las monocapas, las botellas de cultivo con las células inoculadas se procesaron como se mencionó anteriormente. Tras los cambios citopáticos de las monocapas, se identificaron en los sobrenadantes de cultivo de los cuatro pases ciegos el gen *ORF75* del virus OvHV-2 mediante PCR anidada. Como control negativo, se inoculó una botella de 25 cm² con un 80 % de confluencia celular con 200 µL de lisado de capa leucocítica de caballos OvHV-2 negativos.

El título viral se cuantificó a partir de los sobrenadantes libres de células del 4^{to} pase ciego de todas las especies y del 3^{ro} al 14^{vo} pases ciegos de los caballos. Se utilizaron placas de 96 pocillos de fondo plano como describieron Reed y Muench (75). Para el análisis microscópico de las placas, estas se fijaron 72 h postinfección con paraformaldehído al 4% diluido con agua destilada y se tiñeron con cristal violeta al 0.5% diluido en alcohol de 96°.

Para observar los cuerpos de inclusión intranucleares (CI), se inoculó una placa de 24 pocillos con una confluencia celular del 80% con 200 µL de cada uno de los cuatro pases ciegos descritos anteriormente. Las células inoculadas se propagaron con DMEM suplementado con suero fetal bovino al 2% y se incubaron a 37 °C durante 24 h en una atmósfera de CO₂ al 5 %. Posteriormente, se eliminó el sobrenadante y las células se fijaron con paraformaldehído al 4%. Finalmente, se añadió hematoxilina durante 1 min, se lavó con agua destilada y después se tiñó

con eosina durante 30 s. El fondo de cada pocillo se cubrió con glicerol y un cubreobjetos. Los CI intranucleares se observaron bajo un microscopio invertido Olympus (IX71) con un objetivo de 10x (Olympus Corporation). Como control negativo, se dejó una placa de 4 pocillos con una confluencia celular del 80 % y se inoculó con 200 μ L del lisado de capa leucocítica de los caballos OvHV-2 negativos; por lo demás, el procesamiento de la placa fue idéntico al mencionado anteriormente.

5.9 Cinética de replicación viral

La cinética de la replicación viral se realizó a partir de los sobrenadantes libres de células de los pases 4, 5 y 14 del lisado de la capa leucocítica de los caballos. Se inocularon cultivos primarios de testículos de conejo cultivados en placas de fondo plano de 96 pocillos y se procesaron según la técnica de Reed y Muench (75). Brevemente, los cultivos primarios se inocularon con diluciones decuples seriadas de cada una de las muestras por cuadruplicado por dilución. Luego, el inóculo se eliminó en diferentes puntos de tiempo (24, 48, 72, 96 y 120 h post-infección), y las placas se fijaron con paraformaldehído al 4% durante 10 min y se tiñeron con cristal violeta al 0.5%. Los gráficos se realizaron utilizando el software GraphPad Prism 9.5.1 (GraphPad, EE. UU.).

5.10 Secuenciación parcial del gen *ORF75*

La secuenciación parcial del gen *ORF75* se realizó a partir del cuarto pase ciego obtenido mediante la inoculación de los cultivos primarios con el lisado de las capas leucocíticas de las diferentes especies animales (ciervos, ganado lechero, ganado de engorda, ovejas, cabras y caballos). Además, se realizó la secuenciación parcial del control positivo donado por la CPA. Las siete muestras fueron amplificadas por PCR punto final para obtener un fragmento de 422 pb correspondiente a un segmento del gen *ORF75*, y 300 ng de cada producto de PCR fueron secuenciados por electroforesis capilar bidireccional a través de secuenciación Sanger utilizando cebadores de PCR externos como cebadores de secuenciación (MCF 556 y MCF 755) (72). Los

electroferogramas de cada par de secuencias se editaron y ensamblaron con el editor de alineación de secuencias biológicas (BioEdit), v 7.2.0; (76). Las secuencias se alinearon usando el software MEGA 11 (77).

5.11 Análisis Filogenético

Las siete secuencias consenso obtenidas mediante el software BioEdit se compararon con secuencias parciales del gen *ORF75* reportadas en el GenBank (76). Para el análisis filogenético, los alelos de alta y baja similitud para *ORF75* se seleccionaron utilizando BLAST (Basic Local Alignment Search Tool) del NCBI (National Center for Biotechnology) (78). Finalmente, las siete secuencias se analizaron filogenéticamente con secuencias del género *Macavirus* (OvHV-2, AIHV-1 y AIHV-2) y *gammaherpesvirus* humanos tipos 4 y 8 (HHV-4 y HVH-8). El modelo de sustitución se seleccionó con Jmodeltest y el modelo Tamura-Nei fue el más apropiado para este conjunto de datos (79,80). El análisis se realizó con el software MEGA 11 utilizando el método de máxima verosimilitud con 1000 réplicas (77). Las siete secuencias de nucleótidos de consenso del fragmento del gen *ORF75* amplificado en este trabajo se enviaron a la base de datos pública GenBank y se les asignaron los siguientes números de acceso: ON375578 (caballos), ON375579 (cabras), ON375580 (ciervos), ON375581 (ganado lechero)), ON375582 (ganado de engorda), ON375583 (ovejas) y ON375584 (control positivo CPA).

5.12 Elaboración de un suero hiperinmune anti-OvHV-2

Para preparar un suero hiperinmune anti-OvHV-2, seguimos un protocolo de un estudio previo de Orós *et al.* (1997), con algunas modificaciones. Se utilizaron tres conejos albinos Nueva Zelanda de 9 semanas de edad, que pesaban aproximadamente 1,7 kg y eran negativos para OvHV-2 mediante PCR de punto final anidado (81). Se inoculó a los conejos por vía intramuscular con el sobrenadante libre de células del cuarto pase ciego de los caballos (dosis infecciosa de cultivo tisular $10^{4.19}$ TCID₅₀/mL) disuelto en solución salina tamponada con fosfato (PBS) y una suspensión acuosa de adyuvante en gel de hidróxido de aluminio (Alhydrogel® al 2%, InvivoGen).

El sobrenadante del cuarto paso ciego mencionado anteriormente se inactivó con formaldehído al 0.2% diluido en agua destilada. Los conejos se alojaron en jaulas de acero inoxidable con malla de alambre, se alimentaron con gránulos comerciales y tuvieron libre acceso a agua corriente. Los animales se mantuvieron a una temperatura de 23-25°C. Después de un período de aclimatación, los conejos recibieron una inoculación intramuscular semanal durante 5 semanas. Posteriormente, los conejos fueron tranquilizados (acepromazina 1 mg/kg), y sus corazones fueron sangrados y luego sacrificados con una sobredosis de pentobarbital. El suero obtenido se almacenó a -20°C hasta su posterior uso en técnicas de inmunofluorescencia (IF), inmunocitoquímica (ICC) e inmunohistoquímica (IHC).

5.13 Inmunocitoquímica (ICC) e inmunofluorescencia (IF) indirecta

Para realizar las técnicas de ICC e IF indirectas, nos basamos en la metodología descrita por Rossiter (1981), con algunas modificaciones. Se utilizaron 2 placas de 24 pozos con una confluencia celular del 80%, los cuales fueron inoculados con 200µl de cada uno de los cuatro pases ciegos que se obtuvieron anteriormente, y fueron incubados a 37°C durante 72 h. Después de lavar con PBS, las células fueron fijadas con paraformaldehído al 4% diluido en agua destilada durante 10 minutos a temperatura ambiente. Posteriormente las células se permeabilizaron con Tritón X-100 al 0.2% durante 5 minutos a temperatura ambiente. Después de tres lavados con PBS, la peroxidasa endógena fue bloqueada con peróxido de hidrogeno al 3% diluido en agua destilada durante 15 min. Nuevamente se realizaron 3 lavados de las células con agua destilada y se procedió al bloqueo de sitios inespecíficos con albumina sérica bovina (ASB) al 2.5% diluida en tampón Tris-HCl durante 30 min a 37°C. A continuación, las células fueron incubadas con el suero hiperinmune de conejo anti-OvHV-2 diluido 1:5 en albumina al 0.1%, durante 24 h a 4°C. Después de tres lavados con PBS, a la placa para la ICC se le añadió proteína A conjugada con peroxidasa diluida 1:16 en albúmina al 0.1% y se incubó durante 1 h a 37°C. Posteriormente se realizaron tres lavados con PBS y se agregó la mezcla sustrato-cromógeno (peróxido de hidrogeno y 3,3'-diaminobencidina), durante 5 min. La reacción fue detenida con agua destilada (82). Las células con inmunorreactividad positiva al OvHV-2 presentaron una coloración insoluble color marrón en el citoplasma.

Como control negativo, se utilizó una placa de 4 pocillos con una confluencia celular del 80%. Dos de los pozos fueron infectados con 200µl del cuarto pase ciego de los caballos y los otros dos pozos permanecieron sin infectar. En los pozos infectados se utilizó como anticuerpo primario un suero de conejo sano negativo para SA-MCF. Por otro lado, en uno de los pozos no infectados se utilizó como anticuerpo primario el suero hiperinmune de conejo anti-OvHV-2 diluido 1:5 y en el otro pozo sólo se agregó la proteína A conjugada con peroxidasa diluida 1:16 el procesamiento de la placa se realizó como se describió anteriormente.

Para la técnica de IF se procedió de la misma forma que para la técnica de ICC, pero se omitió la inhibición de la peroxidasa endógena y se utilizó como conjugado un anticuerpo secundario acoplado a isotiocianato de fluoresceína (FITC) (anti-IgG de conejo hecho en cabra), diluido 1:20 en ASB al 0.1%. Las células con inmunorreactividad positiva al OvHV-2 presentaron una emisión fluorescente color verde manzana (520nm). Como control negativo de la técnica de IF, se utilizó una placa de 4 pocillos y se procesó de forma similar a la técnica de ICC, con la modificación que se utilizó como conjugado un anticuerpo secundario acoplado a isotiocianato de fluoresceína. La inmunorreactividad presente en las placas fue observada en un microscopio invertido de epifluorescencia Olympus (IX71).

5.14 Inmunohistoquímica

La especificidad del suero hiperinmune anti-OvHV-2 se evaluó en el hígado de un ciervo que murió de forma natural durante el brote de SA-MCF en el rancho de CEIEPAA. En los hepatocitos se observaron CI eosinofílicos citoplasmáticos mediante la técnica de H&E.

La técnica se realizó según lo descrito por Headley *et al.* (2022), con algunas modificaciones (83). Se tomaron secciones de hígado montadas en portaobjetos cargados positivamente (Biocare TM). Después de desparafinar los cortes con xileno, fueron rehidratados con tampón Tris-HCl 0.1 M (pH 7.2) y transferidos a un frasco de tinción Coplin de vidrio con tampón citrato de sodio 0.1 M (pH 6.0) para la recuperación antigénica. Este procedimiento se realizó en una olla de presión durante 10 min a 200°C. Después los portaobjetos se dejaron enfriar a temperatura ambiente (TA) durante 15 min dentro de un frasco Coplin que contenía tampón Tris-

HCl 0.1 M (pH 7.2). Posteriormente, la peroxidasa endógena fue inhibida con peróxido de hidrógeno al 3% diluido en agua destilada. Para reducir la tinción de fondo no específica, los portaobjetos se incubaron durante 1 h a 37°C en una solución que contenía tampón Tris-HCl 0.1M (pH 7.2), leche en polvo al 1% y Tritón X-100 al 0.01%. Esta solución se decantó y los portaobjetos se incubaron durante toda la noche a 4% con el suero hiperinmune de conejo anti-OvHV-2 diluido 1:5 en tampón Tris-HCl 0.1 M (pH 7.2) con ASB al 0.1%. Después de tres lavados con tampón Tris-HCl 0.1 M (pH 7.2), los portaobjetos se incubaron con una IgG anti-conejo acoplada a peroxidasa diluida 1:50 en tampón Tris-HCl 0.1M (pH 7.2), con BSA al 0.1%, durante 1 h a TA.

Después de tres lavados con tampón Tris-HCl 0.1 M (pH 7.2), se agregó a los cortes histológicos la mezcla de peróxido de hidrógeno al 3% y 3,3'-diaminobencidina para revelar la unión del suero hiperinmune anti-OvHV-2 en hepatocitos del ciervo. Finalmente, los cortes fueron contrateñidos con hematoxilina durante 1 min. La inmunorreactividad positiva al OvHV-2, se observó como una tinción insoluble color marrón en el citoplasma de los hepatocitos. Como control negativo, se utilizaron cortes de hígado de ciervo procesados como se describió anteriormente, pero se omitió el suero hiperinmune de conejo anti-OvHV-2.

5.15 Tinción de hígado con Ácido Peryódico de Schiff (PAS)

Los cortes histológicos de hígado de ciervo fueron procesados con el método de PAS. Éste es un método de histoquímica no enzimática que por hidrólisis ácida genera grupos aldehído en hexosas presentes en oligosacáridos unidos covalentemente a proteínas y lípidos. También es útil para identificar glucógeno en células animales y almidón en células vegetales. La tinción de PAS se realizó según la metodología descrita por Fu *et al.* (2017), con algunas modificaciones. Primero se desparafinaron e hidrataron los cortes histológicos, posteriormente se agregó la solución de ácido periódico 0.5% y se incubaron por 5 min, después se enjuagaron con agua destilada y se agregó el reactivo de Schiff el cual se dejó por 15 min (84). Por último, se agregó hematoxilina como contrateñido por 1 min y se observaron al microscopio. Un resultado PAS positivo se considera al observar una coloración magenta que se produce por la reversibilidad al color de la fucsina decolorada por metabisulfito de sodio (reactivo de Schiff), promovida por los aldehídos

generados. El objetivo del empleo de método de PAS en los cortes de hígado de ciervo fue conocer si los CI, previamente identificado con H&E como CI citoplásmicos eosinofílicos, eran PAS positivos, lo que indicaría la presencia de glucoproteínas probablemente virales.

5.16 Tinción de hígado con Feulgen

Algunos cortes histológicos del hígado de ciervo fueron procesados con el método de Feulgen, una histoquímica no enzimática similar al método de PAS, pero que demuestra específicamente la presencia de ADN. Ya que el OvHV-2 es un virus de ADN, utilizamos el método de Feulgen para identificar ADN dentro de los CI de los hepatocitos. Se siguió la metodología descrita por Chieco *et al.* (1999), con algunas modificaciones. El hígado se sometió a una hidrólisis acida débil con ácido clorhídrico 5N (durante 60 min) y luego se trató con reactivo de Schiff (durante 30 min). Este tipo de hidrólisis extrae las purinas a nivel de la unión desoxirribosa-purina del ADN y genera grupos aldehído en la desoxirribosa. Luego los grupos aldehído libres reaccionan con el reactivo de Schiff, como se explicó para el método de PAS (85). Un resultado positivo se revela como una coloración purpura-magenta.

5.17 Animales para desafío

Se utilizaron 5 conejos, albinos de raza Nueva Zelanda de un mes de edad, libres de patógenos. Los conejos se obtuvieron del bioterio de la CPA y se mantuvieron en las instalaciones de la UNAM, de acuerdo con el protocolo de cuidado y uso de animales de laboratorio SICUAE.DC-2020/3-5. Se extrajo sangre de una arteria aural de cada conejo antes de la inoculación y todos fueron negativos a OvHV-2 mediante la técnica de PCR. Posteriormente se les dio un periodo de aclimatación de una semana antes de iniciar la inoculación experimental con el aislamiento viral del OvHV-2.

5.18 Inoculación experimental de conejos con el virus OvHV-2

Un total de tres conejos albinos Nueva Zelanda (Grupo A), fueron inoculados vía intranasal con 1 mL de nuestro aislamiento viral del OvHV-2 obtenido a partir del lisado de capa leucocítica de los caballos (cepa Mex/Eq/19), con número de acceso al GenBank ON375578, de acuerdo con el protocolo de inoculación realizado por Geilbreath *et al.* (2008) y conteniendo una dosis mínima de $10^{5.19}$ TCID₅₀/ 1mL. Una semana después estos conejos fueron de nuevo inoculados con la misma dosis y se evaluaron los signos clínicos observados (86). Los dos conejos sanos sin inocular formaron el “Grupo B”. Todos los conejos (Grupo A y B) fueron sacrificados a los 14 días de inicio de la primera inoculación del grupo A y se tomaron las muestras *post-mortem* correspondientes.

La eutanasia se realizó mediante inyección intramuscular de ketamina y xilazina, seguido de una dosis letal intravenosa de pentobarbital. Durante la necropsia, se tomaron muestras de bazo, hígado, pulmón, riñón y tráquea. Se tomaron tres porciones de cada órgano, una porción se almacenó en formol taponado al 10% y las otras dos se congelaron a -80°C para su posterior análisis por PCR punto final anidada y para intentar el aislamiento viral. Las muestras fijadas fueron procesadas para inclusión y corte en parafina y tinción con H&E para el análisis histopatológico (83). Esta tinción tiñe los núcleos de color azul (basofilia) por la hematoxilina, y el citoplasma y material extracelular se tiñen de color rosado por la eosina (acidofilia o eosinofilia).

5.19 Microscopia Electrónica de Transmisión (MET)

La microscopia electrónica de transmisión se realizó a partir de una muestra de pulmón del conejo #3 (Grupo A), incluida en parafina. Este espécimen fue elegido para hacer la “técnica reversa” para MET ya que se había demostrado la presencia de infiltrado mononuclear intersticial, vasculitis y CI eosinofílicos citoplasmáticos en células del epitelio bronquiolar y del infiltrado mononuclear, algunas de las cuales mostraron cambios nucleares de apoptosis. Además, las muestras de este conejo fueron positivas por PCR al OvHV-2.

El procesamiento de la muestra para la MET se llevó a cabo de la siguiente manera; primero la muestra de 1 mm³ de pulmón, seleccionada de acuerdo con los hallazgos mencionados anteriormente, se desparafinó con xylol durante 5 días y se rehidrató con etanol decreciente hasta tampón de cacodilato de sodio (0.2 M/ pH7.2). Después se fijó con tetraóxido de osmio al 1%, diluido en tampón de cacodilato de sodio (0.1 M/ pH7.2) durante 2 h a 4°C. Después de 3 lavados con el tampón de cacodilato de sodio (0.2 M/ pH7.2), las muestras fueron deshidratadas con etanol creciente (40, 60, 80, 96, 100%) hasta oxido de propileno absoluto, durante 1 h en cada uno de los solventes. Posteriormente las muestras se incluyeron en resina EPON y se realizaron cortes semifinos de 1µm los cuales fueron teñidos con azul de toluidina para visualizar el área más idónea para proceder a la obtención de cortes ultrafinos de 80 nm de grosor con ultra micrótomo automático (29,87). La contrastación de los cortes en rejillas de cobre fue realizada con acetato de plomo y citrato de uranilo. La observación de los cortes se realizó con un microscopio STEM (Zeiss, Croosbean).

5.20 Reaislamiento del OvHV-2

Previamente se hicieron pools de riñón, tráquea, bazo, hígado y pulmón de los tres conejos inoculados experimentalmente (Grupo A), y se realizó una prueba de PCR para identificar que pool estaba positivo y poder realizar el reaislamiento. Sólo se utilizaron los pools de bazo y pulmón ya que son los órganos ideales para realizar el aislamiento de OvHV-2 (61).

Para realizar el reaislamiento se seleccionaron secciones de bazo y pulmón de los conejos desafiados (Grupo A). Las muestras fueron maceradas, centrifugadas a 800 × g por 10 min y filtradas (0.22 µm). Después, el filtrado de bazo y pulmón de los conejos fue utilizado para inocular células del cultivo primario de testículo de conejo, con una confluencia celular del 80%, sembradas en dos botellas de 25 cm². Las células inoculadas se propagaron en medio DMEM suplementado con suero fetal bovino al 2% e incubadas a 37°C con una atmosfera de 5% de CO₂. Cada 24 h fueron observadas utilizando un microscopio invertido marca Olympus (IX71) con objetivo 10x, con la finalidad de observar el ECP característico de los herpesvirus (61). Se realizaron tres pases

ciegos de cada muestra del filtrado (pulmón y bazo). La confirmación del reaislamiento se realizó mediante la técnica de PCR punto final anidada específico para la detección del OvHV-2.

6. RESULTADOS

6.1 Cronología del brote

El 29 de agosto de 2018 se sospechó el primer caso de SA-MCF durante la necropsia de una cabra de seis meses perteneciente al área de cuarentena que había sido recientemente donada al CEIEPAA. El animal presentaba lesiones ulcerativas en lengua y laringe; además, histopatológicamente se observó vasculitis y perivasculitis en diferentes tejidos. En septiembre, 6 cabras del área de cuarentena y 15 vacas Holstein presentaron lesiones ulcerativas en la mucosa oral. La SA-MCF se considera una enfermedad exótica de notificación obligatoria en México, por lo que el 2 de septiembre de 2018 se notificó el brote a la CPA. El 3 de septiembre, la CPA tomó por primera vez muestras de los animales con y sin signos clínicos para confirmar el diagnóstico. Una semana después, la CPA publicó los resultados y se confirmó que las cabras y las vacas lecheras eran negativas para VSV mediante ELISA y PCR. Sin embargo, el 4 de octubre de 2018 6 de las vacas Holstein dieron positivo por PCR para OvHV-2 y negativo para IBRV, PRV y BTV. Para noviembre, la enfermedad se propagó a ciervos, ganado de engorda y ovejas. En ese momento, 21 ciervos presentaron lesiones ulcerativas en la mucosa oral, y 5 muestras de sangre y 3 tejidos de estos animales fueron PCR positivas para OvHV-2 y negativas para IBRV, VSV, PRV, FMDV y CEV. Por otro lado, 8 bovinos Limousine presentaron lesiones ulcerativas y también resultaron positivos para OvHV-2 por PCR. Finalmente, 10 ovejas presentaron lesiones sugestivas de FCM y el 21 de noviembre de 2018 fueron confirmadas como positivas para OvHV-2 por PCR.

En diciembre de 2018, 27 ovejas presentaron lesiones ulcerativas leves en la cavidad oral y, a finales de este mes, el virus se propagó a los caballos; 14 de ellos presentaron lesiones ulcerativas en los labios, aunque solo 2 fueron PCR positivas para OvHV-2 y negativos para VSV por RT-PCR y aislamiento viral (Cuadro 2). La mayoría de las especies se recuperaron en un período de 20 días. Sin embargo, en los ciervos la enfermedad se prolongó unos días más debido a la gravedad de las lesiones ulcerativas en la mucosa oral, que les imposibilitaba comer. Durante el brote, todos los animales de la granja recibieron tratamiento médico a base de estimulantes inmunológicos, vitaminas A, D y E, y se alcalinizó el agua de bebida. En noviembre de 2019 y 2020 hubo dos nuevos brotes. Los animales afectados presentaron signos clínicos similares a los

observados en 2018. Sin embargo, en estos dos nuevos brotes, la especie más afectada fueron los caballos debido a la gravedad de las úlceras. Además, en 2020, las cabras parturientas también presentaron lesiones ulcerativas en la mucosa oral.

6.2 Evaluación *post-mortem*

Los animales afectados durante el brote de SA-MCF en CEIEPAA presentaron úlceras mucogingivales en vestíbulo bucal y lengua, hipersalivación, menor consumo de alimento, pérdida de peso y opacidad corneal (Figura 7). Los dos ciervos (#172 y #174) presentaron una marcada linfadenomegalia retromandibular, lengua congestionada y edematosa con úlceras en la parte dorsal y en la base. Además, se observaron úlceras focales en los pilares ruminales, cubiertas por una pseudomembrana fibrinosa. El hígado estaba ligeramente agrandado y congestionado. Las principales lesiones microscópicas observadas fueron vasculitis y perivasculitis con necrosis fibrinosa en vasos sanguíneos de lengua y rumen con erosión epitelial, edema y neovascularización de la córnea. Los ganglios linfáticos retromandibulares mostraron hiperplasia linfoide. El hígado mostró necrosis hepática multifocal y CI eosinofílica citoplasmática (Figura 8). No se observaron lesiones *post-mortem* en riñón o pulmón.



Figura 7. Lesiones ulcerativas en la mucosa oral de animales afectados con SA-FCM. A) Caballo con úlcera en la punta de la lengua y B) Caballo con úlcera en belfo superior C) Ciervo con úlceras y sangrado en encías y D) Vaca lechera con úlcera en la comisura superior (flechas blancas).

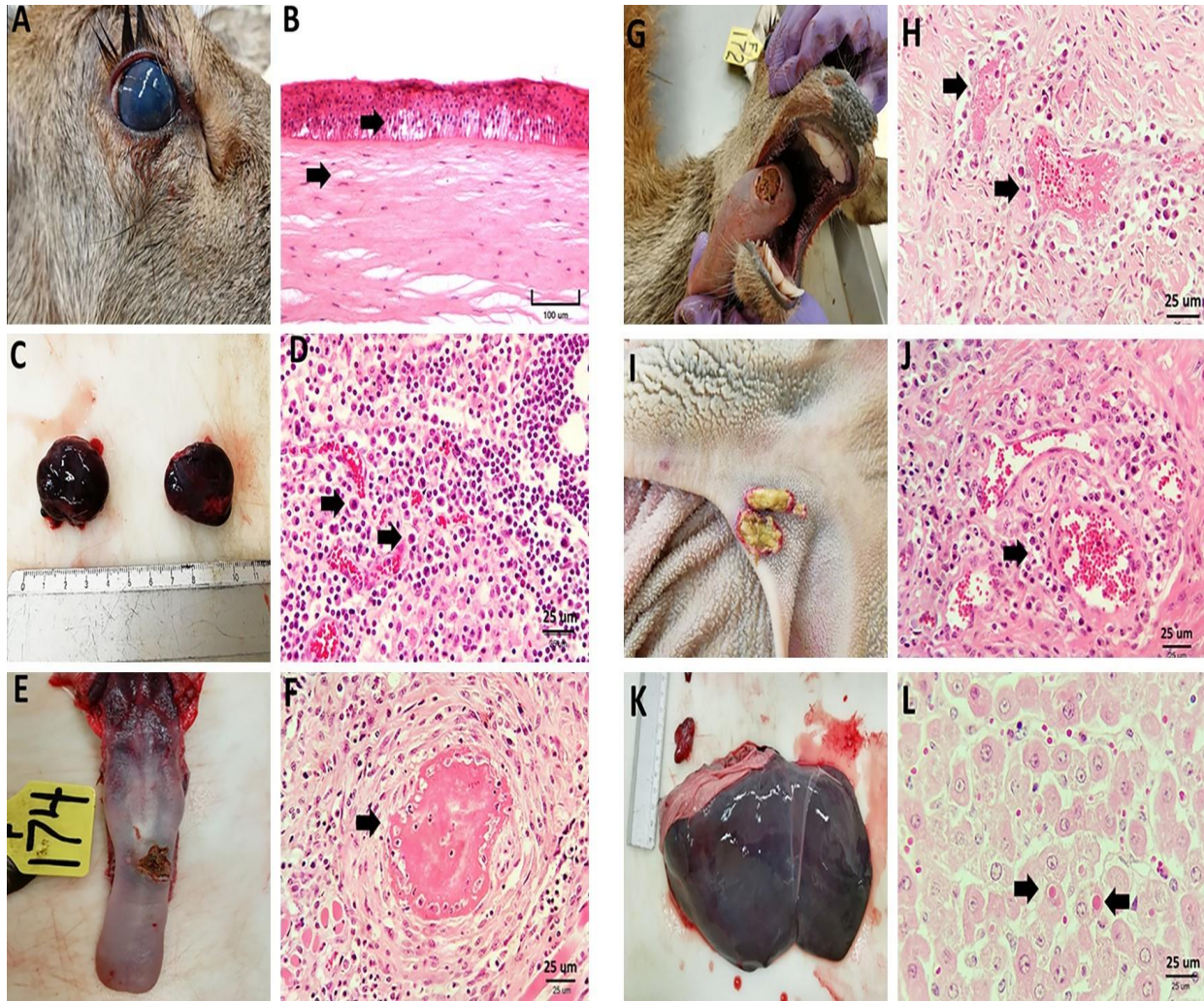


Figura 8. Lesiones *post-mortem* observadas en ciervos afectados durante el brote SA-MCF en Querétaro, México. A- Opacidad corneal, B- Córnea con edema y desprendimiento del epitelio corneal, C- Linfonodos retromandibulares agrandados, congestionados y edematosos, D- Región parafolicular con numerosos linfocitos, células plasmáticas y linfoblastos, E- Lengua con pérdida de la continuidad del epitelio (úlceras) en la porción dorsal, F- Lengua con vasculitis y trombo de fibrina que ocluye totalmente la luz y necrosis fibrinoide, G- Lengua con úlcera en la porción dorsal de la lengua, con incrustación de alimentos, H- Lengua con trombosis e infiltrado perivascular linfoplasmocitario y linfoblástico, I- Rumen con úlceras focales en los pilares recubiertas por una pseudomembrana, J- Rumen con inflamación

perivasculares compuestas por linfocitos, células plasmáticas y linfoblastos, K- Hígado congestionado y agrandado (hepatomegalia), L- Hígado con áreas de necrosis y CI eosinofílicos citoplásmicos.

6.3 Muestras de leucocitos

Se analizaron un total de 213 muestras de leucocitos provenientes de los animales afectados durante el brote de SA-MCF, mediante PCR punto final anidada específica para OvHV-2. De las muestras analizadas, 86 fueron positivas (40.38%) y 127 negativas (59.62%). Las cabras y ovejas presentaron un mayor número de muestras de leucocitos positivos para OvHV-2, mientras que el ganado lechero y los caballos presentaron un menor número de muestras positivas por PCR (Cuadro 2).

Cuadro 2. Especies afectadas, diagnósticos previos y porcentaje de animales positivos para OvHV-2.

Especies afectadas	*Diagnósticos previos/Resultados (PCR)	Población total/enfermos/muertos	**Número total de animales muestreados por la CPA, PCR positivas para OvHV-2 y porcentaje de positivos	***Animales muestreados por la UNAM, PCR positivas para OvHV-2 y porcentaje de positivos
Caballos	VSV/ (-)	39/14/0	35 [2] (5.71%)	39 [9] (23%)
Ganado de engorda	IBRV, VSV, PRV, FMDV, BTV/ (-)	109/8/0	38 [8] (21.05%)	30 [11] (36%)
Ganado lechero	IBRV, VSV, PRV, FMDV, BTV/ (-)	169/15/0	51 [6] (11.76%)	32 [5] (15%)
Cabras Residentes	IBRV, VSV, PRV, FMDV, BTV/ (-)	271/0/0	30 [7] (23.33%)	32 [19] (59%)
Cabras en área de cuarentena	IBRV, VSV, PRV, FMDV, BTV, CEV/ (-)	97/7/0	98 [35] (35.71%)	32 [8] (25%)
Ovejas	IBRV, VSV, PRV, FMDV, BTV, CEV/ (-)	246/37/0	67 [22] (32.83%)	30 [26] (86%)
Ciervos	IBRV, VSV, PRV, FMDV, BTV, CEV/ (-)	103/21/14	17 [8] (47.05%)	18 [8] (44%)
Total		1034/65/14	336[88] (26.19%)	213[86] (40.3%)

Resultados de la PCR punto final anidada para la detección del virus OvHV-2 en muestras de capa leucocítica de las diferentes especies afectadas por SA-MCF en CEIEPAA.

[] = positivo a OvHV-2 por PCR, (%) = porcentaje de animales positivos para OvHV-2.

*Virus de la rinotraqueítis infecciosa bovina (IBRV), virus de la estomatitis vesicular serotipos Indiana y New Jersey (VSV), parapoxvirus (PRV), virus de la fiebre aftosa (FMDV), virus de la lengua azul (BTV), virus del ectima contagioso (CEV).

** Número total de animales muestreados por CPA de agosto a diciembre de 2018

*** Número total de animales muestreados por la UNAM durante enero de 2019

6.4 Aislamiento del virus OvHV-2 en cultivos primarios de testículo de conejo

El ECP causado por el lisado de las capas leucocíticas, se caracterizó por cambios en la morfología del cultivo primario, generó pequeños grupos de células citomegálicas refráctiles entre las 48 y 72 h post-infección y fue similar con los seis pools de lisado de capa leucocítica de las diferentes especies (Figura 9).

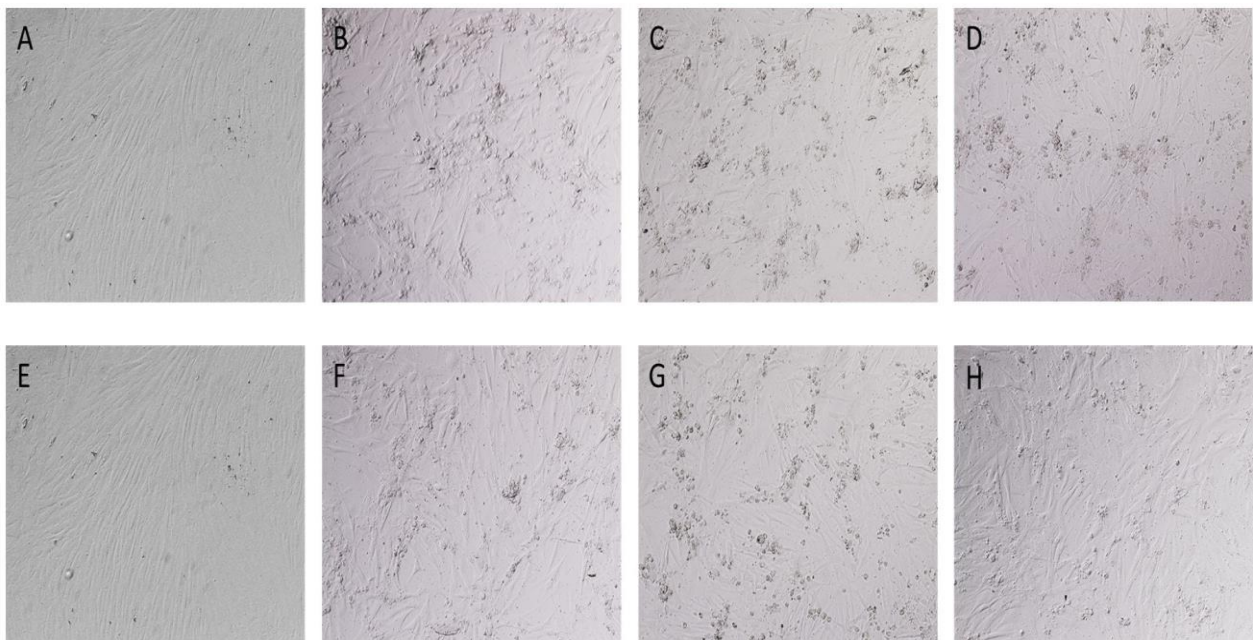


Figura 9. ECP en cultivos primarios de testículo de conejo inoculados con el lisado de capa leucocítica de las diferentes especies animales afectadas durante el brote de SA-MCF a las 72 h post-infección.

(A) Control negativo, (B) cuarto pase ciego de los caballos, (C) cuarto pase ciego de las ovejas, (D) cuarto

pase ciego de las cabras, (E) control negativo, (F) cuarto pase ciego de los ciervos, (G) cuarto pase ciego del ganado lechero, (H) cuarto pase ciego del ganado de engorda. Ampliación: 100X.

Los lisados de las capas leucocíticas de las ovejas y cabras indujeron un marcado ECP, con un 50 % de destrucción de la monocapa desde el primer pase hasta las 72 h y un 100% entre las 96 y las 120 h post-infección. De manera similar, el porcentaje de ECP aumentó desde el segundo pase en adelante (Cuadro 3). Por el contrario, los cultivos primarios inoculados con los pools de lisado de capa leucocítica de los caballos, el ganado lechero, el ganado de engorda y ciervos mostraron poco ECP, que oscilaba entre el 20 y el 30% en el primer y segundo pase, respectivamente. En cambio, en el tercer y cuarto pase, la destrucción de la monocapa aumentó al 50% y 90% a las 72 h post-infección (Cuadro 3).

Cuadro 3. Efecto citopático en cultivos primarios de testículo de conejo.

Especies Afectadas	ECP* 1° pase	ECP* 2° pase	ECP* 3° pase	ECP* 4° pase
Caballos	20-30%	20-30%	50%	90-100%
Ganado de engorda	20-30%	20-30%	20-30%	90-100%
Ganado lechero	20-30%	20-30%	90-100%	90-100%
Cabras	50%	90-100%	90-100%	90-100%
Ovejas	50%	20-30%	20-30%	90-100%
Ciervos	20-30%	20-30%	50%	90-100%

Porcentaje de efecto citopático en cultivos primarios de testículo de conejo.

ECP*= Efecto citopático (los porcentajes reflejan el grado de destrucción de las monocapas celulares).

En los cultivos primarios, los títulos virales obtenidos de los sobrenadantes libres de células del cuarto pase ciego a las 72 h post-infección fueron los siguientes: caballos $10^{4.19}$ TCID₅₀/mL, cabras $10^{3.8}$ TCID₅₀/mL, ciervos $10^{3.3}$ TCID₅₀/mL, ganado lechero $10^{3.5}$ TCID₅₀/mL, ganado de engorda $10_{2.8}$ TCID₅₀/mL y ovejas $10^{3.5}$ TCID₅₀/mL.

Los títulos virales de los sobrenadantes libres de células de los pases 3 a 14 del lisado de capa leucocítica de los caballos, se determinaron a las 72 h post-infección (Figura 10). Determinamos que el título viral del tercer pase fue de $10^{3.33}$ TCID₅₀/mL, mientras que los títulos virales de los pases 4, 5, 6, 7, 8, 9, 10 y 11 oscilaron entre 10^4 TCID₅₀/mL y $10^{4.96}$ TCID₅₀/mL, que eran muy similares. Sin embargo, se observó un aumento en los títulos virales de los pases 12, 13 y 14 con títulos de $10^{5.52}$ TCID₅₀/mL, $10^{6.46}$ TCID₅₀/mL y $10^{6.67}$ TCID₅₀/mL, respectivamente.

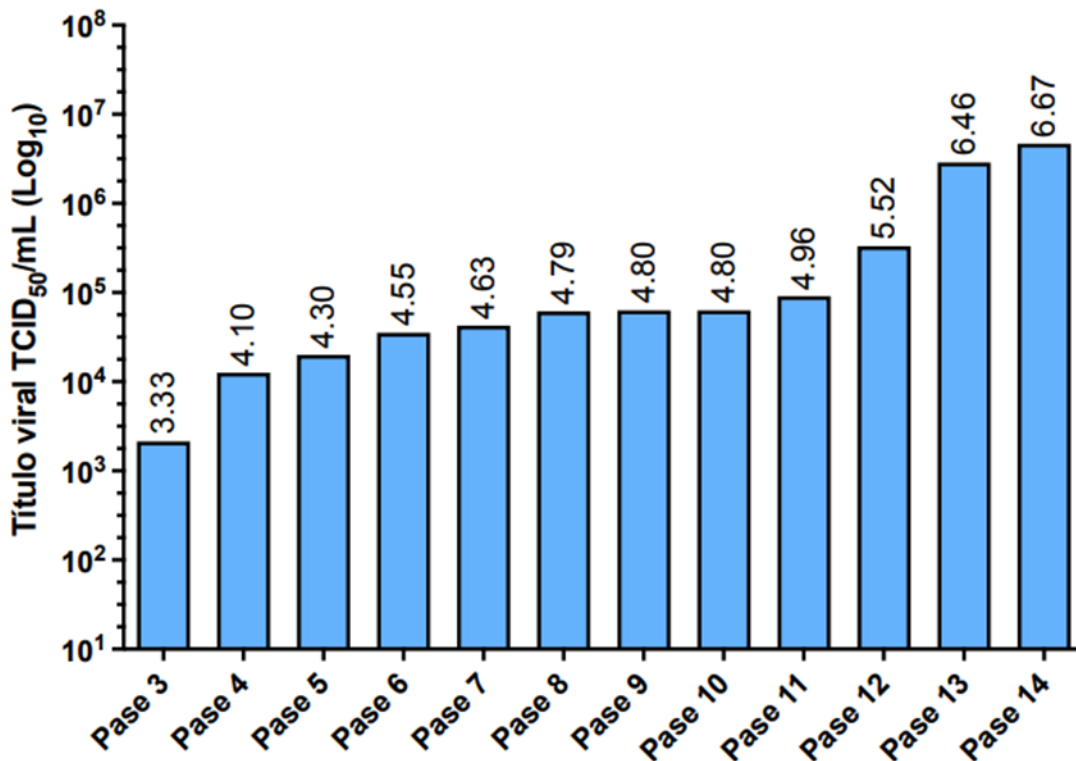


Figura 10. Titulación viral de los sobrenadantes de los pases 3 a 14 de los caballos. El pase continuo del lisado de la capa leucocítica de los caballos en cultivos primarios de testículos de conejo condujo a un aumento en el título viral.

Se observaron CI acidófilos intranucleares en cultivos primarios de testículo de conejo inoculados con los sobrenadantes libres de células de los cuatro pases ciegos a las 24 h post-infección. Sin embargo, en los pocillos que contenían las células inoculadas con sobrenadantes

libres de células de los cuartos pases ciegos de cabras y caballos, se observaron más de cinco CI (Figura 11). Por el contrario, en pocillos inoculados con los sobrenadantes libres de células del cuarto pase ciegos del ganado lechero, ganado de engorda, ovejas y ciervos, se observaron menos de tres CI en todo el pocillo.

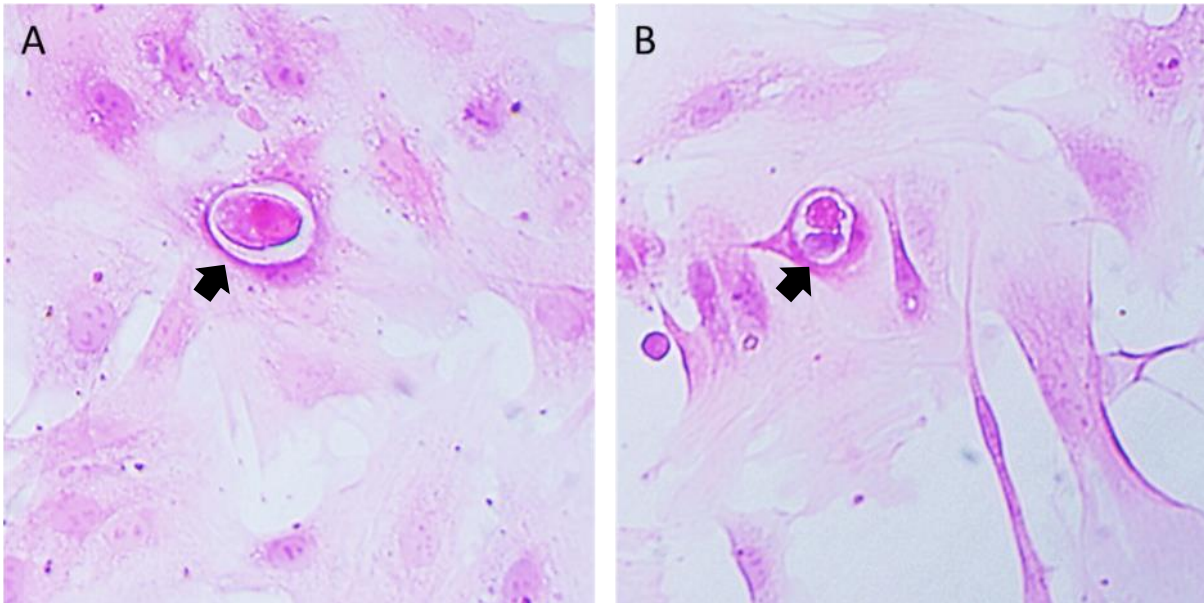


Figura 11. CI acidófilos intranucleares a las 24 h post-infección. (A) Cuarto pase ciego de los caballos, (B) Cuarto pase ciego de las cabras. Las flechas negras indican los CI intranucleares. Tinción H&E. Aumento 200X.

6.5 PCR punto final anidada para la detección de OvHV-2

El ADN se extrajo de los sobrenadantes libres de células de los cuatro pases ciegos obtenidos de la inoculación de los cultivos primarios con los pools de lisado de las capas leucocíticas de las diferentes especies animales afectadas durante el brote de SA-MCF. Los sobrenadantes libres de células de los caballos, cabras y ganado lechero fueron positivos por PCR para OvHV-2 desde el primer pase. Los sobrenadantes libres de células de las ovejas y ciervos fueron positivos hasta el segundo pase. Sin embargo, el sobrenadante libre de células del ganado de engorda fue positivo por PCR hasta el tercer y cuarto pase (Figura 12).

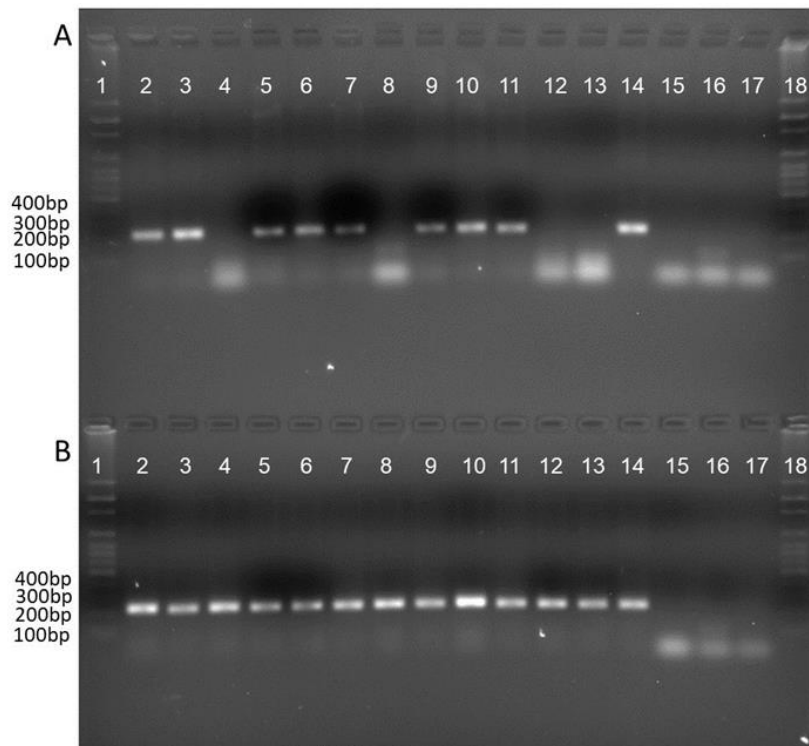


Figura 12. Gel de agarosa (1.5 %) corrido en buffer TAE 1X. (A) PCR anidada del primer y segundo pase ciego del lisado de capa leucocítica en cultivos primarios de testículo de conejo. (1) Marcador de peso molecular 1 kb, (2) primer pase ciego de los caballos, (3) segundo pase ciego de los caballos, (4) primer pase ciego de las ovejas, (5) segundo pase ciego de las ovejas, (6) primer pase ciego de las cabras, (7) segundo pase ciego de las cabras, (8) primer pase ciego de los ciervos, (9) segundo pase ciego de los ciervos, (10) primer pase ciego del ganado lechero, (11) segundo pase ciego del ganado lechero, (12) primer pase ciego del ganado de engorda, (13) segundo pase ciego del ganado de engorda, (14) control positivo, (15) control negativo de amplificación (CNA), (16) control negativo de extracción (CNE), (17) cultivos celulares primarios no inoculados (CCPN), (18) marcador de peso molecular 1 kb. (B) PCR anidada de los pases tres y cuatro del lisado de capa leucocítica en cultivos primarios de testículos de conejo. (1) Marcador de peso molecular de 100 pb, (2) tercer pase ciego de los caballos, (3) cuarto pase ciego de los caballos, (4) tercer pase ciego de las ovejas, (5) cuarto pase ciego de las ovejas, (6) tercer pase ciego de las cabras, (7) cuarto pase ciego de las cabras, (8) tercer pase ciego de los ciervos, (9) cuarto pase ciego de los ciervos, (10) tercer pase ciego del ganado lechero, (11) cuarto pase ciego del ganado lechero, (12) tercer pase ciego del ganado de engorda, (13) cuarto pase ciego del ganado de engorda, (14) control positivo, (15) control negativo de amplificación (CNA), (16) control negativo de extracción (CNE), (17) cultivos celulares primarios no inoculados (CCPN), (18) marcador de peso molecular 1 kb.

6.6 Cinética de replicación viral

El estudio de la cinética de replicación viral mostró que el lisado de la capa leucocítica de los caballos se replicó rápidamente y se pudieron observar sincitios a partir de las 24 h post-infección en el quinto pase y hasta las 72 h en el pase 14 (Figura 13A). Los pases 4 y 5 lograron títulos pico similares de $10^{4.1}$ TCID₅₀/mL y $10^{4.3}$ TCID₅₀/mL a las 72 h post-infección, respectivamente. Sin embargo, el pase 14 logró títulos más altos de $10^{6.6}$ TCID₅₀/mL a las 72 h post-infección. Además, a las 120 h post-infección, los títulos virales disminuyeron (Figura 13).

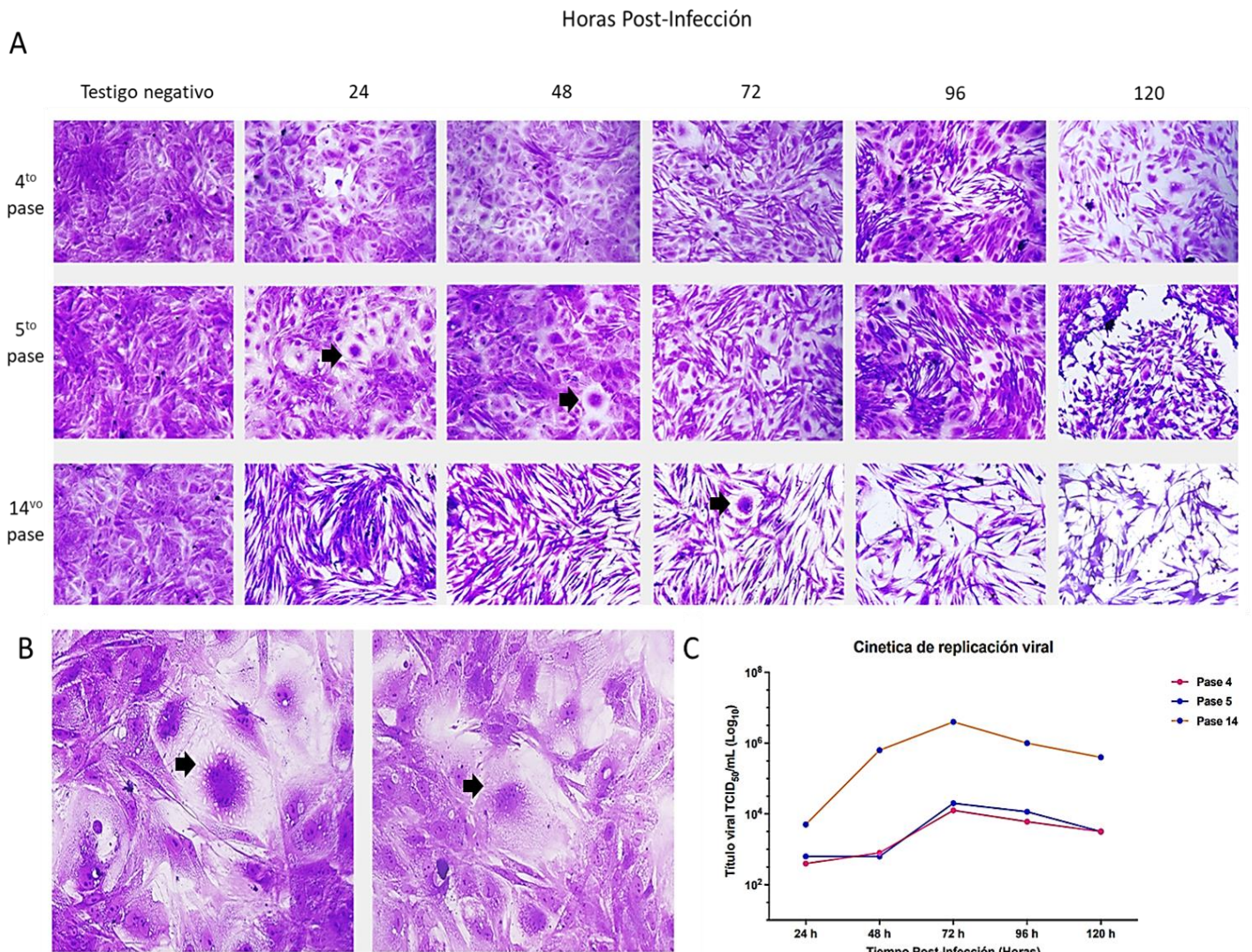


Figura 13. Cinética de replicación de los sobrenadantes libres de células de los pases 4, 5 y 14 del lisado de capa leucocítica de los caballos. (A) Células inoculadas con sobrenadante del cuarto pase ciego, panel superior; sobrenadante del quinto pase, panel central; y sobrenadante del pase 14, panel inferior. Amplificación: 100X. (B) Se observaron sincitios en el quinto pase a las 24 h y 48 h post-infección (flechas negras). (C) Gráfico de títulos virales a las 24, 48, 72, 96 y 120 h post-infección correspondientes a los pases 4, 5 y 14 del lisado de capa leucocítica de los caballos, donde se observa un pico máximo de replicación a las 72 h post-infección.

6.7 Análisis Filogenético

El alineamiento de las secuencias parciales de 422 pb del gen *ORF75* indicó que las seis secuencias parciales de los sobrenadantes libres de células del cuarto pase de las diferentes especies afectadas por SA-MCF y el control positivo de OvHV-2 compartían 98%- 99% de identidad de nucleótidos con otras secuencias *ORF75* parciales obtenidas de la base de datos GenBank. Con respecto a la estructura de la topología inferida, el análisis indicó que nuestras siete secuencias parciales presentan alta homología con *Macavirus*, reportados en diferentes partes del mundo y separados del clado de los *Rhadinovirus* (human gammaherpesvirus 8) y de los *lymphocryptovirus* (herpesvirus gamma humano 4), que se encuentra en diferentes clados (Figura 14).

Por otro lado, las secuencias parciales de *ORF75* de los seis sobrenadantes libres de células del cuarto pase en comparación con la secuencia BJ1035, presentaron una sustitución no sinónima en la posición 1213, cambiando el aminoácido (AA) de lisina (K) a treonina (T) (Cuadro 4); sin embargo, la secuencia parcial de las ovejas presentó una segunda mutación en la posición 1314, cambiando el AA cisteína (C) por glicina (G) (Cuadro 4), por lo que se clasificaron como *ORF75*0201* debido al número de sustituciones según a la clasificación de Russell *et al.* (2014).

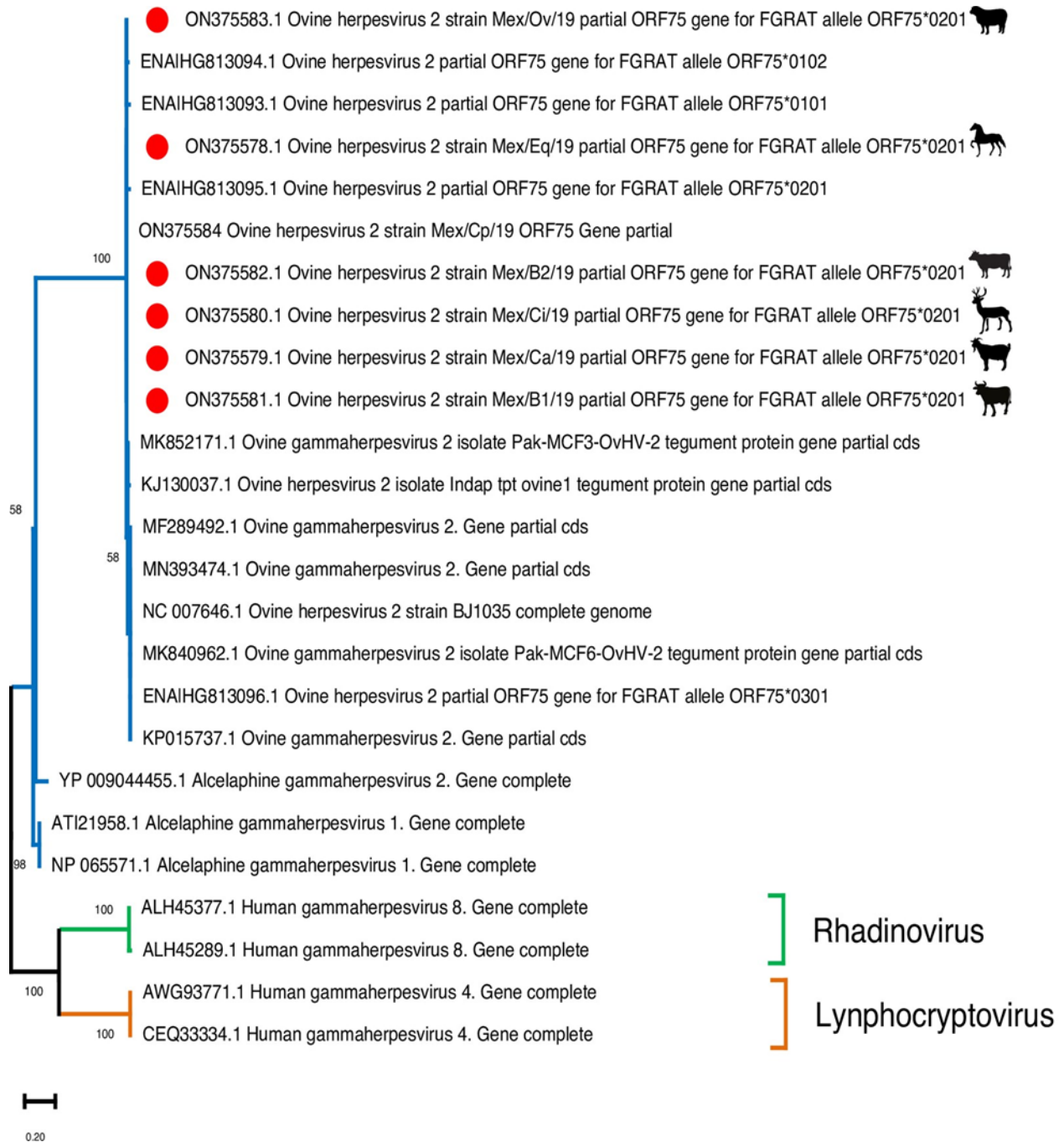


Figura 14. Análisis filogenético de las secuencias parciales del gen *ORF75*. El árbol está a escala y la barra indica el número de sustituciones por sitio. Los aislamientos mexicanos están marcados con un círculo rojo.

Cuadro 4. Diversidad genética de secuencias *ORF75* mexicanas en comparación con el gen de referencia BJ1035.

GEN <i>ORF75</i>	NT	NT	NT	AA	NT	NT	NT	AA
	[3637]	[3637]	[3637]	[1213]	[3940]	[3941]	[3942]	[1314]
*REF NC_007646.1	A	A	A	LYS	T	G	C	CYS
BJ1035								
ON375578.1	A	C	G	THR	-	-	-	NA
(CABALLOS)								
ON375579.1	A	C	G	THR	-	-	-	NA
(CABRAS)								
ON375580.1	A	C	G	THR	-	-	-	NA
(CIERVOS)								
ON375581.1	A	C	G	THR	-	-	-	NA
(GANADO LECHERO)								
ON375582.1	A	C	G	THR	-	-	-	NA
(GANADO DE ENGORDA)								
ON375583.1	A	C	G	THR	G	G	C	GLY
(OVEJAS)								

*Ref = referencia, () = especie de origen, NT = nucleótido, AA = aminoácido, [] = posición, NA = no aplica.

6.8 Inmunocitoquímica (ICC) e inmunofluorescencia (IF) indirecta

Se observó inmunorreactividad citoplasmática positiva al suero hiperinmune de conejo anti-OvHV-2 en todos los pocillos inoculados con los sobrenadantes libres de células de los cuatro pases ciegos de los caballos, cabras, ganado lechero, ganado de engorda, ovejas y ciervos. Sin embargo, con el tercer pase ciego de los caballos y cabras, se observó una mayor proporción de células (40% y 50% de la monocapa) con inmunorreactividad positiva al suero de conejo (Figura 15). En contraste, los pozos inoculados con el tercer y cuarto pase del ganado de engorda, ganado

lechero, ovejas y ciervos presentaron menor proporción de células (10% de la monocapa), con inmunorreactividad citoplasmática (Figura 15). Se observó una emisión verde manzana a 520 nm por IF y un precipitado marrón por ICC.

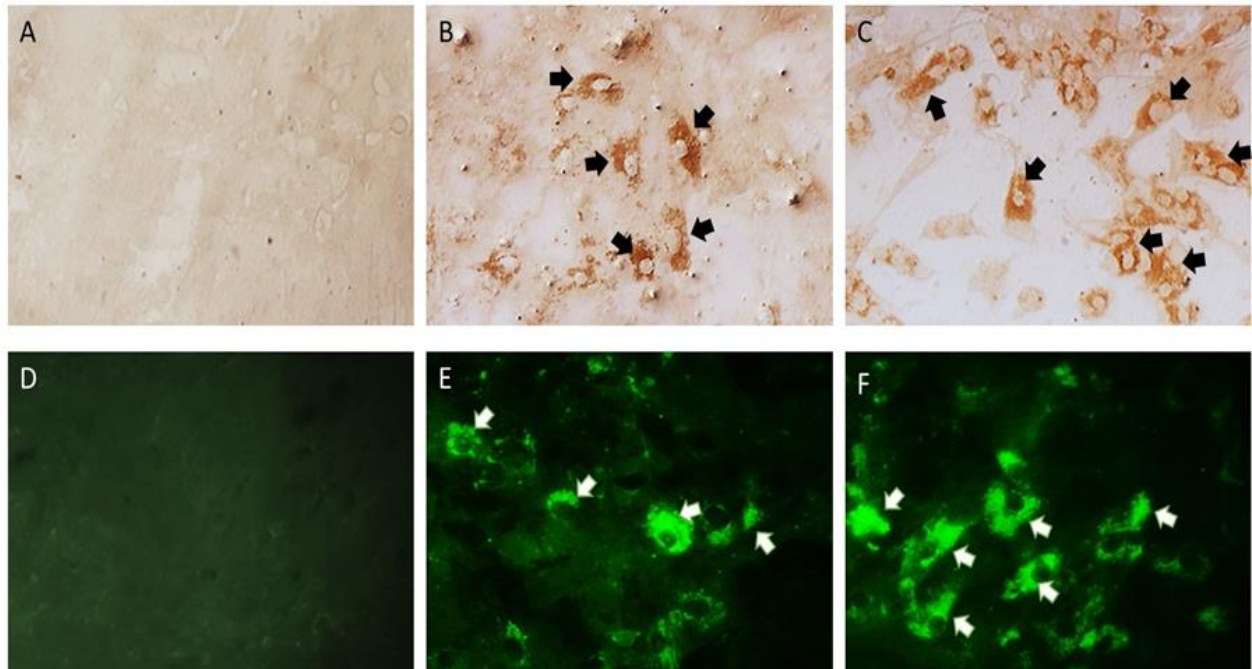


Figura 15. Inmunorreactividad citoplasmática con las técnicas de ICC e IF en cultivos celulares primarios de testículo de conejo. Inmunorreactividad citoplasmática con las técnicas ICC e IF en cultivos celulares primarios de testículo de conejo. (A) control negativo ICC, (B) ICC del tercer pase de los caballos, (C) ICC del tercer pase de las cabras, (D) control negativo IF, (E) IF del tercer pase de los caballos, (F) IF del tercer pase de las cabras. Las flechas indican la inmunorreactividad citoplasmática que aparece como un color marrón insoluble en ICC y un color verde manzana en IF. Aumento: 200X.

6.9 Inmunohistoquímica enzimática de hígado

Los CI yuxtaneucleares de los hepatocitos del ciervo afectado fueron inmunorreactivos al suero hiperinmune de conejo anti-OvHV-2. Además, también se observó una ligera inmunorreactividad intranuclear en los hepatocitos (Figura 16).

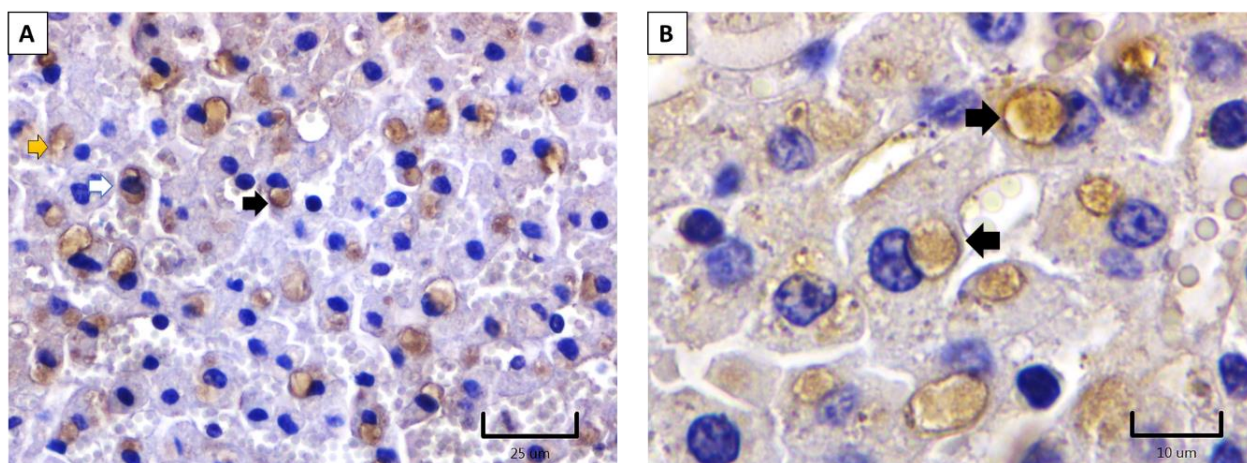


Figura 16. Inmunohistoquímica de hígado de ciervo. (A) y (B) Inmunorreactividad a antígenos OvHV-2 con suero hiperinmune de conejo en CI citoplasmáticos (flechas negras), dentro del citoplasma (flechas amarillas) y en el núcleo de los hepatocitos (flechas blancas).

6.10 Identificación del contenido de los CI en hígado

Los CI yuxtaneucleares, que fueron eosinofílicos y OvHV-2-positivos, también fueron PAS-positivos y Feulgen-positivos. El interior de los CI mostró una tinción PAS positiva difusa, mientras que la tinción con Feulgen fue observada como gránulos aislados dentro del CI (de 1 a 6 gránulos). Otras estructuras citoplasmáticas de forma alargada también fueron Feulgen-positivos, que fueron identificadas como mitocondrias, sin descartar de que algunas en forma de gránulos sean partículas virales (Figura 17).

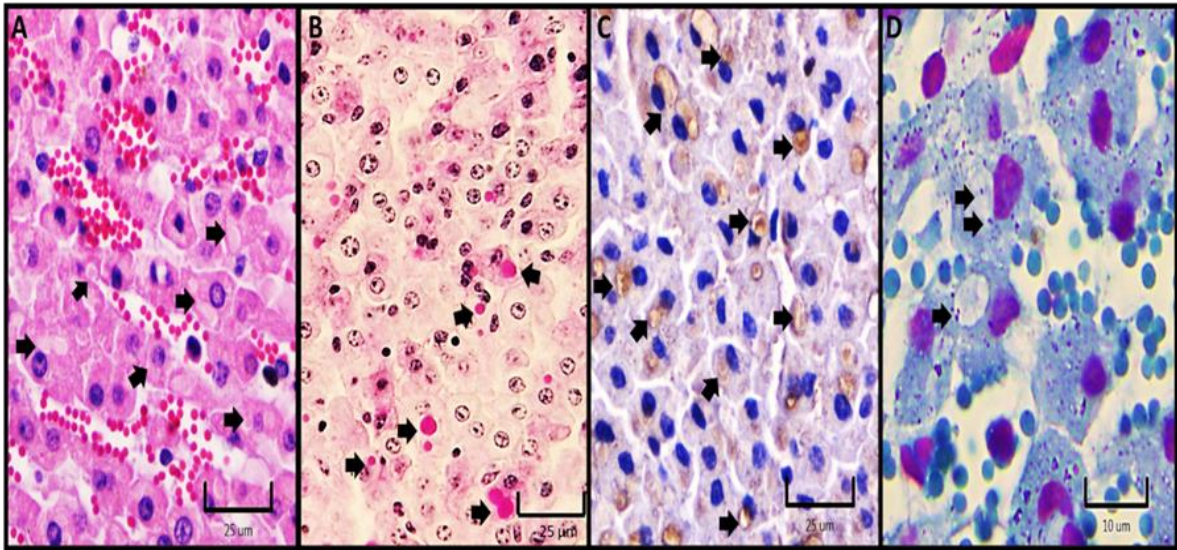


Figura 17. Características tintoriales y morfológicas de los cuerpos de inclusión citoplasmáticos (CI) yuxtannucleares en hepatocitos de un ciervo que murió por SA-MCF secundaria a infección natural por OvHV-2. A) CI eosinofílicos, B) CI PAS positivos, C) CI inmunorreactivos al suero anti-OvHV-2, D) CI con partículas o gránulos Feulgen positivos.

6.11 Signos clínicos en conejos inoculados con el virus OvHV-2

Los tres conejos (Grupo A) inoculados con el aislamiento del OvHV-2 cepa Mex/Eq/19, presentaron disminución en el consumo de alimento posterior a la segunda inoculación y dos días después se recuperaron. Además, uno de los animales presentó adinamia y se aisló del grupo. Ningún otro signo clínico fue observado. Los conejos del grupo B (conejos sanos), no presentaron signos clínicos y sus órganos fueron negativos al OvHV-2 mediante la técnica de PCR punto final anidada.

6.12 Lesiones macroscópicas e histológicas en conejos

Las principales lesiones macroscópicas en los conejos inoculados experimentalmente (Grupo A), fueron esplenomegalia y riñones ligeramente pálidos. Los conejos sanos sin inocular (Grupo B), no presentaron ninguna lesión. Las alteraciones histopatológicas del grupo A, fueron predominantemente en pulmón y bazo. Las lesiones pulmonares fueron más graves en el conejo #2 (Grupo A), donde se observó hiperplasia linfoide intrapulmonar del tejido linfoide asociado a bronquios y bronquiolos (BALT), obstrucción pulmonar, bronquiolos con desprendimiento de células de Clara, cuerpos de inclusión en macrófagos alveolares y zonas de enfisema pulmonar e infiltrado mononuclear en la pared alveolar. Además, el conejo #1 presentó vasculitis, hemorragia alveolar y congestión vascular.

Con respecto al riñón, los conejos #1 y #3 no presentaron lesiones, a diferencia del conejo #2 que presentó lesiones moderadas, entre ellas dilatación y detritos celulares en túbulos colectores de la corteza y médula, además de infiltrado linfoide con células plasmáticas perivascular y peritubular en región yuxtacortical y médula exterior.

Las lesiones histológicas en hígado fueron muy leves, el conejo #1 presentó ligera congestión vascular, esteatosis microvesicular y focos de necrosis con infiltrado mononuclear y eosinofilia. El conejo #2 presentó lesiones moderadas, una ligera congestión vascular e infiltrado mononuclear difuso periportal y focos de infiltrado mononuclear en lobulillos y de distribución difusa. El conejo #3 no presentó ninguna lesión hepática. El bazo de los tres conejos pertenecientes al grupo A presentaron hiperplasia linfoide muy leve en el conejo #1 y #3, aunque en el conejo #2 fue de tal magnitud que no se podía distinguir la pulpa roja. La tráquea de los tres conejos no presentó ninguna lesión. Los dos conejos control negativos pertenecientes al grupo “B”, no presentaron ninguna lesión histológica (Figura 18).

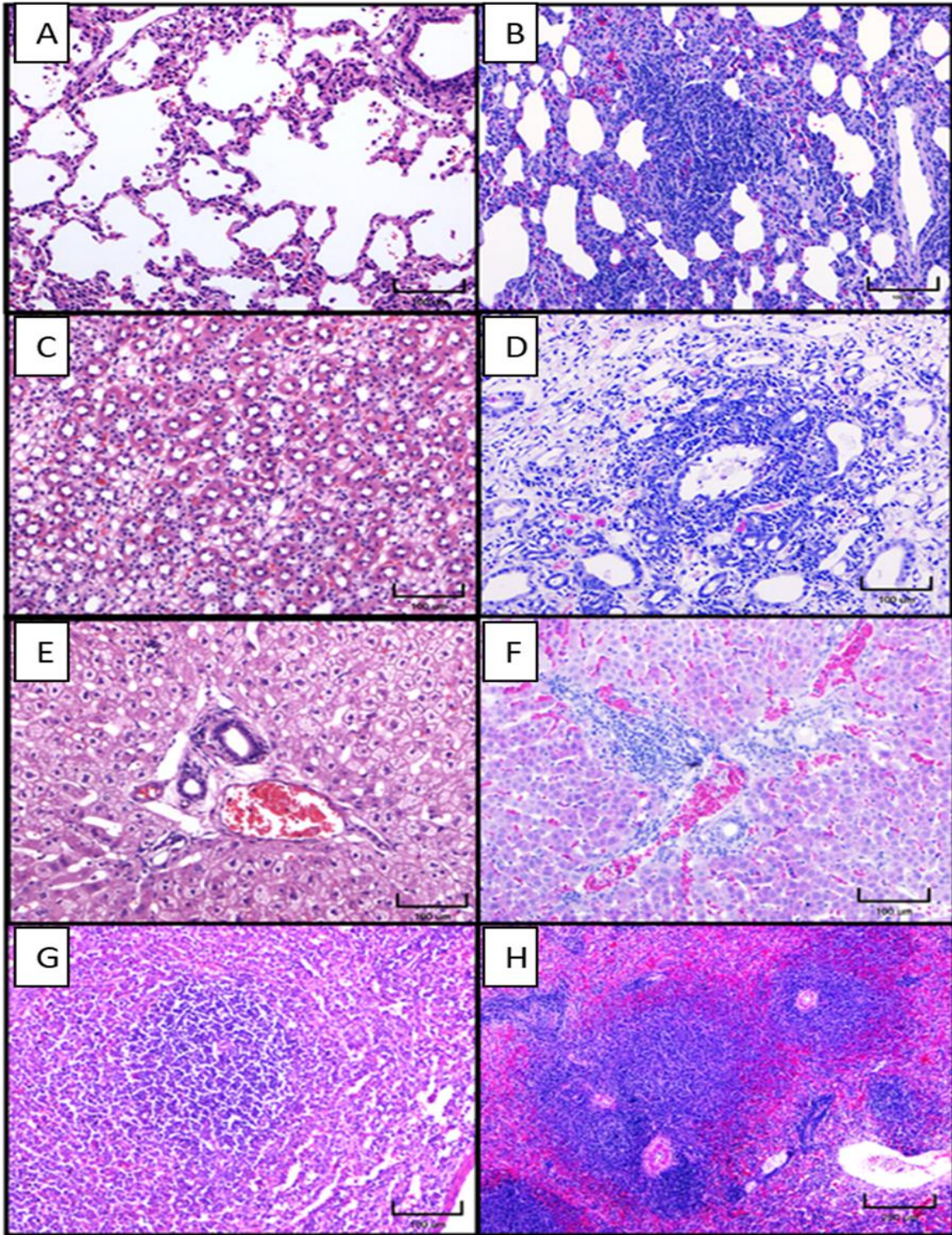


Figura 18. Lesiones microscópicas de los conejos desafiados con el aislamiento de los caballos. A) Pulmón de conejo sano, B) Pulmón con infiltrado mononuclear en pared alveolar; C) Riñón de conejo sano,

D) Riñón con infiltrado linfoide peritubular; E) Hígado de conejo sano, F) Hígado con infiltrado mononuclear difuso periportal; G) Bazo de conejo sano, H) Bazo con hiperplasia linfoide.

6.13 Microscopia electrónica de transmisión (MET)

La MET demostró la presencia de estructuras similares a cápsides virales rodeadas de heterocromatina en regiones centrales y periféricas de núcleos de apariencia normal y apoptótica. Algunas cápsides mostraron una localización extranuclear e intranuclear en la misma célula. También fue posible observar estructuras similares a cápsides virales yuxtannucleares junto a cuerpos densos. Ocasionalmente se observaron en citoplasma estructuras con morfología similar a un herpesvirus de casi 150nm de diámetro (Figuras 18, 19, 20 y 21). Las células que presentaron estas estructuras virales estuvieron localizadas en el intersticio pulmonar, algunas parecidas a fibroblastos y otras a células mononucleares.

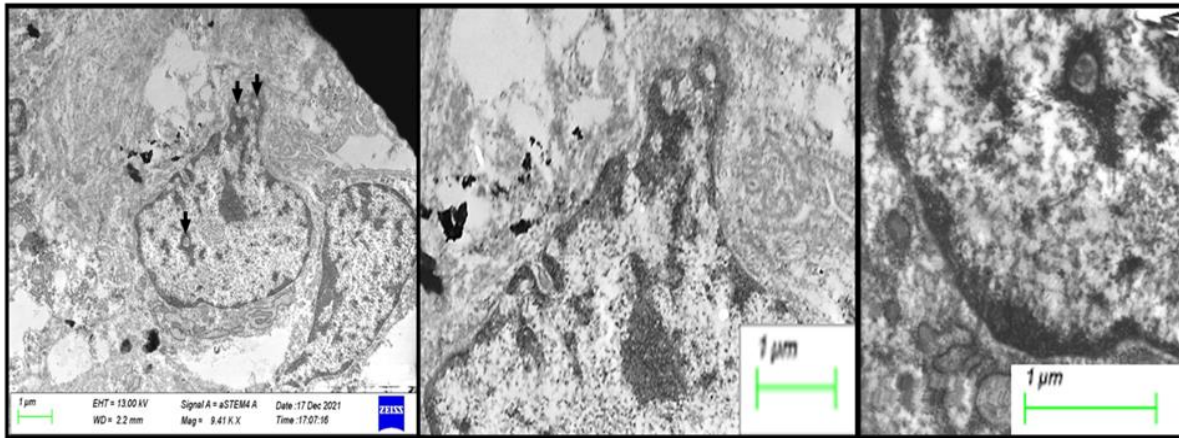


Figura 19. Micrografías electrónicas de pulmón de conejo inoculado por vía intranasal con el aislamiento viral del OvHV-2 a partir de leucocitos de caballo. Cápsides virales en la periferia del núcleo y una rodeada de heterocromatina (Flechas negras). Técnica reversa para MET. 9 410X (izquierda). Al centro y a la derecha amplificación electrónica de las cápsides señaladas con flechas.

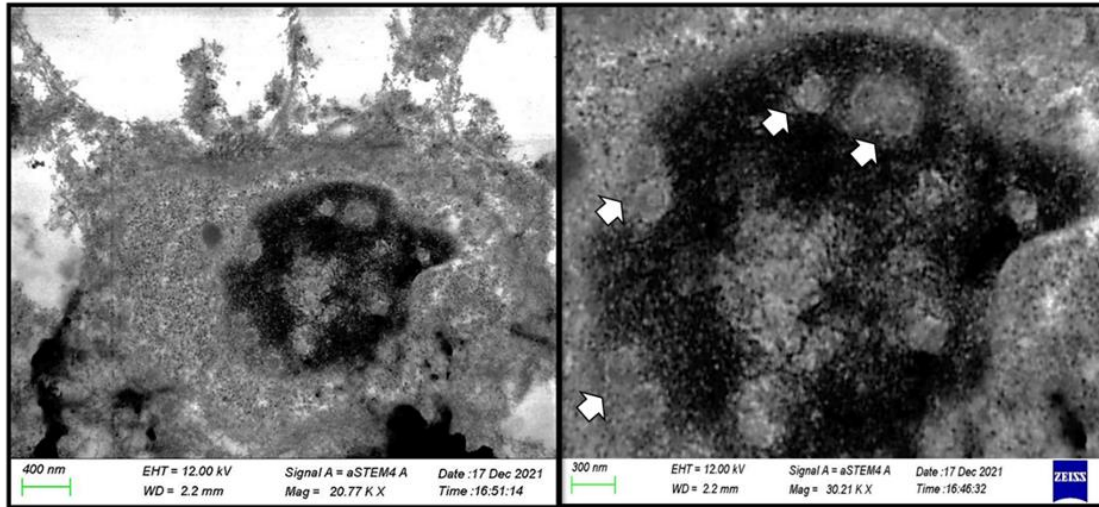


Figura 20. Micrografías electrónicas de pulmón de conejo inoculado por vía intranasal con el aislamiento viral del OvHV-2 a partir de leucocitos de caballo. Estructuras similares a cápsides virales localizadas entre la heterocromatina condensada en un núcleo con cambios apoptóticos. Técnica reversa para MET. 20 770X (izquierda), 30 210X (derecha).

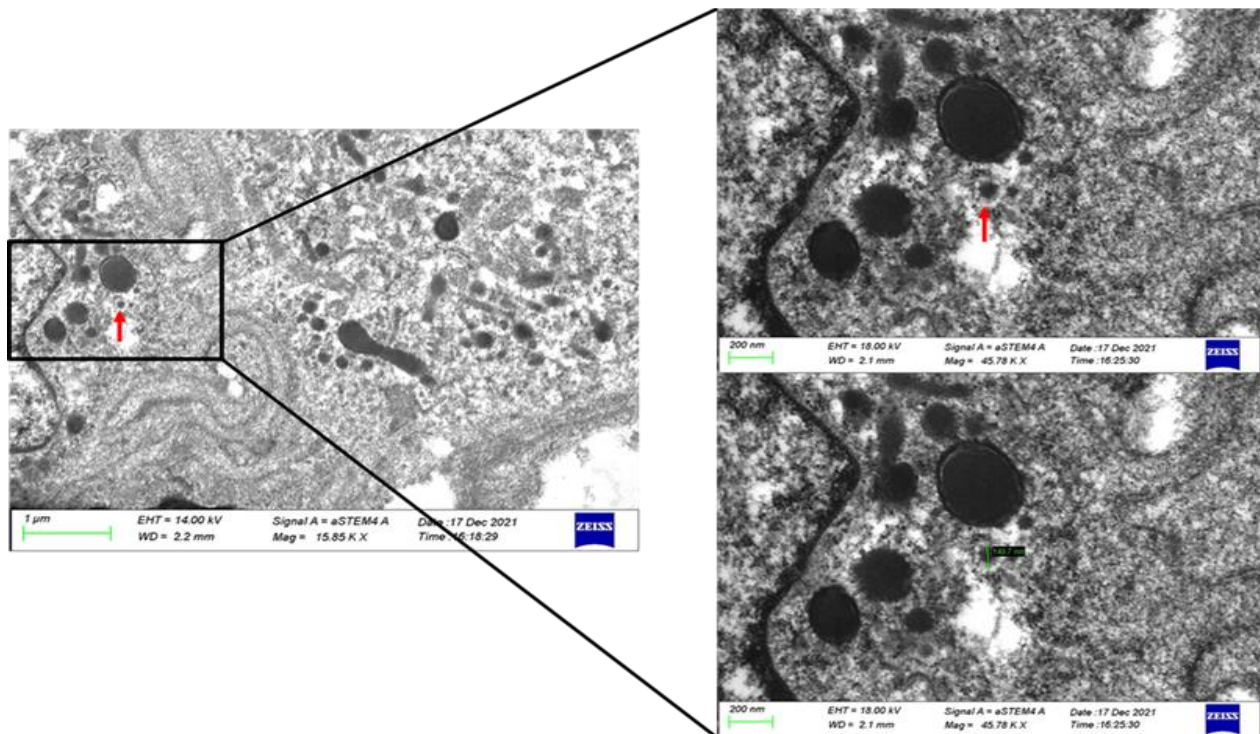


Figura 21. Micrografías electrónicas de pulmón de conejo inoculado por vía intranasal con el aislamiento viral del OvHV-2 a partir de leucocitos de caballo. A) Estructura similar a cápside viral en

citoplasma yuxtannuclear (flecha roja), junto a varios cuerpos electrodensos B) Imagen a mayor aumento, donde se puede observar el tamaño de la cápside viral de 149.7 nm (flecha amarilla). Técnica reversa para MET. 15 850X (izquierda), 45 780X (derecha).

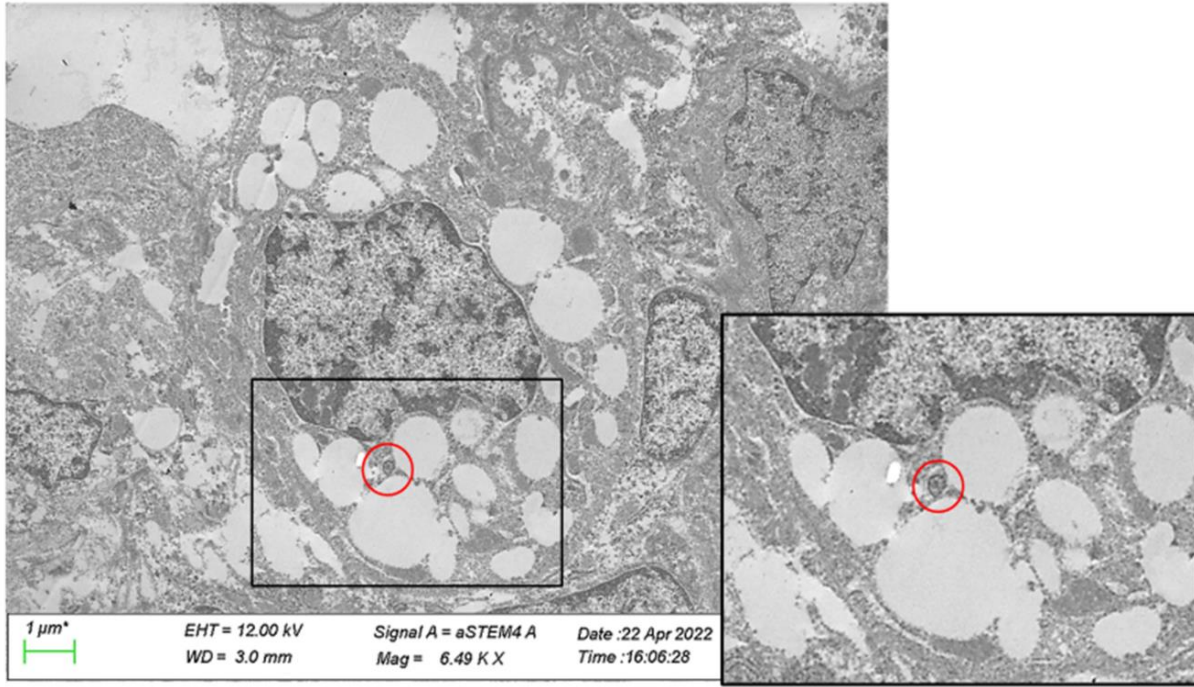


Figura 22. Micrografías electrónicas de pulmón de conejo inoculado por vía intranasal con el aislamiento viral del OvHV-2 a partir de leucocitos de caballo. A) Estructura citoplasmática similar a un herpesvirus (círculo rojo). Técnica reversa para MET. 6 490X (izquierda), amplificación electrónica (derecha).

6.14 Reaislamiento del virus OvHV-2

Los cultivos primarios inoculados con el macerado de pulmón de los tres conejos inoculados experimentalmente presentaron un marcado ECP desde las 72 h post-infección a partir del segundo pase, con una destrucción de la monocapa de más del 50% (Figura 23). Con respecto a los cultivos primarios inoculados con el macerado de bazo, no se observó ningún efecto citopático en el primer y segundo pase. Sin embargo, en el tercer pase se pudo observar una destrucción del 30% de la monocapa a partir de las 72 h post-infección.

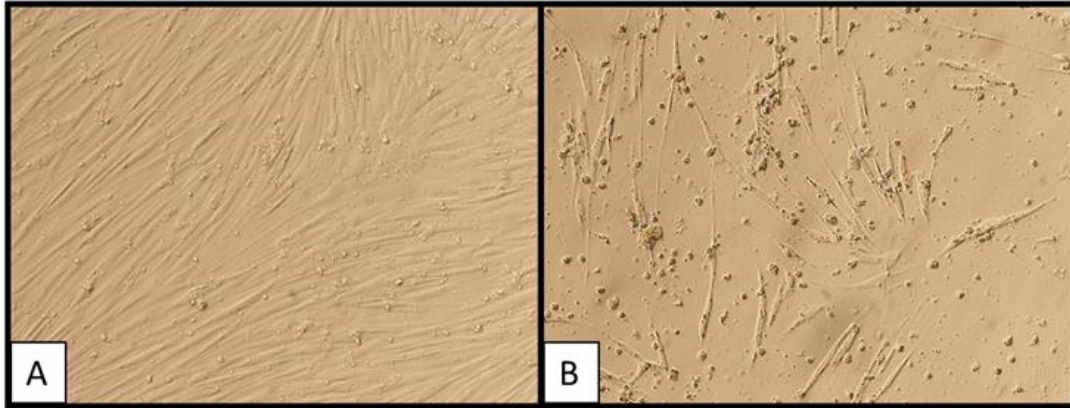
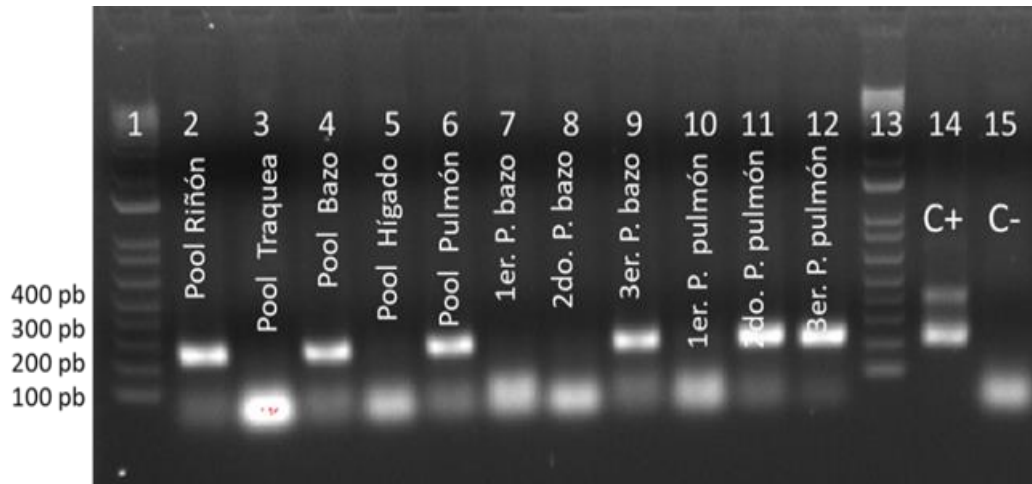


Figura 23. Reaislamiento del virus OvHV-2, en cultivos primarios de testículo de conejo. A) control negativo, B) Segundo pase del reaislamiento del virus OvHV-2 a partir del macerado de pulmón, ECP a las 72 h post-infección.

6.15 Detección del OvHV-2 mediante PCR punto final anidada en reaislamientos

Los macerados de riñón, bazo y pulmón de los conejos inoculados experimentalmente con el aislamiento del caballo fueron positivos al OvHV-2 por PCR punto final anidada al OvHV-2, mientras que los macerados de tráquea e hígado fueron negativos. Con respecto a los reaislamientos, sólo fue positivo al OvHV-2 en el tercer pase ciego del macerado de bazo. Por otro lado, el segundo y tercer pase ciego del macerado de pulmón fueron positivos al OvHV-2 por PCR (Figura 24).



Gel de agarosa al 1.5% corrido en buffer TAE 1X.

Figura 24. Prueba de PCR punto final anidada en órganos de conejos inoculados experimentalmente con OvHV-2. Carril 1- MPM- Marcador de peso molecular, carril 2- Macerado de riñón, carril 3- Macerado de tráquea, carril 4- Macerado de bazo, carril 5- Macerado de hígado, carril 6- Macerado de pulmón, carril 7- Primer pase ciego de bazo, carril 8- Segundo pase ciego de bazo, carril 9- Tercer pase ciego de bazo, carril 10- Primer pase ciego de pulmón, carril 11- Segundo pase ciego de pulmón, carril 12- Tercer pase ciego de pulmón, carril 13- MPM-marcador de peso molecular, 14- C+ control positivo, 15- C- control negativo de amplificación.

7. DISCUSIÓN

En este estudio describimos un brote de SA-MCF ocurrido en el rancho CEIEPAA, ubicado en Tequisquiapan, estado de Querétaro, México. Durante este brote se afectaron varias especies de animales, entre ellas caballos, ovejas, cabras, ganado lechero, ganado de engorda y ciervos. Estos animales, presentaron signos típicos de la forma clínica cabeza-ocular, compatibles con otros brotes de SA-MCF, reportados en diferentes partes del mundo (35). Las lesiones microscópicas de vasculitis y perivasculitis en diferentes órganos, además de diversos grados de trombosis e hiperplasia de ganglios linfáticos observadas en los ciervos que murieron durante el brote de SA-MCF, coincide con las lesiones reportadas en ciervos cola blanca (88).

En nuestro estudio utilizamos leucocitos de los animales afectados para realizar el aislamiento del OvHV-2, siendo una aproximación similar a lo reportado por Hristov *et al.* (2016), quienes utilizaron leucocitos de bisontes, muestras de sangre completa, de pulmón y de bazo de los diferentes animales afectados por SA-MCF para hacer el aislamiento del OvHV-2 (61).

Para el aislamiento *in vitro* del OvHV-2 se utilizaron cultivos primarios de testículo de conejo. De hecho, el uso de cultivos primarios ya ha sido reportado anteriormente para el aislamiento del AIHV-1 y AIHV-2 (62–64). En nuestro estudio, observamos un ECP marcado a las 72 h post-infección de los cultivos primarios de testículo a partir del tercer pase ciego. El ECP fue identificado como pequeños focos de células citomegálicas refráctiles, lo cual coincide con lo descrito durante los aislamientos de AIHV-1 y de OvHV-2 de camellos afectados por SA-MCF. El ECP fue identificado como pequeños focos de células citomegálicas refráctiles, lo cual coincide con lo descrito durante los aislamientos de AIHV-1 y de OvHV-2 de camellos afectados por SA-MCF (61,89).

En el presente estudio, los títulos del cuarto pase ciego de los caballos, cabras, ovejas, ciervos, ganado de engorda y ganado lechero obtenidos en cultivos celulares primarios de testículos de conejo oscilaron entre $\log 10^{2.8}$ y $\log 10^{4.19}$ TCID₅₀/mL. Por otro lado, el sobrenadante libre de células de los caballos alcanzó su pico más alto en el pase 14 a las 72 h post-infección ($10^{6.6}$ TCID₅₀/mL). Estos resultados indicaron que la propagación del virus OvHV-2 en cultivos primarios de testículos de conejo condujo a un aumento en los títulos virales en cada pase. Este

título viral es similar al encontrado por Hristov *et al.* (2016) de 10^6 TCID₅₀/mL en células de riñón bovino Madin-Darby (MDBK) después del pase 19 (61). Este aumento en los títulos virales en pases más altos podría deberse a que en los primeros pases, el virus está predominantemente asociado a células, y después de cinco pases, hay un período durante el cual el genoma viral sufre reordenamientos, lo que lleva a la atenuación viral y resulta en una mejor célula. rendimientos libres de virus. Sin embargo, esto solo se ha demostrado en AIHV-1 (90).

En los cultivos primarios de testículo de conejo infectados con los lisados de leucocitos, identificamos CI eosinofílicos intranucleares. Estos CI coinciden con los reportados por Hristov *et al.* (2016). La formación y relevancia de estas estructuras son explicados más adelante.

El OvHV-2 se identificó en cultivos primarios de testículo de conejo mediante PCR punto final anidada dirigida a un fragmento de 238 pb del gen *ORF75*, con una mayor intensidad a partir del tercer y cuarto pase en todos los sobrenadantes libres de células de las diferentes especies afectadas. Estos resultados indican que se requieren varios pases ciegos para generar mejores rendimientos de virus libres de células y lograr la adaptabilidad del virus a la célula, de acuerdo con el informe de Hristov *et al.* (2016) (61).

El lisado de la capa leucocítica de los caballos se replicó con una cinética similar en los pases 4 y 5; sin embargo, en el pase 14 alcanzó un título más alto. La replicación viral pudo detectarse a partir de las 24 h post-infección debido a la formación de sincitios solo en el pase 5 y 14. El ECP aumentó gradualmente, alcanzando un máximo a las 72 h post-infección y la disminución del título viral a las 120 h post-infección podría deberse a la muerte de las células. Con estos resultados, podemos inferir que los cultivos primarios de testículos de conejo soportan la replicación del OvHV-2. Nuestros resultados concuerdan con los de Hristov *et al.* (2016), en el que el aislamiento de la capa leucocítica del bisonte se caracterizó por pequeños sincitios a las 24 h post-infección, y entre las 60 y las 72 h post-infección donde hubo más del 50% de destrucción de la monocapa (61).

Además, el diagnóstico definitivo se confirmó mediante secuenciación parcial del fragmento de 422 pb del gen *ORF75*. Las siete secuencias de los sobrenadantes libres de células del cuarto pase de las diferentes especies afectadas por SA-MCF y el control positivo de OvHV-2 comparten una identidad de nucleótidos del 98 % al 99 % entre ellas y con las secuencias de OvHV-2 reportadas en diferentes regiones del mundo. Estos resultados se alinean con los informados por Martins *et*

al. (2017), quienes secuenciaron 13 muestras positivas de bovinos de diferentes áreas de Brasil y encontraron una similitud del 97 % al 100 % con OvHV-2 de varias otras regiones del mundo (91).

En el presente estudio, las secuencias *ORF75* se clasificaron como *ORF75*0201* por presentar al menos una sustitución no sinónima, cambio de lisina (K) a treonina (T); esto indica que el agente infeccioso que afectó a todos los animales durante el brote de 2018 con SA-MCF fue la misma cepa de OvHV-2. Por otro lado, nuestros resultados difieren de los de Russell *et al.* (2014) donde encontraron que el alelo principal en 18 muestras era *ORF75*0101*, eran similares a la secuencia de referencia BJ1035 (92,93). Podemos inferir que en México el alelo que más circula es el *ORF75*0201*. Sin embargo, para la caracterización genética y estudios epidemiológicos sería necesario secuenciar los genes *ORF50* y *Ov9.5*, siendo este último el más importante para estudios de este tipo (92). En este sentido, y con los resultados presentados anteriormente, podríamos inferir que las cabras y las ovejas fueron las fuentes de infección (transmisión entre especies) o como potenciales reservorios capaces de transmitir la enfermedad a especies susceptibles (caballos, ciervos, ganado lechero y ganado de engorda) debido a su cercanía entre ellos y compartir pastizales.

La inmunorreactividad intracitoplasmática a OvHV-2 en los cultivos primarios de testículo de conejo infectados con los lisados de leucocitos y en los CI intracitoplasmáticos e intranucleares de hepatocitos de un ciervo que murió de forma natural por SA-MCF, demuestra que la inmunización de conejos con la suspensión del aislado de OvHV-2 inactivado fue eficiente y que los anticuerpos presentes en el suero hiperinmune reconocen antígenos de OvHV-2, tanto en la infección experimental de células en cultivo como en ciervos infectados naturalmente. Estos resultados concuerdan con los reportados por Headley *et al.* (2022), quienes identificaron inmunorreactividad intracitoplasmática en múltiples tejidos utilizando un anticuerpo monoclonal (mAb-15A), dirigido a un epítipo conservado entre todos los *Macavirus* (94).

Además, los CI intracitoplasmáticos en los hepatocitos de un ciervo que murió durante el brote de SA-MCF fueron eosinofílicos. Estos CI eosinofílicos también han sido identificados en neuronas de vacas clínicamente diagnosticadas con SA-MCF (47). Previamente, hace 76 años, Goss *et al.* (1947) reportaron resultados similares en células de Purkinje y en células epiteliales de mucosas. La presencia de CI intracitoplasmáticos, como los observados en hepatocitos del ciervo mencionado, podría deberse a sitios de acumulación y retención de proteínas virales y celulares.

Estructuras similares, identificadas con microscopía electrónica de transmisión como cuerpos densos, podrían corresponder a cúmulos macromoleculares y son muy comunes en células humanas infectadas por citomegalovirus. La mayoría de estas estructuras están secuestradas en vesículas derivadas del aparato de Golgi y algunos de estos cuerpos densos están ubicados cerca o en contacto con la cubierta nuclear, por lo que se ha propuesto que “inyectan” proteínas virales a través de los poros nucleares y que son necesarias para el ensamblaje viral (95). Con el empleo de los métodos de H&E, PAS y Feulgen en los cortes histológicos de hígado de ciervo se demostró que los CI intracitoplasmáticos contienen proteínas básicas, glucoproteínas probablemente virales y ADN. El contenido de los CI concuerda con lo reportado por Nelson *et al.* (2013), quienes identificaron la acumulación de proteína viral en el citoplasma, debida a una replicación viral abortiva en hospedadores susceptibles terminales infectados con OvHV-2 (33). Por todo lo antes mencionado, podemos inferir que los CI intracitoplasmáticos que solo se han descrito en los hospedadores susceptibles en nuestro caso el ciervo, podrían ser una acumulación de proteínas y glucoproteínas virales, proteínas celulares, y ADN necesarios para el ensamblaje de los viriones que se están sintetizando en el núcleo, y además de viriones abortivos.

La inoculación de los conejos con el aislamiento obtenido a partir de los leucocitos de los caballos (cepa Mex/Eq/19), reprodujo los signos clínicos y las lesiones de SA-MCF, lo que destaca el uso de los conejos como modelo experimental y que coincide con lo reportado por Cunha *et al.* (2013) y por Gailbreath *et al.* (2008) (15,18).

En nuestro estudio de MET observamos cápsides virales en núcleo y viriones, con morfología similar a herpesvirus, en el citoplasma de células presentes en el intersticio pulmonar, algunas parecidas a fibroblastos y otras a células mononucleares, algunas con aspecto apoptótico del núcleo. Estas estructuras virales también se han descrito por Cunha *et al.* (2008) en secreciones nasales de ovinos infectados por OvHV-2 (29). Además de compartir una morfología típica de los herpesvirus (96).

Por último, hicimos el reisolamiento de OvHV-2 a partir del pulmón y del bazo de los conejos desafiados (Grupo A), positivos por PCR punto final anidada al OvHV-2. Estos órganos contienen una gran carga de copias de ADN del OvHV-2, entre 66,900 y 61,200, de acuerdo con lo reportado por Gailbreath *et al.* (2008) y posteriormente confirmado por Hristov *et al.* (2016) en animales

afectados por SA-MCF (61,86). Por lo tanto, además de usar los leucocitos de animales infectados con SA-MCF, se sugiere utilizar pulmón y bazo para realizar el aislamiento del virus OvHV-2.

8. CONCLUSIONES

1. El brote de SA-MCF que afectó a los animales del CEIEPAA, en Tequisquiapan, Querétaro, fue causado por el virus OvHV-2.
2. Fue demostrado, por primera vez en México, que los caballos son susceptibles a la infección por OvHV-2 y desarrollan SA-MCF.
3. La SA-MCF debe ser considerada en el diagnóstico diferencial de las enfermedades vesiculares en caballos.
4. Los cultivos primarios de testículo de conejo fueron susceptibles y permisibles para la replicación viral del OvHV-2.
5. Se demostró la adaptabilidad del aislamiento de los caballos en los cultivos primarios, logrando un aumento en el título viral en pases consecutivos.
6. Las secuencias parciales mexicanas del gen *ORF75*, compartían entre el 98% al 99% de identidad de nucleótidos entre ellas y con las secuencias de OvHV-2 reportadas en diferentes regiones del mundo, y el alelo ORF75*0201 fue el que afectó a todos los animales en el CEIEPAA durante el brote de SA-MCF del 2018.
7. Los conejos pueden ser infectados con OvHV-2 y replican algunas de las características histopatológicas y clínicas de SA-MCF.
8. Los CI pueden ser considerados dentro de los criterios diagnósticos de infección por OvHV-2 y SA-MCF de acuerdo las características histológicas, histoquímicas, inmunohistológicas y ultraestructurales, tanto en infecciones *in vitro*, experimentales y naturales *in vivo*.

9. REFERENCIAS

1. Russell GC, Stewart JP, Haig DM. Malignant catarrhal fever: A review. *The Veterinary Journal* [Internet]. 2009 Mar 1 [cited 2023 Mar 2];179(3):324–35. Available from: <https://linkinghub.elsevier.com/retrieve/pii/S1090023307003899>
2. Davison AJ, Eberle R, Ehlers B, Hayward GS, McGeoch DJ, Minson AC, et al. The order Herpesvirales. [cited 2023 Mar 2]; Available from: <http://www.>
3. Current ICTV Taxonomy Release. <https://ictv.global/taxonomy>. 2023.
4. Davison AJ. Herpesvirus systematics. *Vet Microbiol*. 2010 Jun;143(1):52–69.
5. Ensser A, Pflanz R, Fleckenstein B. Primary structure of the alcelaphine herpesvirus 1 genome. *J Virol* [Internet]. 1997 Sep [cited 2023 Mar 2];71(9):6517–25. Available from: <https://journals.asm.org/journal/jvi>
6. Taus NS, Herndon DR, Traul DL, Stewart JP, Ackermann M, Li H, et al. Comparison of ovine herpesvirus 2 genomes isolated from domestic sheep (*Ovis aries*) and a clinically affected cow (*Bos bovis*). *Journal of General Virology* [Internet]. 2007 Jan 1 [cited 2023 Mar 2];88(1):40–5. Available from: <https://www.microbiologyresearch.org/content/journal/jgv/10.1099/vir.0.82285-0>
7. Hart J, Ackermann M, Jayawardane G, Russell G, Haig DM, Reid H, et al. Complete sequence and analysis of the ovine herpesvirus 2 genome. *Journal of General Virology* [Internet]. 2007 Jan 1 [cited 2023 Mar 2];88(1):28–39. Available from: <https://www.microbiologyresearch.org/content/journal/jgv/10.1099/vir.0.82284-0>
8. Li H, O’toole D, Kim O, Oaks JL, Crawford TB. Malignant catarrhal fever-like disease in sheep after intranasal inoculation with ovine herpesvirus-2. *Brief Communications J Vet Diagn Invest*. 2005;17:171–5.
9. PLOWRIGHT W. Malignant Catarrhal Fever in East Africa: I.—Behaviour of the Virus in Free-living Populations of Blue Wildebeest (*Gorgon taurinus taurinus*, Burchell). *Res Vet Sci*. 1965 Jan 1;6(1):56–68.
10. Li H, Taus NS, Jones C, Murphy B, Evermann JF, Crawford TB. A devastating outbreak of malignant catarrhal fever in a bison feedlot. *J Vet Diagn Invest* [Internet]. 2006 [cited 2023 Mar 2];18(1):119–23. Available from: <https://pubmed.ncbi.nlm.nih.gov/16566270/>
11. HOFFMANN D, SOBIRONINGSIH S, CLARKE BC, YOUNG PJ, SENDOW I. Transmission and virological studies of a malignant catarrhal fever syndrome in the Indonesian swamp buffalo (*Bubalus bubalis*). *Aust Vet J* [Internet]. 1984 Apr 1 [cited 2023 Mar 2];61(4):113–6. Available from: <https://onlinelibrary.wiley.com/doi/full/10.1111/j.1751-0813.1984.tb07202.x>
12. Taus NS, Oaks JL, Gailbreath K, Traul DL, O’Toole D, Li H. Experimental aerosol infection of cattle (*Bos taurus*) with ovine herpesvirus 2 using nasal secretions from infected sheep. *Vet Microbiol*. 2006 Aug 25;116(1–3):29–36.

13. O'toole D, Taus NS, Montgomery DL, Oaks JL, Crawford TB, Li H. Intra-nasal Inoculation of American Bison (*Bison bison*) with Ovine Herpesvirus-2 (OvHV-2) Reliably Reproduces Malignant Catarrhal Fever.
14. Costa ÉA, Bomfim MRQ, Da Fonseca FG, Drumond BP, Coelho FM, Vasconcelos AC, et al. Ovine Herpesvirus 2 Infection in Foal, Brazil. *Emerg Infect Dis* [Internet]. 2009 May [cited 2023 Mar 2];15(5):844. Available from: [/pmc/articles/PMC2687043/](https://pubmed.ncbi.nlm.nih.gov/19111111/)
15. Gailbreath KL, Taus NS, Cunha CW, Knowles DP, Li H. Experimental infection of rabbits with ovine herpesvirus 2 from sheep nasal secretions. *Vet Microbiol*. 2008 Nov 25;132(1–2):65–73.
16. Li H, Cunha CW, Taus NS. Malignant catarrhal fever: understanding molecular diagnostics in context of epidemiology. *Int J Mol Sci* [Internet]. 2011 Oct [cited 2023 Mar 2];12(10):6881–93. Available from: <https://pubmed.ncbi.nlm.nih.gov/22072925/>
17. Anderson IE, Buxton D, Campbell I, Russell G, Davis WC, Hamilton MJ, et al. Immunohistochemical Study of Experimental Malignant Catarrhal Fever in Rabbits. *J Comp Pathol*. 2007 Feb 1;136(2–3):156–66.
18. Cunha CW, O'Toole D, Taus NS, Knowles DP, Li H. Are rabbits a suitable model to study sheep-associated malignant catarrhal fever in susceptible hosts? *Vet Microbiol* [Internet]. 2013 May 3 [cited 2023 Mar 2];163(3–4):358–63. Available from: <https://linkinghub.elsevier.com/retrieve/pii/S0378113513000485>
19. Buxton D, Reid HW, Finlayson J, Pow I. Pathogenesis of 'sheep-associated' malignant catarrhal fever in rabbits. *Res Vet Sci*. 1984 Mar 1;36(2):205–11.
20. Plowright W, Ferris RD, Scott GR. Blue wildebeest and the aetiological agent of bovine malignant catarrhal fever. *Nature* [Internet]. 1960 [cited 2023 Mar 2];188(4757):1167–9. Available from: <https://pubmed.ncbi.nlm.nih.gov/13736396/>
21. Li H, Snowden G, O'Toole D, Crawford TB. Transmission of ovine herpesvirus 2 in lambs. *J Clin Microbiol* [Internet]. 1998 [cited 2023 Mar 2];36(1):223–6. Available from: <https://journals.asm.org/journal/jcm>
22. Hüsey D, Janett F, Albin S, Stäuber N, Thun R, Ackermann M. Analysis of the pathogenetic basis for shedding and transmission of ovine gamma herpesvirus 2. *J Clin Microbiol* [Internet]. 2002 Dec 1 [cited 2023 Mar 2];40(12):4700–4. Available from: <https://journals.asm.org/doi/10.1128/JCM.40.12.4700-4704.2002>
23. Li H, Hua Y, Snowden G, Crawford TB. Levels of ovine herpesvirus 2 DNA in nasal secretions and blood of sheep: implications for transmission. *Vet Microbiol*. 2001 Apr 19;79(4):301–10.
24. Li H, Taus NS, Lewis GS, Kim O, Traul DL, Crawford TB. Shedding of ovine herpesvirus 2 in sheep nasal secretions: The predominant mode for transmission. *J Clin Microbiol* [Internet]. 2004 Dec [cited 2023 Mar 2];42(12):5558–64. Available from: <https://journals.asm.org/doi/10.1128/JCM.42.12.5558-5564.2004>

25. Selman IE, Wiseman A, Wright NG, Murray M. Transmission studies with bovine malignant catarrhal fever. *Vet Rec* [Internet]. 1978 Mar 1 [cited 2023 Mar 2];102(12):252–7. Available from: <https://europepmc.org/article/med/644823>
26. Pierson RE, Storz J, McChesney AE, Thake D. Experimental transmission of malignant catarrhal fever. *Am J Vet Res*. 1974;35(No.4):523–5.
27. Li H, Cunha CW, Davies CJ, Gailbreath KL, Knowles DP, Oaks JL, et al. Ovine herpesvirus 2 replicates initially in the lung of experimentally infected sheep. *Journal of General Virology* [Internet]. 2008 Jul 1 [cited 2023 Mar 2];89(7):1699–708. Available from: <https://www.microbiologyresearch.org/content/journal/jgv/10.1099/vir.0.2008/000554-0>
28. Meier-Trummer CS, Ryf B, Ackermann M. Identification of peripheral blood mononuclear cells targeted by Ovine herpesvirus-2 in sheep. *Vet Microbiol*. 2010 Mar 24;141(3–4):199–207.
29. Cunha CW, Traul DL, Taus NS, Oaks JL, O’Toole D, Davitt CM, et al. Detection of ovine herpesvirus 2 major capsid gene transcripts as an indicator of virus replication in shedding sheep and clinically affected animals. *Virus Res*. 2008 Mar 1;132(1–2):69–75.
30. Taus NS, Schneider DA, Oaks JL, Yan H, Gailbreath KL, Knowles DP, et al. Sheep (*Ovis aries*) airway epithelial cells support ovine herpesvirus 2 lytic replication in vivo. *Vet Microbiol*. 2010 Sep 28;145(1–2):47–53.
31. Cunha CW, Gailbreath KL, O’Toole D, Knowles DP, Schneider DA, White SN, et al. Ovine herpesvirus 2 infection in American bison: virus and host dynamics in the development of sheep-associated malignant catarrhal fever. *Vet Microbiol* [Internet]. 2012 Oct 12 [cited 2023 Mar 2];159(3–4):307–19. Available from: <https://linkinghub.elsevier.com/retrieve/pii/S0378113512002702>
32. Meier-Trummer CS, Tobler K, Hilbe M, Stewart JP, Hart J, Campbell I, et al. Ovine herpesvirus 2 structural proteins in epithelial cells and M-cells of the appendix in rabbits with malignant catarrhal fever. *Vet Microbiol* [Internet]. 2009 Jun 12 [cited 2023 Mar 2];137(3–4):235–42. Available from: <https://linkinghub.elsevier.com/retrieve/pii/S0378113509000510>
33. Nelson DD, Taus NS, Schneider DA, Cunha CW, Davis WC, Brown WC, et al. Fibroblasts express OvHV-2 capsid protein in vasculitis lesions of American bison (*Bison bison*) with experimental sheep-associated malignant catarrhal fever. *Vet Microbiol* [Internet]. 2013 Oct 25 [cited 2023 Mar 2];166(3–4):486–92. Available from: <https://linkinghub.elsevier.com/retrieve/pii/S0378113513003830>
34. OIE. Malignant catarrhal fever. In: *OIE Manual of Diagnostic Tests and Vaccines for Terrestrial Animal*,. Fifth. France; 2004. 570–579 p.
35. O’toole D, Li H, Sourk C, Montgomery DL, Crawford TB. Malignant catarrhal fever in a bison (*Bison bison*) feedlot, 1993-2000. *J Vet Diagn Invest*. 2002;14:183–93.
36. Palmer MV, Thacker TC, Madison RJ, Koster LG, Swenson SL, Li H. Active and Latent Ovine Herpesvirus-2 (OvHV-2) Infection in a Herd of Captive White-tailed Deer (*Odocoileus virginianus*).

- J Comp Pathol [Internet]. 2013 Aug 1 [cited 2023 Mar 2];149(2–3):162–6. Available from: <https://linkinghub.elsevier.com/retrieve/pii/S0021997513000194>
37. Reid HW, Buxton D, McKelvey WA, Milne JA, Appleyard WT. Malignant catarrhal fever in Père David's deer. *Vet Rec* [Internet]. 1987 [cited 2023 Mar 2];121(12):276–7. Available from: <https://pubmed.ncbi.nlm.nih.gov/3672838/>
 38. Berezowski JA, Appleyard GD, Crawford TB, Haigh J, Li H, Middleton DM, et al. BRIEF COMMUNICATIONS An outbreak of sheep-associated malignant catarrhal fever in bison (*Bison bison*) after exposure to sheep at a public auction sale. *J Vet Diagn Invest*. 2005;17:55–8.
 39. Rech RR, Schild AL, Driemeier D, Garmatz SL, Oliveira FN, Riet-Correa F, et al. Malignant catarrhal fever in cattle in Rio Grande do Sul, Brazil: epidemiology, clinical signs and pathology. *Pesquisa Veterinária Brasileira* [Internet]. 2005 [cited 2023 Mar 2];25(2):97–105. Available from: <http://www.scielo.br/j/pvb/a/snHFypBVPZqwt6QcD8gwMVD/abstract/?lang=en>
 40. Collery P, Foley A. An outbreak of malignant catarrhal fever in cattle in the Republic of Ireland. *Vet Rec* [Internet]. 1996 Jul 6 [cited 2023 Mar 2];139(1):16–7. Available from: <https://pubmed.ncbi.nlm.nih.gov/8819289/>
 41. Frölich K, Li H, Müller-Doblies U. SEROSURVEY FOR ANTIBODIES TO MALIGNANT CATARRHAL FEVER-ASSOCIATED VIRUSES IN FREE-LIVING AND CAPTIVE CERVIDS IN GERMANY. *J Wildl Dis* [Internet]. 1998 Jan 1 [cited 2023 Mar 2];34(4):777–82. Available from: <https://meridian.allenpress.com/jwd/article/34/4/777/122072/SEROSURVEY-FOR-ANTIBODIES-TO-MALIGNANT-CATARRHAL>
 42. Desmecht D, Cassart D, Rollin F, Coignoul F, Tham KM. Molecular and clinicopathological diagnosis of non-wildebeest associated malignant catarrhal fever in Belgium. *Veterinary Record* [Internet]. 1999 Apr 1 [cited 2023 Mar 2];144(14):388–388. Available from: <https://onlinelibrary.wiley.com/doi/full/10.1136/vr.144.14.388>
 43. Yus E, Guitián J, Díaz A, Sanjuán ML. Outbreak of malignant catarrhal fever in cattle in Spain. *Vet Rec* [Internet]. 1999 Oct 16 [cited 2023 Mar 2];145(16):466–7. Available from: <https://pubmed.ncbi.nlm.nih.gov/10576285/>
 44. Dabak M, Bulut H. Outbreak of malignant catarrhal fever in cattle in Turkey. *Vet Rec* [Internet]. 2003 Feb 22 [cited 2023 Mar 2];152(8):240–1. Available from: <https://pubmed.ncbi.nlm.nih.gov/12625541/>
 45. Rossiter PB. Antibodies to malignant catarrhal fever virus in sheep sera. *J Comp Pathol* [Internet]. 1981 [cited 2023 Mar 2];91(2):303–11. Available from: <https://pubmed.ncbi.nlm.nih.gov/7047584/>
 46. Wilson PR. Advances in health and welfare of farmed deer in New Zealand. *N Z Vet J* [Internet]. 2002 [cited 2023 Mar 2];50(3 Suppl):105–9. Available from: <https://pubmed.ncbi.nlm.nih.gov/16032253/>
 47. Aluja A, Rocha TC De, Velázquez A. Fiebre catarral maligna. *Rev Mex Cienc Pecu*. 1969;

48. Li H, Cunha CW, Taus NS, Knowles DP. Malignant catarrhal fever: inching toward understanding. *Annu Rev Anim Biosci* [Internet]. 2014 [cited 2023 Mar 2];2:209–33. Available from: <https://pubmed.ncbi.nlm.nih.gov/25384141/>
49. Pierson RE, Thake D, McChesney AE, Storz J. An epizootic of malignant catarrhal fever in feedlot cattle. *J Am Vet Med Assoc*. 1973;163(No.4):349–50.
50. Lankester F, Lugelo A, Kazwala R, Keyyu J, Cleaveland S, Yoder J. Correction: The Economic Impact of Malignant Catarrhal Fever on Pastoralist Livelihoods. *PLoS One* [Internet]. 2019 Sep 1 [cited 2023 Mar 2];14(9). Available from: <https://pubmed.ncbi.nlm.nih.gov/31557267/>
51. Schultheiss PC, Collins JK, Spraker TR, DeMartini JC. Epizootic malignant catarrhal fever in three bison herds: differences from cattle and association with ovine herpesvirus-2. *J Vet Diagn Invest* [Internet]. 2000 [cited 2023 Mar 2];12(6):497–502. Available from: <https://pubmed.ncbi.nlm.nih.gov/11108448/>
52. O’Toole D, Li H, Miller D, Williams WR, Crawford TB. Chronic and recovered cases of sheep-associated malignant catarrhal fever in cattle. *Vet Rec* [Internet]. 1997 [cited 2023 Mar 2];140(20):519–24. Available from: <https://pubmed.ncbi.nlm.nih.gov/9178482/>
53. Headley SA, de Oliveira TES, Cunha CW. A review of the epidemiological, clinical, and pathological aspects of malignant catarrhal fever in Brazil. *Braz J Microbiol* [Internet]. 2020 Sep 1 [cited 2023 May 16];51(3):1405–32. Available from: <https://pubmed.ncbi.nlm.nih.gov/32542424/>
54. Li H, McGuire TC, Müller-Doblies UU, Crawford TB. A simpler, more sensitive competitive inhibition enzyme-linked immunosorbent assay for detection of antibody to malignant catarrhal fever viruses. *J Vet Diagn Invest* [Internet]. 2001 [cited 2023 Mar 2];13(4):361–4. Available from: <https://pubmed.ncbi.nlm.nih.gov/11478614/>
55. Powers JG, VanMetre DC, Collins JK, Dinsmore RP, Carman J, Patterson G, et al. Evaluation of ovine herpesvirus type 2 infections, as detected by competitive inhibition ELISA and polymerase chain reaction assay, in dairy cattle without clinical signs of malignant catarrhal fever. *J Am Vet Med Assoc* [Internet]. 2005 Aug 15 [cited 2023 Mar 2];227(4):606–11. Available from: <https://pubmed.ncbi.nlm.nih.gov/16117071/>
56. Hüsey D, Stäuber N, Leutenegger CM, Rieder S, Ackermann M. Quantitative fluorogenic PCR assay for measuring ovine herpesvirus 2 replication in sheep. *Clin Diagn Lab Immunol* [Internet]. 2001 [cited 2023 Jun 12];8(1):123–8. Available from: <https://pubmed.ncbi.nlm.nih.gov/11139205/>
57. Baxter SIF, Pow I, Bridgen A, Reid HW. PCR detection of the sheep-associated agent of malignant catarrhal fever. *Arch Virol* [Internet]. 1993 Mar [cited 2023 Mar 6];132(1–2):145–59. Available from: <https://link.springer.com/article/10.1007/BF01309849>
58. Cunha CW, Otto L, Taus NS, Knowles DP, Li H. Development of a multiplex real-time PCR for detection and differentiation of malignant catarrhal fever viruses in clinical samples. *J Clin Microbiol* [Internet]. 2009 Aug [cited 2023 Jun 12];47(8):2586–9. Available from: <https://pubmed.ncbi.nlm.nih.gov/19494077/>

59. Li H, Snowden G, Crawford TB. Production of malignant catarrhal fever virus-free sheep. *Vet Microbiol* [Internet]. 1999 Mar 1 [cited 2023 Jun 12];65(2):167–72. Available from: <https://pubmed.ncbi.nlm.nih.gov/10078600/>
60. Traul DL, Taus NS, Oaks JL, O’Toole D, Rurangirwa FR, Baszler T V., et al. Validation of nonnested and real-time PCR for diagnosis of sheep-associated malignant catarrhal fever in clinical samples. *J Vet Diagn Invest* [Internet]. 2007 [cited 2023 Jun 12];19(4):405–8. Available from: <https://pubmed.ncbi.nlm.nih.gov/17609352/>
61. Hristov M V., Peshev RD. Isolation and identification of malignant catarrhal fever virus in cell cultures. *Bulg J Vet Med*. 2016;19(4):263–73.
62. Plowright W, Ferris RD, Scott GR. Blue wildebeest and the aetiological agent of bovine malignant catarrhal fever. *Nature* [Internet]. 1960 [cited 2023 May 16];188(4757):1167–9. Available from: <https://pubmed.ncbi.nlm.nih.gov/13736396/>
63. Plowright W, Ferris RD. The Preparation of Bovine Thyroid Monolayers for use in Virological Investigations. *Res Vet Sci*. 1961 Apr 1;2(2):149–53.
64. Castro AE, Daley GG, Zimmer MA, Whitenack DL, Jensen J. Malignant catarrhal fever in an Indian gaur and greater kudu: experimental transmission, isolation, and identification of a herpesvirus. *Am J Vet Res* [Internet]. 1982 Jan 1 [cited 2023 May 16];43(1):5–11. Available from: <https://europepmc.org/article/MED/7091816>
65. Handley JA, Sargan DR, Herring AJ, Reid HW. Identification of a region of the alcelaphine herpesvirus-1 genome associated with virulence for rabbits. *Vet Microbiol* [Internet]. 1995 [cited 2023 Mar 2];47(1–2):167–81. Available from: <https://pubmed.ncbi.nlm.nih.gov/8604548/>
66. Wright H, Stewart JP, Ireri RG, Campbell I, Pow I, Reid HW, et al. Genome re-arrangements associated with loss of pathogenicity of the γ -herpesvirus alcelaphine herpesvirus-1. *Res Vet Sci* [Internet]. 2003 [cited 2023 Mar 2];75(2):163–8. Available from: <https://pubmed.ncbi.nlm.nih.gov/12893166/>
67. Goss LW, Cole CR, Kissling RE. The Pathology of Malignant Catarrhal Fever (Bovine Epitheliosis): With Special Reference to Cytoplasmic Inclusions. *Am J Pathol* [Internet]. 1947 Sep 1 [cited 2023 May 16];23(5):837–41. Available from: <https://www.ncbi.nlm.nih.gov/pmc/articles/pmid/19970964/?tool=EBI>
68. Severi B, Landini MP, Cenacchi G, Zini N, Maraldi NM. Human cytomegalovirus nuclear and cytoplasmic dense bodies. *Arch Virol* [Internet]. 1992 Mar [cited 2023 Mar 2];123(1–2):193–207. Available from: <https://pubmed.ncbi.nlm.nih.gov/1372496/>
69. Li H, Cunha CW, Taus NS. Malignant catarrhal fever: understanding molecular diagnostics in context of epidemiology. *Int J Mol Sci* [Internet]. 2011 Oct [cited 2023 May 16];12(10):6881–93. Available from: <https://pubmed.ncbi.nlm.nih.gov/22072925/>
70. Pérez-Guiot A, Páez-Trejo A, Domínguez-Hernández Y, Carranza-Velázquez J, Hernández-García D, Carrisoza-Urbina I, et al. Pakistan Veterinary Journal Malignant Catarrhal Fever Associated with

- Ovine Gammaherpesvirus-2 in Domestic Ruminants in Queretaro, Mexico. [cited 2023 Jun 12]; Available from: <http://dx.doi.org/10.29261/pakvetj/2022.076>
71. English D, Andersen BR. Single-step separation of red blood cells. Granulocytes and mononuclear leukocytes on discontinuous density gradients of Ficoll-Hypaque. *J Immunol Methods* [Internet]. 1974 [cited 2023 May 16];5(3):249–52. Available from: <https://pubmed.ncbi.nlm.nih.gov/4427075/>
 72. Baxter SIF, Pow I, Bridgen A, Reid HW. PCR detection of the sheep-associated agent of malignant catarrhal fever. *Arch Virol* [Internet]. 1993 Mar [cited 2023 May 16];132(1–2):145–59. Available from: <https://pubmed.ncbi.nlm.nih.gov/8352654/>
 73. High Pure PCR Template Preparation Kit Rapidly purify genomic DNA for diverse applications. [cited 2023 Mar 6]; Available from: www.roche-applied-science.com
 74. Li H, Shen DT, O’toole D, Knowles DP, Gorham JR, Crawford TB, et al. Investigation of sheep-associated malignant catarrhal fever virus infection in ruminants by PCR and competitive inhibition enzyme-linked immunosorbent assay. *J Clin Microbiol* [Internet]. 1995 [cited 2023 Mar 6];33(8):2048–53. Available from: <https://journals.asm.org/doi/10.1128/jcm.33.8.2048-2053.1995>
 75. Reed LJ, Muench H. A simple method of estimating fifty per cent endpoints. *Am J Epidemiol* [Internet]. 1938 May 1 [cited 2023 Mar 6];27(3):493–7. Available from: <https://academic.oup.com/aje/article/27/3/493/99616>
 76. Hall T. BIOEDIT: A USER-FRIENDLY BIOLOGICAL SEQUENCE ALIGNMENT EDITOR AND ANALYSIS PROGRAM FOR WINDOWS 95/98/ NT. 1999;
 77. Tamura K, Stecher G, Kumar S. MEGA11: Molecular Evolutionary Genetics Analysis Version 11. *Mol Biol Evol* [Internet]. 2021 Jul 1 [cited 2023 May 16];38(7):3022–7. Available from: <https://pubmed.ncbi.nlm.nih.gov/33892491/>
 78. Johnson M, Zaretskaya I, Raytselis Y, Merezhuk Y, McGinnis S, Madden TL. NCBI BLAST: a better web interface. *Nucleic Acids Res* [Internet]. 2008 Jul 1 [cited 2023 Mar 6];36(suppl_2):W5–9. Available from: https://academic.oup.com/nar/article/36/suppl_2/W5/2505810
 79. Posada D. jModelTest: phylogenetic model averaging. *Mol Biol Evol* [Internet]. 2008 Jul [cited 2023 Jun 18];25(7):1253–6. Available from: <https://pubmed.ncbi.nlm.nih.gov/18397919/>
 80. Tamura K, Nei M. Estimation of the number of nucleotide substitutions in the control region of mitochondrial DNA in humans and chimpanzees. *Mol Biol Evol* [Internet]. 1993 May 1 [cited 2023 May 16];10(3):512–26. Available from: <https://academic.oup.com/mbe/article/10/3/512/1016366>
 81. Orós J, Poveda JB, Rodríguez JL, Franklin CL, Fernández A. Natural cilia-associated respiratory bacillus infection in rabbits used for elaboration of hyperimmune serum against *Mycoplasma* sp. *Zentralbl Veterinarmed B* [Internet]. 1997 [cited 2023 May 16];44(5):313–7. Available from: <https://pubmed.ncbi.nlm.nih.gov/9270356/>

82. Rossiter PB. Immunofluorescence and immunoperoxidase techniques for detecting antibodies to malignant catarrhal fever in infected cattle. *Trop Anim Health Prod* [Internet]. 1981 [cited 2023 Mar 2];13(4):189–92. Available from: <https://pubmed.ncbi.nlm.nih.gov/7046177/>
83. Headley SA, de Lemos GAA, Dall Agnol AM, Xavier AAC, Depes VCA, Yasumitsu CY, et al. Ovine gammaherpesvirus 2 infections in cattle without typical manifestations of sheep-associated malignant catarrhal fever and concomitantly infected with bovine coronavirus. *Braz J Microbiol* [Internet]. 2022 Mar 1 [cited 2023 May 16];53(1):433–46. Available from: <https://pubmed.ncbi.nlm.nih.gov/34780031/>
84. Fu DA, Campbell-Thompson M. Periodic acid-schiff staining with diastase. *Methods in Molecular Biology* [Internet]. 2017 [cited 2023 Mar 6];1639:145–9. Available from: https://link.springer.com/protocol/10.1007/978-1-4939-7163-3_14
85. Chieco P. The Feulgen reaction 75 years on Identification of innovative microRNA-based biomarkers and anti-cancer strategies for the treatment of hepatocellular carcinoma View project Image Cytometry View project. Article in *Histochemistry and Cell Biology* [Internet]. 1999 [cited 2023 Mar 6]; Available from: <https://www.researchgate.net/publication/12896440>
86. Gailbreath KL, Taus NS, Cunha CW, Knowles DP, Li H. Experimental infection of rabbits with ovine herpesvirus 2 from sheep nasal secretions. *Vet Microbiol*. 2008 Nov 25;132(1–2):65–73.
87. Devan KS, Walther P, von Einem J, Ropinski T, Kestler HA, Read C. Detection of herpesvirus capsids in transmission electron microscopy images using transfer learning. *Histochem Cell Biol* [Internet]. 2019 Feb 5 [cited 2023 Mar 6];151(2):101–14. Available from: <https://link.springer.com/article/10.1007/s00418-018-1759-5>
88. Brown CC, Bloss LL. An epizootic of malignant catarrhal fever in a large captive herd of white-tailed deer (*Odocoileus virginianus*). *J Wildl Dis* [Internet]. 1992 [cited 2023 May 16];28(2):301–5. Available from: <https://pubmed.ncbi.nlm.nih.gov/1602586/>
89. Rossiter PB. A lack of readily demonstrable virus antigens in the tissues of rabbits and cattle infected with malignant catarrhal fever virus. *Br Vet J* [Internet]. 1980 [cited 2023 May 16];136(5):478–83. Available from: <https://pubmed.ncbi.nlm.nih.gov/6784880/>
90. Wright H, Stewart JP, Ireri RG, Campbell I, Pow I, Reid HW, et al. Genome re-arrangements associated with loss of pathogenicity of the γ -herpesvirus alcelaphine herpesvirus-1. *Res Vet Sci* [Internet]. 2003 [cited 2023 May 16];75(2):163–8. Available from: <https://pubmed.ncbi.nlm.nih.gov/12893166/>
91. Martins M de SN, Castro AMMG de, Lima M dos S, Pinto V da SC, Silva TG da, Fava C Del, et al. Malignant Catarrhal Fever in Brazilian cattle presenting with neurological syndrome. *Braz J Microbiol* [Internet]. 2017 Apr 1 [cited 2023 May 16];48(2):366–72. Available from: <https://pubmed.ncbi.nlm.nih.gov/28081979/>
92. Russell GC, Scholes SF, Twomey DF, Courtenay AE, Grant DM, Lamond B, et al. Analysis of the genetic diversity of ovine herpesvirus 2 in samples from livestock with malignant catarrhal fever. *Vet Microbiol* [Internet]. 2014 Aug 6 [cited 2023 May 16];172(1–2):63–71. Available from: <https://pubmed.ncbi.nlm.nih.gov/24846753/>

93. Hart J, Ackermann M, Jayawardane G, Russell G, Haig DM, Reid H, et al. Complete sequence and analysis of the ovine herpesvirus 2 genome. *J Gen Virol* [Internet]. 2007 Jan [cited 2023 May 16];88(Pt 1):28–39. Available from: <https://pubmed.ncbi.nlm.nih.gov/17170433/>
94. Headley SA, de Lemos GAA, Dall Agnol AM, Xavier AAC, Depes VCA, Yasumitsu CY, et al. Ovine gammaherpesvirus 2 infections in cattle without typical manifestations of sheep-associated malignant catarrhal fever and concomitantly infected with bovine coronavirus. *Brazilian Journal of Microbiology* [Internet]. 2022 Mar 1 [cited 2023 Mar 6];53(1):433–46. Available from: <https://link.springer.com/article/10.1007/s42770-021-00653-6>
95. Severi B, Landini MP, Cenacchi G, Zini N, Maraldi NM. Human cytomegalovirus nuclear and cytoplasmic dense bodies. *Arch Virol* [Internet]. 1992 Mar [cited 2023 Mar 6];123(1–2):193–207. Available from: <https://link.springer.com/article/10.1007/BF01317149>
96. Riaz A. Recent Understanding of the Classification and Life Cycle of Herpesviruses: A Review Detection and Molecular Characterization of Mastitis, Mammilitis and Reproductive tract disorders causing Herpesviruses in Dairy Cattles View project Establishing animal gut microbial species catalogue by metagenomic sequencing View project. 2017 [cited 2023 Mar 6]; Available from: <https://www.researchgate.net/publication/320033956>
97. O’Toole D, Li H. The pathology of malignant catarrhal fever, with an emphasis on ovine herpesvirus 2. *Vet Pathol* [Internet]. 2014 Mar [cited 2023 May 16];51(2):437–52. Available from: <https://pubmed.ncbi.nlm.nih.gov/24503439/>
98. Russell GC, Stewart JP, Haig DM. Malignant catarrhal fever: A review. *Veterinary Journal*. 2009 Mar;179(3):324–35.
99. Amoroso MG, Galiero G, Fusco G. Genetic characterization of ovine herpesvirus 2 strains involved in water buffaloes malignant catarrhal fever outbreaks in Southern Italy. *Vet Microbiol*. 2017 Feb 1;199:31–5.
100. Li H, Brooking A, Cunha CW, Highland MA, O’Toole D, Knowles DP, et al. Experimental induction of malignant catarrhal fever in pigs with ovine herpesvirus 2 by intranasal nebulization. *Vet Microbiol* [Internet]. 2012 Oct 12 [cited 2022 Nov 6];159(3–4):485–9. Available from: <https://pubmed.ncbi.nlm.nih.gov/22560763/>
101. Foyle KL, Fuller HE, Higgins RJ, Russell GC, Willoughby K, Rosie WG, et al. Malignant catarrhal fever in sika deer (*Cervus nippon*) in the UK. *Vet Rec* [Internet]. 2009 Oct 10 [cited 2022 Nov 6];165(15):445–7. Available from: <https://pubmed.ncbi.nlm.nih.gov/19820260/>
102. Costa ÉA, Bomfim MRQ, Da Fonseca FG, Drumond BP, Coelho FM, Vasconcelos AC, et al. Ovine Herpesvirus 2 Infection in Foal, Brazil - Volume 15, Number 5—May 2009 - Emerging Infectious Diseases journal - CDC. *Emerg Infect Dis* [Internet]. 2009 May [cited 2022 Oct 26];15(5):844–5. Available from: https://wwwnc.cdc.gov/eid/article/15/5/08-1664_article
103. Gailbreath KL, Taus NS, Cunha CW, Knowles DP, Li H. Experimental infection of rabbits with ovine herpesvirus 2 from sheep nasal secretions. *Vet Microbiol*. 2008 Nov 25;132(1–2):65–73.

104. Li H, Cunha CW, Taus NS. Malignant Catarrhal Fever: Understanding Molecular Diagnostics in Context of Epidemiology. *International Journal of Molecular Sciences* 2011, Vol 12, Pages 6881-6893 [Internet]. 2011 Oct 18 [cited 2022 Oct 26];12(10):6881–93. Available from: <https://www.mdpi.com/1422-0067/12/10/6881/htm>
105. Nelson DD, Taus NS, Schneider DA, Cunha CW, Davis WC, Brown WC, et al. Fibroblasts express OvHV-2 capsid protein in vasculitis lesions of American bison (*Bison bison*) with experimental sheep-associated malignant catarrhal fever. *Vet Microbiol*. 2013 Oct 25;166(3–4):486–92.
106. Sood R KNBS. *Emerging and Re-emerging Infectious Diseases of Livestock*. 2017. 347–362 p.
107. O’Toole D, Li H, Sourk C, Montgomery DL, Crawford TB. Malignant Catarrhal Fever in a Bison (*Bison Bison*) Feedlot, 1993–2000. *J Vet Diagn Invest* [Internet]. 2002 Jun 25 [cited 2022 Oct 26];14(3):183–93. Available from: <https://journals.sagepub.com/doi/10.1177/104063870201400301>
108. O’Toole D, Li H, Sourk C, Montgomery DL, Crawford TB. Malignant catarrhal fever in a bison (*Bison bison*) feedlot, 1993-2000. *J Vet Diagn Invest* [Internet]. 2002 [cited 2023 May 16];14(3):183–93. Available from: <https://pubmed.ncbi.nlm.nih.gov/12033673/>
109. Traul DL, Taus NS, Oaks JL, O’Toole D, Rurangirwa FR, Baszler T V., et al. Validation of nonnested and real-time PCR for diagnosis of sheep-associated malignant catarrhal fever in clinical samples. *J Vet Diagn Invest* [Internet]. 2007 [cited 2023 May 16];19(4):405–8. Available from: <https://pubmed.ncbi.nlm.nih.gov/17609352/>
110. Wan SK, Castro AE, Heuschele WP, Ramsay EC. Enzyme-linked immunosorbent assay for the detection of antibodies to the alcelaphine herpesvirus of malignant catarrhal fever in exotic ruminants. *Am J Vet Res* [Internet]. 1988 Feb 1 [cited 2023 May 16];49(2):164–8. Available from: <https://europepmc.org/article/med/3348526>
111. Rossiter PB. Immunofluorescence and immunoperoxidase techniques for detecting antibodies to malignant catarrhal fever in infected cattle. *Trop Anim Health Prod* [Internet]. 1981 [cited 2023 May 16];13(4):189–92. Available from: <https://pubmed.ncbi.nlm.nih.gov/7046177/>
112. Herring A, Reid H, Inglis N, Pow I. Immunoblotting analysis of the reaction of wildebeest, sheep and cattle sera with the structural antigens of alcelaphine herpesvirus-1 (malignant catarrhal fever virus). *Vet Microbiol* [Internet]. 1989 [cited 2023 May 16];19(3):205–15. Available from: <https://pubmed.ncbi.nlm.nih.gov/2718352/>
113. Sentsui H, Nishimori T, Nagai I, Nishioka N. Detection of sheep-associated malignant catarrhal fever virus antibodies by complement fixation tests. *J Vet Med Sci* [Internet]. 1996 [cited 2023 May 16];58(1):1–5. Available from: <https://pubmed.ncbi.nlm.nih.gov/8645750/>
114. Li H, Shen DT, Knowles DP, Gorham JR, Crawford TB. Competitive inhibition enzyme-linked immunosorbent assay for antibody in sheep and other ruminants to a conserved epitope of malignant catarrhal fever virus. *J Clin Microbiol* [Internet]. 1994 [cited 2023 May 16];32(7):1674–9. Available from: <https://pubmed.ncbi.nlm.nih.gov/7523438/>

115. Mushi EZ, Plowright W. A microtitre technique for the assay of malignant catarrhal fever virus and neutralising antibody. *Res Vet Sci.* 1979 Sep 1;27(2):230–2.
116. Decaro N, Tinelli A, Pratelli A, Martella V, Tempesta M, Buonavoglia C. First two confirmed cases of malignant catarrhal fever in Italy. *New Microbiol [Internet].* 2003 Oct 1 [cited 2023 May 16];26(4):339–44. Available from: <https://europepmc.org/article/med/14596344>
117. Dubuisson J, Thiry E, Bublot M, Sneyers M, Boulanger D, Guillaume J, et al. Production and characterization of monoclonal antibodies to bovid herpesvirus-4. *Vet Microbiol [Internet].* 1989 [cited 2023 May 16];19(4):305–15. Available from: <https://pubmed.ncbi.nlm.nih.gov/2546320/>
118. Li D, Shen DT, Davis WC, Knowles DP, Gorham JR, Crawford TB. Identification and characterization of the major proteins of malignant catarrhal fever virus. *J Gen Virol [Internet].* 1995 [cited 2023 May 16];76 (Pt 1)(1):123–9. Available from: <https://pubmed.ncbi.nlm.nih.gov/7844521/>
119. Alhajri SM, Cunha CW, Knowles DP, Li H, Taus NS. Evaluation of glycoprotein Ov8 as a potential antigen for an OvHV-2-specific diagnostic assay. *PLoS One [Internet].* 2018 Jul 1 [cited 2023 May 16];13(7). Available from: <https://pubmed.ncbi.nlm.nih.gov/29966004/>
120. Plowright W, Ferris RD. The Preparation of Bovine Thyroid Monolayers for use in Virological Investigations. *Res Vet Sci.* 1961 Apr 1;2(2):149–53.
121. Castro AE, Daley GG, Zimmer MA, Whitenack DL, Jensen J. Malignant catarrhal fever in an Indian gaur and greater kudu: experimental transmission, isolation, and identification of a herpesvirus. *Am J Vet Res [Internet].* 1982 Jan 1 [cited 2023 Mar 6];43(1):5–11. Available from: <https://europepmc.org/article/med/7091816>
122. Li H, Taus NS, Jones C, Murphy B, Evermann JF, Crawford TB. A devastating outbreak of malignant catarrhal fever in a bison feedlot. *J Vet Diagn Invest [Internet].* 2006 [cited 2023 May 16];18(1):119–23. Available from: <https://pubmed.ncbi.nlm.nih.gov/16566270/>
123. Aluja A; Rocha T.C; Velázquez A. Fiebre catarral maligna Fiebre catarral maligna. *Técnica Pecuaria.* 1969;1–8.
124. Pérez-Guiot A, Páez-Trejo A, Domínguez-Hernández Y, Carranza-Velázquez J, Hernández-García D, Carrisoza-Urbina I, et al. Pakistan Veterinary Journal Malignant Catarrhal Fever Associated with Ovine Gammaherpes virus-2 in Domestic Ruminants in Queretaro, Mexico. [cited 2023 May 16]; Available from: <http://dx.doi.org/10.29261/pakvetj/2022.076>
125. English D, Andersen BR. Single-step separation of red blood cells, granulocytes and mononuclear leukocytes on discontinuous density gradients of Ficoll-Hypaque. *J Immunol Methods.* 1974 Aug 1;5(3):249–52.
126. Baxter SIF, Pow I, Bridgen A, Reid HW. PCR detection of the sheep-associated agent of malignant catarrhal fever. *Archives of Virology* 1993 132:1 [Internet]. 1993 Mar [cited 2022 Oct 25];132(1):145–59. Available from: <https://link.springer.com/article/10.1007/BF01309849>
127. High Pure PCR Template Preparation Kit. 2020;

128. Li H, Shen DT, O'toole D, Knowles DP, Gorham JR, Crawford TB, et al. Investigation of sheep-associated malignant catarrhal fever virus infection in ruminants by PCR and competitive inhibition enzyme-linked immunosorbent assay. *J Clin Microbiol* [Internet]. 1995 [cited 2022 Oct 26];33(8):2048–53. Available from: <https://journals.asm.org/doi/10.1128/jcm.33.8.2048-2053.1995>
129. Posada D. jModelTest: Phylogenetic Model Averaging. *Mol Biol Evol* [Internet]. 2008 Jul 1 [cited 2023 May 16];25(7):1253–6. Available from: <https://academic.oup.com/mbe/article/25/7/1253/1045159>
130. Orós J, Poveda JB, Rodríguez JL, Franklin CL, Fernández A. Natural Cilia-Associated Respiratory Bacillus Infection in Rabbits Used for Elaboration of Hyperimmune Serum Against *Mycoplasma* sp. *Journal of Veterinary Medicine, Series B*. 1997;44(5):313–7.
131. Rossiter PB. Immunofluorescence and immunoperoxidase techniques for detecting antibodies to malignant catarrhal fever in infected cattle. *Trop Anlm Hlth Prod*. 1981;13–189.
132. Headley SA, de Lemos GAA, Dall Agnol AM, Xavier AAC, Depes VCA, Yasumitsu CY, et al. Ovine gammaherpesvirus 2 infections in cattle without typical manifestations of sheep-associated malignant catarrhal fever and concomitantly infected with bovine coronavirus. *Brazilian Journal of Microbiology* [Internet]. 2022 Mar 1 [cited 2022 Oct 26];53(1):433–46. Available from: <https://link.springer.com/article/10.1007/s42770-021-00653-6>
133. O'Toole D, Li H, Sourk C, Montgomery DL, Crawford TB. Malignant catarrhal fever in a bison (*Bison bison*) feedlot, 1993-2000. *J Vet Diagn Invest* [Internet]. 2002 [cited 2023 May 16];14(3):183–93. Available from: <https://pubmed.ncbi.nlm.nih.gov/12033673/>
134. Goss LW, Cole CR, Kissling RE. The Pathology of Malignant Catarrhal Fever (Bovine Epitheliosis): With Special Reference to Cytoplasmic Inclusions*. *Am J Pathol* [Internet]. 1947 Sep 1 [cited 2022 Oct 26];23(5):837. Available from: <https://www.ncbi.nlm.nih.gov/pmc/articles/PMC1934312/>
135. Severi B, Landini MP, Cenacchi G, Zini N, Maraldi NM. Human cytomegalovirus nuclear and cytoplasmic dense bodies. *Arch Virol* [Internet]. 1992 Mar [cited 2023 May 16];123(1–2):193–207. Available from: <https://pubmed.ncbi.nlm.nih.gov/1372496/>
136. Nelson DD, Taus NS, Schneider DA, Cunha CW, Davis WC, Brown WC, et al. Fibroblasts express OvHV-2 capsid protein in vasculitis lesions of American bison (*Bison bison*) with experimental sheep-associated malignant catarrhal fever. *Vet Microbiol* [Internet]. 2013 Oct 25 [cited 2023 May 16];166(3–4):486–92. Available from: <https://pubmed.ncbi.nlm.nih.gov/23953727/>

10. Artículos científicos generados durante el desarrollo de los estudios de doctorado.

Comparative Immunology, Microbiology and Infectious Diseases 80 (2022) 101736



Contents lists available at ScienceDirect

Comparative Immunology, Microbiology and Infectious Diseases

journal homepage: www.elsevier.com/locate/cimid



Assessment of the hemagglutinating activity of the *Porcine orthorubulavirus*

Ricardo Rodrigo Albarrán-Rodríguez^a, Hector Castillo-Juarez^{b,1}, Francisco Rivera-Benítez^c, Gabriel R. Campos-Montes^d, Blanca Espinosa^e, Tania Lucia Madrigal-Valencia^a, Erika Nayeli Salazar Jimenez^a, Humberto Ramírez-Mendoza^{a,*}

^a Departamento de Microbiología e Inmunología, Facultad de Medicina, Veterinaria y Zootecnia, Universidad Nacional Autónoma de México, Ciudad Universitaria, Circuito Exterior, Coyoacán, C.P. 04510 Mexico City, Mexico

^b Departamento de Producción Agrícola y Animal, Universidad Autónoma Metropolitana, Unidad Xochimilco, Calzada del Hueso 1100, Coyoacán, C.P. 04960 Mexico City, Mexico

^c Centro Nacional de Investigación Disciplinaria en Salud Animal e Inocuidad, Instituto Nacional de Investigaciones Forestales, Agrícolas y Pecuarias, Km. 15.5 Carretera México-Toluca, C.P. 05110 Mexico City, Mexico

^d Departamento El Hombre y su Ambiente, Universidad Autónoma Metropolitana, Unidad Xochimilco, Calzada del Hueso 1100, Coyoacán, C.P. 04960 Mexico City, Mexico

^e Departamento de Bioquímica, Instituto Nacional de Enfermedades Respiratorias, SSA, Calzada de Tlalpan 4502, Belisario Domínguez Secc 16, Tlalpan, C.P.14080 Mexico City, Mexico

ARTICLE INFO

Keywords

Porcine orthorubulavirus
Blue eye disease
Hemagglutinating activity
Diagnosis

ABSTRACT

Blue eye disease (BED) in pigs is caused by *Porcine orthorubulavirus* (PRV) of the *Paramyxoviridae* family. It is an endemic disease in swine production in the central region of Mexico and causes nervous signs and high mortality in suckling pigs, pneumonia in growing pigs, orchitis in boars and mummification during gestation. PRV hemagglutinates most red blood cells (RBCs) of domestic species. For serological diagnosis, the hemagglutination inhibition test is used, and in this test, guinea pig, bovine and chicken RBCs have been commonly used. In this investigation, hemagglutination with PRV was evaluated using the RBCs of seven domestic species (chicken, bovine, horse, pig, dog, guinea pig and rabbit). In the hemagglutination test, the following parameters were evaluated: temperature (25 °C and 37 °C), bottoms of the wells (V and U), erythrocyte concentration (0.5%, 0.75%, and 1%), and reading time (15, 30, 45, 60 and 90 min). Significant differences ($P < 0.001$) were found in most of the evaluated treatments. The best hemagglutination results were obtained with chicken, bovine and horse RBCs. The hemagglutination titer is higher (2 dilutions) when using chicken RBCs than when using bovine or horse RBCs. If chicken RBCs are used in the inhibition of hemagglutination, the test will be more sensitive, while it is more specific when bovine or horse RBCs are used. The hemagglutination readings are imprecise when using RBCs from dogs, pigs, guinea pigs and rabbits. RBCs from these species should not be used for the diagnosis or investigation of PRV.

1. Introduction

Porcine orthorubulavirus (PRV) is a member of the *Paramyxoviridae* family and the Mononegavirales order [1,2,3]. This virus is the causal agent of blue eye disease (BED) in pigs. PRV affects piglets of less than 15 days of age, causing high mortality (90–100%) associated to neurological disorders [4]. In weaned pigs, growth retardation and reduced feed

conversion efficiency, interstitial pneumonia are observed [5]. In gestational gilts, the virus is able to cross the placental barrier, which leads to embryonic reabsorptions, stillbirths, and mummifications [6]. In boars in stud, the main affectionation is the presence of orchitis and, although there is recovery, the virus remains in the semen for long periods; hence, viral elimination is slow [7,8]. Corneal opacity occurs in 1–5% of pigs in all stages [4].

* Correspondence to: Departamento de Microbiología e Inmunología, Facultad de Medicina Veterinaria y Zootecnia, Universidad Nacional Autónoma de México, Ciudad Universitaria, Colonia Copilco, Coyoacán, C.P. 04510 Mexico City, Mexico.

E-mail addresses: ricardo-pxol@hotmail.com (R.R. Albarrán-Rodríguez), rivera.francisco@inifap.gob.mx (F. Rivera-Benítez), gabocamo@gmail.com (G.R. Campos-Montes), bespinosa1118@yahoo.com.mx (B. Espinosa), a.nia.90@hotmail.com (T.L. Madrigal-Valencia), erika-alex16@hotmail.com (E.N.S. Jimenez), betosram@comunidad.unam.mx, betosram@yahoo.es (H. Ramírez-Mendoza).

¹ Deceased, March 18, 2019.

<https://doi.org/10.1016/j.cimid.2021.101736>

Received 27 February 2021; Received in revised form 28 November 2021; Accepted 29 November 2021

Available online 1 December 2021

0147-9571/© 2021 Elsevier Ltd. All rights reserved.

The hemagglutinating capacity of enveloped viruses is mediated by the recognition and the binding of the hemagglutinin glycoprotein with a variant of sialic acid (Sia) or of neuraminic acid (Neu) on the surface of RBCs. For PRV, it is known that its receptor is NeuAc α 2,3 Gal [9] which was identified through infectivity inhibition assays in monolayers of Vero cells with the lectin from *Maackia amurensis*, which completely inhibited the infectivity, as it is specific for the NeuAc α 2,3 Gal disaccharide. With aid of lectins, it has been possible to establish that the NeuAc α 2,3 Gal receptor is present differentially in organs of newly born and adult pigs [10] which seems to correspond to the clinical manifestation of the different stages.

It is common to use the hemagglutination inhibition test for the serological diagnosis of viruses that agglutinate, but before performing this test, it must be established that the virus possesses from 4 to 8 hemagglutinating units (HAUs) in RBCs adequate for each virus to be evaluated.

PRV is capable of agglutinating RBCs of most domesticated species [4]; however, there are more NeuAc α -2,6-Gal molecules than NeuAc α -2,3-Gal molecules on the surfaces of RBCs from humans (blood group O), turkeys, pigs, and guinea pigs, whereas in chicken and goose RBCs, the concentrations of these sialic acids are the reverse [11].

Due to the variability in the concentration of sialic acid in RBCs of the different species, the goal of this study was to assess the hemagglutinating behavior of PRV in dog, chicken, guinea pig, cow, horse, rabbit, and pig RBCs.

2. Materials and methods

2.1. RBCs

We obtained RBCs from five animals of each of the following species: domestic chickens, horses, pigs, rabbits, guinea pigs, dogs, and bovine. The five animals of each species were common animals, of similar age (provided by the different teaching centers of the Veterinary School of the National Autonomous University of Mexico, UNAM). Blood samples were taken with Alsever's anticoagulant at a 1:1 proportion.

Washing of RBCs was performed by mixing the blood and the anticoagulant with a phosphate buffer solution (PBS, pH 7.4). Then, samples were centrifuged at 400 x g for 10 min; this process was repeated until the supernatant was completely transparent. From the five blood samples of each species, suspensions at 0.5%, 0.75%, and 1% were made [12].

2.2. Virus

The PRV strain used was PAC-3/EF413173 (Jalisco/1992) virus was replicated in a cell culture of the ovine choroidal plexus in 75-mL flasks for 72 h. Cultures were grown in Dulbecco's modified Eagle's medium (DMEM) supplemented with 5% fetal bovine serum (FBS) and maintained at 37°C with 5% CO₂. When cells were 80% confluent, they were inoculated with viral suspension.

The infected cell culture was subjected to three cycles of heat-shock to obtain the highest amount of viral particles. This solution was centrifuged at 1500 x g for 30 min to eliminate detritus, and the supernatant was recovered and stored at -70 °C in aliquots. Viral stocks were titrated with the same cells. Tenfold serial dilutions (10⁻¹ to 10⁻⁹) of virus were prepared and added to cells. After three days, the supernatants were collected and analyzed using a hemagglutination (HA) assay with 0.5% chicken RBCs.

2.3. Hemagglutination test

Polystyrene 96-well microtiter plates of two types, U- and V-shaped, were used (Thermo Fisher cat. 2205, Thermo Fisher cat. 2605). Both types of microtiter plates (U- and V-shaped) were supplemented with 50 μ L of PBS (pH 7.4) to dilute the virus; 50 μ L of the virus was placed in the

Table 1

Levels * of explanatory variables evaluated for hemagglutination to the *Porcine orthorubulavirus*.

Variable	Levels assessed
Species	chicken, bovine, horse, pig, rabbit, guinea pig, dog
Erythrocyte concentration (%)	0.5, 0.75, 1.0
Reading time (minutes)	15, 30, 45, 60, 90
Incubation temperature (°C)	25, 37
Plate bottom shape	"U" bottom, "V" bottom
Volume (μ L)	25, 50

* All possible combinations were made with the various levels of each variable.

first well. Serial double dilutions were performed, starting with 1:2 and continuing to 1:4096.

Once the virus had been diluted, 50 μ L of each erythrocyte suspension was added (final volume 100 μ L per well). Three replicates were performed for each treatment. Each replicate was made in different plates so that the readings could be performed by three different people. This same procedure was followed with 25- μ L volumes. By diluting the virus to 25- μ L volumes, the volume of each well was of 50 μ L (25 μ L of diluted virus and 25 μ L of RBCs). Reading times were at 15, 30, 45, 60, and 90 min, the erythrocyte suspensions were 0.5, 0.75%, and 1% and tests were evaluated at 37 °C and 25 °C.

All the aforementioned procedures were performed with the RBCs of each animal of the seven species. RBCs suspended in PBS were used as negative controls for each test. The time of sedimentation was assessed in these RBCs. The different levels for each explanatory variable are summarized in Table 1.

To assess the hemagglutination reading, three categories were determined, and values of 0, 1 and 2 were assigned and were considered ordinal variables. The first category was assigned the number (0), which corresponds to the elapsed time from the time the RBCs were placed in the wells until the time when the reading could be made; here, it was not yet possible to differentiate the sedimentation of control RBCs and hemagglutination.

The number (1) was assigned to the elapsed time at which it was clearly possible to perform the reading of both the sedimentation and hemagglutination. The number (2) was assigned to the elapsed time at which the reading of hemagglutination and sedimentation was not accurate and corresponds to the elution phenomenon. The assignment of the samples to the corresponding level was made from the mode of the evaluation resulting from 3 different observers for each sample.

The data were analyzed using ordinal logistic regression analysis to evaluate the differences in reading type over time between species and subsequently to determine the effects involved in the response of each species.

3. Results

3.1. Results according to the erythrocyte species used

The statistical analysis in Tables A1-A3 describe the three stages corresponding to hemagglutination. The first stage corresponds to the start of the test (it was assigned the value of 0). The second stage corresponds to hemagglutination and sedimentation (it was assigned the value of 1). The last stage corresponds to elution or the reading of hemagglutination and sedimentation was not accurate (it was assigned the value of 2). These three stages allow to visualize the difference in the hemagglutination of the erythrocytes of the different species. The erythrocyte species and the time of observation were related ($P < 0.001$) to the results of the test categories.

In general, as the observation time elapsed, the number of cases without hemagglutination decreased (Table A1).

At 60 min, hemagglutination was present in at least 90% of the wells in which chicken, bovine and horse RBCs were used; in the latter (horse), at minute 90, hemagglutination was achieved in 99.2% of wells. In the

other species, wells did not reach 70% hemagglutination at 60 min. Regarding rabbit RBCs, hemagglutination was achieved in only 1.7% of wells (Table A2).

In all cases, the percentage of wells that presented elution increased with advancing time, except for horse RBCs, which did not present the phenomenon during the whole observation time (Table A3).

The average titer of hemagglutination is different for each type of erythrocytes from the different species. There is a differential dilution in the hemagglutinating titer between the chicken and bovine erythrocytes; there is a 2-times higher titer between the guinea pig and bovine erythrocytes, and the difference in the hemagglutinating titer is also much higher (1.26 times) between the dog and bovine erythrocytes. In addition to these differences among the averages, the standard deviation must also be considered, which is quite wide with pig, rabbit, guinea pig and dog erythrocytes. At the moment of titrating the virus through hemagglutination, there can be a difference of more than two viral dilutions when different erythrocyte species are used. Titers of the hemagglutination inhibition test will be different when using erythrocytes of different species; hence, they cannot be used randomly.

3.2. Analysis of the effects within a species

For all species, the assessed effects (bottom of plate, erythrocyte concentration, viral suspension volume, and incubation temperature) were generally significant ($P < 0.05$), except for the viral suspension volume effect with the chicken RBCs and the incubation temperature with the horse RBCs (Table B1).

3.3. Bottom of well (U- and V-shaped)

In the readings at 60 min, the wells with chicken and horse RBCs presented mild discrepancies in their distribution regarding the presence of hemagglutination between the U-shaped wells (50.0% for both species) and the V-shaped wells (46.7% for chicken and 47.5% for horse). For bovine RBCs, the percentage was the same for both types of wells (45%). For pig RBCs, the U-shaped plates presented a lower percentage of wells with hemagglutination (11.7% vs. 20%), contrasting with the guinea pig (30.8% vs. 35.0%) and dog RBCs (28.3% vs. 30.8%); hemagglutination readings with rabbit RBCs were 0.8% for both types of plates.

3.4. Erythrocyte concentration (0.5%, 0.75%, and 1.0%)

For chicken, bovine, and horse RBCs, the distribution of samples with hemagglutination was homogeneous with the three concentrations used. For the remainder of the species, the 1% erythrocyte concentration had the highest percentage of wells with hemagglutination.

3.5. Viral suspension volume (25 and 50 μ L)

No difference was observed in the percentages of wells with hemagglutination at 60 min based on the viral suspension volumes of 25 and 50 μ L when using chicken (47.5% vs. 49.2%) or rabbit (0.8% at both levels) RBCs. The 25- μ L volume presented higher percentages of hemagglutination than the 50- μ L volume with horse (50% vs. 40%) and pig RBCs (21.7% vs. 10.0%). Conversely, the 50- μ L volume had higher percentages of hemagglutination with respect to the 25- μ L volume in bovine (50% vs. 40%), guinea pig (50% vs. 15.8%), and dog RBCs (44.2% vs. 15.0%).

3.6. Incubation temperature (25 °C and 37 °C)

At 60 min, horse RBCs revealed no differences between temperatures in the percentages of wells with hemagglutination (48.3% for 25 °C and 49.2% for 37 °C), whereas small differences were detected in the percentages of hemagglutination with chicken (50% for 25 °C and 46.7%

for 37 °C) and bovine (44.2% for 25 °C and 45.8% for 37 °C) RBCs; in both cases, the wells without hemagglutination presented elution at 37 °C. The guinea pig RBCs did not present differences between temperatures in the percentages of hemagglutination (32.5% for 25 °C and 33.3% for 37 °C); however, the percentage of wells without hemagglutination was higher at 25 °C. For dog and pig RBCs, higher percentages of hemagglutination were found at 25 °C (38.3% at 25 °C and 20.8% at 37 °C for dog and 27.5% at 25 °C and 4.2% at 37 °C for pig); in both species, elution occurred more often at 37 °C. Rabbit RBCs presented the highest percentages of elution at 37 °C, and no hemagglutination occurred from 30 min onward.

It is important to know the moment at which elution occurs because in the laboratories, many sera are evaluated, and it is frequently observed that there is a time interval of 30 min between the first and the last readings for each plate. In our work, with guinea pig RBCs at 37 °C, elution occurred at 45 min in volumes of 25- μ L and 50- μ L in U- and V-shaped plates at erythrocyte concentrations of 0.75% and 1%. When U-shaped plates were used, the sedimentation of guinea pig RBCs was nonspecific at concentrations of 0.50% and 0.75% at 25 °C.

4. Discussion

Moreno Lopez et al., in the research publication that characterized the virus and classified it as *Porcine rubulavirus*, used the hemagglutination test, and the authors described that the test was performed using conventional methods, and elution was observed after a few minutes; however, some doubts arose. For example, what is the conventional methodology for hemagglutination? What amount of time corresponded to the few minutes needed for the elution to occur? These questions reveal that both the methodology and the results are not precise. In this work, in the results of the hemadsorption test, elution was observed in all cell cultures when using guinea pig RBCs [13].

Among the first research works on the BED virus in pigs, it was described that the virus hemagglutinates RBCs from different species (chicken, guinea pig, human groups A, B, and AB, mouse, rat, bovine, horse, goat, and sheep); it is also described that elution was observed with all RBCs of all analyzed species between 30 and 60 min at 37 °C (Stephano HA et al., 1988). However, the publication does not describe what parameters were used in the test, such as erythrocyte concentration, type of plate, time elapsed for the readings, volume of the viral suspension, and the volume of the erythrocyte suspension [4].

Subsequently, other authors used guinea pig RBCs at 1% in V-shaped plates, and the readings were performed once sedimentation was observed. In this investigation, they only evaluated three piglets [14].

Other authors, aiming at knowing the prevalence of the virus in different states of Mexico, used the hemagglutination inhibition test. The test was performed with guinea pig RBCs at 37 °C. Mexico consists of 32 states; in this work, pig sera samples were obtained from 27 states. Of these, 10 states had animals with antibodies against the BED [15]. The geographical conditions and the characteristics of porcine production in some of these states with positive results, but that had always been disease-free, were analyzed, and serology indicated that there were animals with antibodies against this disease. This was due to the lack of standardization of the hemagglutination and hemagglutination inhibition tests, leading to false positive results.

All of these research on PRV have used guinea pig RBC. In the present research, we found that they were the least indicated for the hemagglutination test, because when guinea pig RBCs were used for the hemagglutination inhibition test against the BED, false-positive sera could be obtained because the sedimentation that is observed in the test does not correspond to the inhibition of hemagglutination but rather to the elution.

In the hemagglutination or the hemagglutination inhibition test for BED diagnosis, the species of RBCs to be used, the reading time, the erythrocyte concentrations, the temperature at which to perform the test, and the type of plate to be used have not been standardized.

Because of this, the hemagglutination inhibition test currently performed for *Porcine orthorubulavirus* is not reliable for diagnosis because laboratories use different RBCs from chicken, cows, or guinea pigs. In the current research, we observed that when modifying any of these parameters, the results change concomitantly.

Our results led us to conclude that it is not possible to use RBCs from different animal species randomly because the results differ when modifying the erythrocyte source, the erythrocyte concentration, the temperature, the type of plate and the reading time. Here, we observed that the best reading time when using chicken RBCs is between 30 and 60 min at 25 °C with U-shaped plates in a volume of 50 µL, whereas at 37 °C, elution is observed at 60 min. With bovine and horse RBCs, reliable readings of hemagglutination can be obtained starting at 60 min and even after 90 min, though no elution was observed after 6 h of observation (not quantified). Rabbit RBCs revealed that reliable readings could only be made with high erythrocyte concentrations (1%) and in V-shaped plates. At lower erythrocyte concentrations and in U-shaped plates, no sedimentation of RBCs occurred, not even in the wells with RBCs lacking the virus (control). When assessing hemagglutination with pig RBCs, the readings were not accurate during the entire evaluation time. Dog RBCs yielded less reliable hemagglutination readings. Chicken RBCs were the most reliable to perform the hemagglutination reading and had a low variation coefficient when assessing the hemagglutination-sedimentation and elution times. Guinea pig and RBCs should not be used in hemagglutination, the elution of RBCs occurs in less time when the hemagglutination is performed at 37 °C.

These differences in the hemagglutinating titer observed among the RBCs of the different species allows the inference that the hemagglutination inhibition test will be more specific when using bovine RBCs and more sensitive when using chicken RBCs.

We found a difference in the sedimentation time. With chicken RBCs, sedimentation began at 30 min, whereas with bovine and horse RBCs, sedimentation began after 60 min. With rabbit RBCs, no sedimentation was observed, especially when using U-shaped plaques.

5. Conclusions

To perform hemagglutination with the PRV, the best parameters are to use chicken RBCs with U-shaped bottom plaques, at room temperature (25 °C), at a 0.5% RBCs concentration, the reading time must be between 30 and 60 min, and with diluent volumes of 50 µL, of the virus of 50 µL, and of RBCs of 50 µL.

Horse and bovine RBCs can also be used with the same parameters mentioned before; however, the hemagglutination titer is between 2 dilutions lower than that observed with chicken RBCs. The reading time must be from 60 min on, and no elution is observed for several hours.

In the hemagglutination or the hemagglutination inhibition test for the PRV, guinea pig, pig, dog, or rabbit RBCs should not be used because readings are not accurate.

Ethical statement

The blood samples were taken by the responsible veterinarians and no permissions were necessary to collect the specimens used in the study.

Author's contributions

Albarrán-Rodríguez, Madrigal-Valencia, Salazar-Jimenez; contributed to main experiments. Castillo-Juarez and Campos Montes contributed to the statistical analysis. Espinosa B. contributed to revision

of the manuscript. Ramírez-Mendoza and Rivera-Benitez designed the experiment and drafted the manuscript.

Conflict of interest

The authors declare that they have no conflict of interest.

Data Availability

The data that support the findings of this study are available from the corresponding author.

Acknowledgements

Funding. This study was partially financed by PAPIIT-UNAM (IT-201918) and SEP-CONACYT (no. CB-2016-01-284863).

Appendix A

See Tables A1–A3

Table A1

Percentage of wells without hemagglutination at different times in the seven species (category 0: time at starting the test in which no defined sedimentation was observed).

Species	Time of observation (min)				
	15	30	45	60	90
<i>Chicken</i>	17.5	1.7	0.8	0.0	0.0
<i>Bovine</i>	90.8	29.2	12.5	7.5	1.7
<i>Horse</i>	83.3	17.5	3.3	2.5	0.8
<i>Pig</i>	89.2	67.5	41.7	28.3	16.7
<i>Rabbit</i>	87.5	44.5	23.3	14.2	7.5
<i>Guinea pig</i>	90.8	58.3	40.8	25.8	20.0
<i>Dog</i>	83.3	48.3	12.5	9.2	0.8

In each species, 120 wells were distributed in two types of plates (U and V), three erythrocyte concentrations (0.5%, 0.75%, and 1.0%), two different viral suspension volumes (25 µL and 50 µL), and two incubation temperatures (25 °C and 37 °C).

Table A2

Percentage of wells with hemagglutination at different times in the seven different species (category 1: interval of time in which agglutination and sedimentation was observed).

Species	Time of observation (min)				
	15	30	45	60	90
<i>Chicken</i>	79.2	95.8	96.7	96.7	92.5
<i>Bovine</i>	9.2	70.8	85.8	90.0	93.3
<i>Horse</i>	16.7	82.5	96.7	97.5	99.2
<i>Pig</i>	10.8	23.3	30.8	31.7	34.2
<i>Rabbit</i>	4.2	6.7	6.7	1.7	0.8
<i>Guinea pig</i>	9.2	36.7	53.3	65.8	66.7
<i>Dog</i>	16.7	38.3	60.0	59.2	55.8

In each species, 120 wells were distributed in two types of plates (U and V), three erythrocyte concentrations (0.5%, 0.75%, and 1.0%), two different viral suspension volumes (25 µL and 50 µL), and two incubation temperatures (25 °C and 37 °C).

Table A3

Percentage of wells with elution at different times in seven different species (category 2: the reading of hemagglutination and sedimentation was not accurate and corresponds to the elution phenomenon).

Species	Time of observation (min)				
	15	30	45	60	90
Chicken	3.3	2.5	2.5	3.3	7.5
Bovine	0.0	0.0	1.7	2.5	5.0
Horse	0.0	0.0	0.0	0.0	0.0
Pig	0.0	9.2	27.5	40.0	49.2
Rabbit	8.3	48.7	70.0	84.2	91.7
Guinea pig	0.0	5.0	5.8	8.3	13.3
Dog	0.0	13.3	27.5	31.7	43.3

In each species, 120 wells were distributed in two types of plates (U and V), three erythrocyte concentrations (0.5%, 0.75%, and 1.0%), two different viral suspension volumes (25 μ L and 50 μ L), and two incubation temperatures (25 °C and 37 °C).

Table B1

Levels of significance for the factors involved in hemagglutination tests to detect the PRV responsible for the BED using RBCs from seven different species, considering a logistic regression analysis.

Species*	Bottom of the well	Viral volume	Erythrocyte concentration	Incubation temperature	Observation time
Chicken	<0.0001	0.0704	<0.0001	0.0003	<0.0001
Bovine	0.0003	<0.0001	<0.0001	0.0011	<0.0001
Horse	0.0217	<0.0001	<0.0001	0.3756	<0.0001
Pig	<0.0001	<0.0001	<0.0001	<0.0001	<0.0001
Rabbit	<0.0001	0.0370	<0.0001	<0.0001	<0.0001
Guinea pig	<0.0001	<0.0001	<0.0001	0.0014	<0.0001
Dog	<0.0001	<0.0001	<0.0001	<0.0001	<0.0001

* Previous analysis detected significant differences among species ($P < 0.0001$). Levels of effects: bottom of well (U and V shaped), viral volume (25 μ L and 50 μ L), erythrocyte concentration (0.5, 0.75, 1%), temperature (25°C, 37°C), observation time (15, 30, 45, 60, 90 min).

References

- [1] B. Rima, A. Balkema-Buschmann, W.G. Dundon, P. Duprex, A. Easton, R. Fouchier, G. Kurath, R. Lamb, B. Lee, P. Rota, L. Wang, Ictv report consortium. ICTV virus taxonomy profile: paramyxoviridae, *J. Gen. Virol.* 100 (2019) 1593–1594, <https://doi.org/10.1099/jgv.0.001328>.
- [2] B. Rima, A. P. Collins, R. Easton, G. Fouchier, R.A. Kurath, B. Lamb, A. Lee, P. Maisner, L.F. Rota, Wang, Problems of classification in the family Paramyxoviridae, *Arch. Virol.* 163 (2018) 1395–1404, <https://doi.org/10.1007/s00705-018-3720-2>.
- [3] L.F. Wang, E. Hansson, M. Yu, K.B. Chua, N. Mathe, G. Cramer, B.K. Rima, J. Moreno-López, B.T. Eaton, Full-length genome sequence and genetic relationship of two paramyxoviruses isolated from bat and pigs in the Americas, *Arch. Virol.* 152 (2007) 1259–1271, <https://doi.org/10.1007/s00705-007-0959-4>.
- [4] H.A. Stephano, G.M. Gay, T.C. Ramirez, Encephalomyelitis, reproductive failure and corneal opacity (blue eye) in pigs, associated with a paramyxovirus infection, *Vet. Record* 10 (1988) 2–6, <https://doi.org/10.1136/vr.122.1.6>.
- [5] J.F. Rivera-Benitez, S. Cuevas-Romero, A. Pérez-Torres, J. Reyes-Leyva, J. Hernández, H. Ramírez-Mendoza, Respiratory disease in growing pigs after Porcine rubulavirus experimental infection, *Virus Res.* 176 (2013) 137–143, <https://doi.org/10.1016/j.virusres.2013.05.017>.
- [6] P. Hernández-Jauregui, H. Ramírez-Mendoza, C. Mercado García, J. Moreno-López, S. Kennedy, Experimental porcine rubulavirus (La Piedad-Michoacán virus) infection in pregnant cells, *J. Comp. Pathol.* 130 (2004) 1–6, [https://doi.org/10.1016/S0021-9975\(03\)00058-6](https://doi.org/10.1016/S0021-9975(03)00058-6).
- [7] H. Ramírez-Mendoza, P. Hernández-Jauregui, J. Reyes-Leyva, E. Zenteno, J. Moreno-López, S. Kennedy, Lesions in the reproductive tract of boars experimentally infected with porcine rubulavirus, *J. Comp. Pathol.* 117 (1997) 237–252, [https://doi.org/10.1016/S0021-9975\(97\)80018-7](https://doi.org/10.1016/S0021-9975(97)80018-7).
- [8] J.F. Rivera-Benitez, R. Martínez Bautista, A. Pérez Torres, A.C. García-Contreras, J. Reyes-Leyva, J. Hernández, H. Ramírez-Mendoza, Persistence of porcine rubulavirus in experimentally infected boars, *Vet. Microbiol.* 162 (2013) 491–498, <https://doi.org/10.1016/j.vetmic.2012.10.037>.
- [9] J. Reyes-Leyva, B. Espinosa, G. Santos, R. Zenteno, J. Hernández, V. Vallejo, E. Zenteno, Purification and characterization of the Hemagglutinin-Neuraminidase of Porcine rubulavirus LPMV, *Glycoconj. J.* 16 (1999) 517–522, <https://doi.org/10.1023/A:1007022021301>.
- [10] V. Vallejo, J. Reyes-Leyva, J. Hernández, H. Ramírez, P. Delanoy, E. Zenteno, Differential expression of sialic acid on porcine organs during the maturation process, *Comp. Biochem. Physiol.* 126 (2000) 415–442, [https://doi.org/10.1016/S0305-0491\(00\)00213-3](https://doi.org/10.1016/S0305-0491(00)00213-3).
- [11] T. Ito, Y. Suzuki, H. Kida, Receptor specificity of influenza A viruses correlates with the agglutination of rbc from different animal species, *Virology* 499 (1997) 493–499, <https://doi.org/10.1006/vim.1996.8323>.
- [12] F.G. Barleson, T.M. Chambers, D.L. Wiedbrauk, *Virology: A Laboratory Manual*, Academic Press Inc, 1992.
- [13] J. Moreno-López, P. Correa-Girón, A. Martínez, A. Ericsson, Characterization of a paramyxovirus isolated from the brain of a piglet in Mexico, *Arch. Virol.* 91 (1986) 221–231, <https://doi.org/10.1007/BF01314282>.
- [14] F. McNeilly, I. Walker, G.M. Allan, J.C. Foster, T. Linne, M. Merza, P. Hernandez, S. Kennedy, B. Adair, A comparative study on the use of virus and antibody detection techniques for the diagnosis of La Piedad-Michoacán paramyxovirus (LPMV) infection in pigs, *J. Vet. Diagn. Investig.* 9 (1997) 3–9, <https://doi.org/10.1177/104063879700900102>.
- [15] M. Fuentes, R. Carreon, H. Ramírez, M.E. Trujillo, I. Fraire, Pilot study about the frequency of blue eye paramyxovirus antibodies in Mexican pigs, *Vet. México* 23 (1992) 37–39.



Research paper

Comparison of hemagglutination inhibition tests, immunoperoxidase monolayer assays, and serum neutralizing tests in detecting antibodies against blue eye disease in pigs



Diego Rafael Hidalgo-Lara^a, Jazmín De la Luz-Armendáriz^b, José Francisco Rivera-Benítez^c, Luis Gomez-Nuñez^c, Erika Nayeli Salazar-Jiménez^a, Tania Lucia Madrigal-Valencia^a, Humberto Ramírez-Mendoza^{a,*}

^a Departamento de Microbiología e Inmunología, Facultad de Medicina Veterinaria y Zootecnia, UNAM, Mexico City, Mexico

^b Departamento de Medicina y Zootecnia de Rumiantes, Facultad de Medicina Veterinaria y Zootecnia, UNAM, Mexico City, Mexico

^c Centro Nacional de Investigación Disciplinaria en Salud Animal e Inocuidad, Instituto Nacional de Investigaciones Forestales, Agrícolas y Pecuarias, Mexico City, Mexico

ARTICLE INFO

Keywords:

Porcine orthorubulavirus
Blue eye disease
Serological tests
Immunoperoxidase test
Hemagglutination inhibition test
Serum neutralizing test

ABSTRACT

Blue eye disease (BED) of pigs was identified in the early 1980s in La Piedad, Michoacan, Mexico. The causal agent is *Porcine orthorubulavirus* (PRV), which affects pigs of all ages, producing nervous, respiratory, and reproductive disorders. BED is geographically endemic to the center of Mexico, where 75% of the country's swine industry is concentrated. Due to its adverse effects on the swine industry and the risk of dissemination to other countries, it is essential to have reliable diagnostic methods for BED. The objective of this study was to establish the optimal conditions for three serological tests, hemagglutination inhibition (HI), immunoperoxidase monolayer assay (IPMA), and serum neutralization (SN), and to compare their sensitivity, specificity, κ coefficient, and predictive values. Twelve different HI protocols (9408 tests), one SN protocol and one IPMA protocol (784 tests, each) were evaluated. Forty-nine sera were analyzed, and thirty-seven sera showed true positive results, while twelve showed true negative results. The κ coefficient was used to assess the variation in each test. The best HI protocol registered a sensitivity and specificity of 89 and 100%, respectively, the IPMA test showed values of 85 and 100%, and the SN test registered a sensitivity of 91% and a specificity of 96%. One of the disadvantages of the HI test is that when chicken red blood cells (RBCs) are used, elution occurs in a short incubation time, which would decrease the specificity. The use of bovine RBCs increases the specificity of the test and makes it more stable, but it decreases the sensitivity. The results of HI and SN revealed the importance of eliminating the complement system of the serum and removing other inhibitors to avoid test nonspecificity. The IPMA test does not use an active virus; hence, it is considered safe and does not present any risk of disseminating PRV.

1. Introduction

Blue eye disease (BED) of pigs was first described in 1980 in the City of La Piedad, state of Michoacán, Mexico. Numerous outbreaks of encephalitis accompanied by corneal opacity and high mortality in piglets have been reported (Stephano et al., 1988). The causative virus was classified as belonging to the *Paramyxoviridae* family, *Rubulavirinae* subfamily, *Orthorubulavirus* genus, and *Porcine orthorubulavirus* (PRV) species (ICTV, 2019). PRV is an enveloped, negative-sense single-

stranded RNA virus. The receptor binding protein (RBP) possesses hemagglutinating activity, and the fusion protein possesses syncytium-forming properties (Moreno-López et al., 1986). Gene sequencing revealed that PRV is related to human mumps virus (41%), simian virus 5 (43%), human parainfluenza type 2 virus (38%) and type 4 virus (35%). Their identity is very high for the hemagglutinin-neuraminidase (HN) protein (Berg et al., 1991; Sundqvist et al., 1992).

Clinical signs of BED vary according to the age of the pigs, the production system, their management, and the presence of other diseases

* Corresponding author at: Departamento de Microbiología e Inmunología, Facultad de Medicina Veterinaria y Zootecnia, Universidad Nacional Autónoma de México, Ciudad Universitaria, Colonia Copilco, Alcaldía Coyoacán, C.P. 04510 Ciudad de México, Mexico.

E-mail address: betosram@comunidad.unam.mx (H. Ramírez-Mendoza).

<https://doi.org/10.1016/j.jim.2021.113088>

Received 11 October 2020; Received in revised form 31 May 2021; Accepted 22 June 2021

Available online 26 June 2021

0022-1759/© 2021 Elsevier B.V. All rights reserved.

(Stephano et al., 1988). Epidemiological evaluations have indicated that the disease is endemic to the central and central-western zones of Mexico (Escobar-López et al., 2012). A humoral immune response is detected in the first week postinfection, with titers of 4–8 (\log_2) being obtained in hemagglutination inhibition (HI) and sero-neutralization (SN) tests. Immunoelectrophoretic assays showed that HN is the most immunogenic protein, as determined by the presence of specific antibodies in 85.7% of the sera evaluated in the second week after infection and 100% of the sera starting in the third week. For serological diagnosis, the most commonly used test is HI; other tests used for serological diagnosis are indirect immunofluorescence (IFI) and SN tests and enzyme-linked immunosorbent assays (ELISAs) (McNeilly et al., 1997; Nordengrahn et al., 1999).

Currently, no commercial ELISA test is available for BED in Mexico. At the end of the 1990s, a competitive ELISA test developed in Sweden (Svanova Biotech AB, Uppsala, Sweden) was distributed; however, it was later discontinued. When PRV is endemic to a farm, the immunity level must be evaluated through serological tests that provide titer values. Their results will indicate how long passive immunity will last and provide information about the titer of antibodies in replacement sows, breeding sows, and boars. The initial HI technique was highly distrusted for serological diagnosis because the first epidemiological investigations gave false-positive results in areas where the disease had never been present (Fuentes et al., 1992). Regarding the HI, SN, and IPMA tests for the diagnosis of PRV, no consensus exists yet for the procedures and minimal conditions for their development. Moreover, the presence of nonspecific hemagglutination and inhibitors in the sera of pigs requires that the sera be subjected to specific treatments before performing serological tests. For the abovementioned reasons, it is necessary to standardize sensitive and specific techniques to obtain reliable, precise, and reproducible results that can be implemented in monitoring and disease control programs. This study focuses on the standardization of the techniques to reduce false-positive results.

2. Materials and methods

2.1. Serum samples

Samples were obtained from the serum bank of the *Centro Nacional de Investigación Disciplinaria en Salud Animal e Inocuidad* (CENID-SAI), pertaining to the *Instituto Nacional de Investigaciones Forestales, Agrícolas y Pecuarias* (INIFAP) and the *Laboratorio de Virología Molecular* of the *Departamento de Microbiología e Inmunología* of the *Facultad de Medicina Veterinaria y Zootecnia* of the *Universidad Nacional Autónoma de México* (FMVZ-UNAM). Forty-nine sera were assessed with each test, each with four replicates (intra- and interassay). Thirty-seven sera were positive and twelve were negative. The origins of these sera were as follows: 28 sera showing positivity specifically for the PAC-3 strain from animals challenged with PRV, 9 sera raised against different PRV strains, corresponding to viral isolates from 1984 to 2013, and 12 nonimmune sera. The most important reference point was the clinical history of the animal from which the sample was obtained. Knowing the origin of the serum makes the interpretation of the sensitivity, specificity, and *kappa* coefficient more reliable.

2.2. Kappa coefficient

For the sensitivity and specificity values to be reliable, it is important to ascertain that the sera are either positive or negative. The sensitivity of a diagnostic test indicates the probability of being diagnosed as positive in the presence of disease. Sensitivity was calculated according to the following formula: sensitivity = a (true positive)/a + c (true positive + false negative). The specificity of a diagnostic test indicates the probability of being diagnosed as negative in the absence of disease. Specificity was calculated according to the following formula: specificity = d (true negative)/b + d (false positive + true negative).

The *kappa* coefficient reflects the degree of agreement among diagnostic tests. Agreement among tests indicates their soundness (validity), whereas their disagreement suggests that the tests are not reliable (although it is possible that the tests agree by being consistently incorrect). The *kappa* coefficient takes into account random agreement. The expected proportion (EP) agreement is calculated, which is the sum of the expected proportion of agreement for the positive and negative results. The proportion of expected random agreement (both positive), EP+ = [(a + b)/n] x [(a + c)/n]; the proportion of expected random agreement (both negative), EP- = [(c + d)/n] x [(b + d)/n]. Therefore, EP = (EP+) + (EP-). The *kappa* coefficient is the relation between the observed agreement (OA) beyond randomness and the maximal possible agreement (MA) beyond randomness, that is: *kappa* = OA/MA and agreement observed beyond randomness, OA = OP-EP. The proportional agreement observed between both tests, OP = (a + d)/n, where n = (a + b + c + d) and maximal possible agreement beyond randomness, MA = 1 - EP. Thus, *kappa* = OA/MA, and OA and MA are calculated depending on EP (Parikh et al., 2008; Thrusfield, 2018).

2.3. Interpretation of the kappa coefficient

To evaluate the test variability, the *kappa* coefficient was calculated (Landis and Koch, 1977). The *kappa* coefficient was interpreted as follows: $\kappa \leq 0.20$ (low), $0.21 \leq \kappa \leq 0.40$ (mild), $0.41 \leq \kappa \leq 0.60$ (moderate), $0.61 \leq \kappa \leq 0.80$ (good), $\kappa \geq 0.81$ (very good).

2.4. Virus

The PAC-3 strain of PRV (Jalisco/1992; Access No. EF413173 of GenBank) was replicated in a cell culture of pig kidney epithelial cells (PK-15) in Dulbecco's minimum essential medium (D-MEM) supplemented with 2% fetal bovine serum. The virus was titrated with the Reed and Muench method to obtain the 50% infectious dose (TCID_{50%}) and through hemagglutination to determine hemagglutinating units (HAU).

2.5. Hemagglutination inhibition (HI) assay

Twelve protocols were evaluated for the HI test. Different concentrations of viruses and red blood cells (RBCs) were used in the protocols. The different protocols evaluated are presented in Table 1.

The sera were pre-treated by the following: 100 μ L of serum (heat-inactivated at 56 °C), 200 μ L of kaolin, and 200 μ L of chicken or bovine erythrocytes (10%) were homogenized and maintained at 4 °C for 24 h. Once the erythrocytes and kaolin were sedimented, the supernatant was extracted and maintained at -20 °C until use. For the test, 50 μ L aliquots

Table 1
Variables analyzed in the HI test.

Test	HAU	RBCs type	Serum treatment
HI 1	4	Chicken	Without treatment
HI 2	8	Chicken	Without treatment
HI 3	4	Chicken	Heat inactivated
HI 4	8	Chicken	Heat inactivated
HI 5	4	Chicken	Heat inactivated, adsorbed with kaolin and 10% chicken RBCs
HI 6	8	Chicken	Heat inactivated, adsorbed with kaolin and 10% chicken RBCs
HI 7	4	Bovine	Without treatment
HI 8	8	Bovine	Without treatment
HI 9	4	Bovine	Heat inactivated
HI 10	8	Bovine	Heat inactivated
HI 11	4	Bovine	Heat inactivated, adsorbed with kaolin and 10% bovine RBCs
HI 12	8	Bovine	Heat inactivated, adsorbed with kaolin and 10% bovine RBCs

All of the tests were carried out using 0.5% RBCs.

of the serum samples were deposited in U-bottom 96-well plates with 50 μ L of PBS, and double serial dilutions were performed, starting from 1:2 (sera without treatment) or 1:10 (sera with complete treatment) to dilutions of 1:256 or 1:1280. Then, 50 μ L of the PRV adjusted to 4 or 8 HAU was added to each well. The plates were incubated for 30 min at room temperature. Afterward, 50 μ L of chicken or bovine RBCs at 0.5% were added to each well in the plate, and readings were taken at 30 min when the chicken erythrocytes were used or 90 min when the bovine erythrocytes were used. The titer of hemagglutination inhibitory antibodies was expressed as the reciprocal of the maximal dilution at which the serum inhibited the hemagglutinating activity of the virus. For data analyses, all of the titers obtained in the test were transformed to \log_2 (Hernández et al., 1998).

2.6. Serum-neutralization (SN)

The test was performed according to Hernández et al., 1998, with slight modifications. The serum sample was diluted with D-DEM. Double serial dilutions of all sera were performed (from 1:2 to 1:4096) in a flat 96-well microplate, with a final volume of 50 μ L. Then, 50 μ L of PRV adjusted to 300 TCID_{50%} was added, and the plate was incubated at room temperature for 30 min. Finally, 100 μ L of a suspension of PK-15 cells (10^4 cells/well) was added, and the mixture was incubated for 72 h at 37 °C in a 5% CO₂ atmosphere. The end point was determined through hemagglutination in the supernatants. The titer of the neutralizing antibodies corresponded to the reciprocal of the last serum dilution that completely neutralized the production of the hemagglutinating virus (Hernández et al., 1998).

2.7. Immunoperoxidase monolayer assay (IPMA)

This test was performed according to Pileri et al. (2014) with slight modifications. Monolayers of PK-15 cells were cultured in 96-well plates. The cell cultures were infected with 300 TDIC_{50%} of the PRV. The plates were incubated at 37 °C in a 5% CO₂ atmosphere for 48 h and then fixed in 4% paraformaldehyde. Washes with PBS were performed, and the activity of the endogenous peroxidase was blocked with a 3% hydrogen peroxide solution in methanol for 30 min. Double serial dilutions of the serum were performed (from 1:2 to 1:4096), and incubation with the dilutions was performed for 30 min at room temperature. After three PBS washes, 50 μ L of Protein A-HRP (diluted 1:300) was added to all wells, and the plates were incubated at room temperature for 30 min. PBS washes were performed again, and 50 μ L of the 3-amino-9-ethylcarbazole substrate was added. The reaction was allowed to develop for 10 min, and the plates were washed with PBS and examined with an inverted microscope.

3. Results

3.1. Hemagglutination inhibition

With the different protocols of the HI test, a higher average titer was obtained when the serum was not inactivated and not adsorbed. These sera corresponded to the HI 1, HI 2, HI 3 and HI 4 protocols. The average titers were 6.7, 6.3, 6.8, and 6.3 \log_2 , respectively. Some negative control sera without previous treatment were positive, indicating that several sera showed false-positive results. In those sera that received only one previous inactivation at 56 °C for 30 min, the titers remained very similar, but there were still some negative sera presenting as positive when using either chicken or bovine RBCs at 4 or 8 HAU. Negative sera, where only the complement was inactivated, corresponded to sera HI 3, HI 4, HI 9, and HI 10, and the average titers were 1.44, 1.26, 0.76, and 0.48 \log_2 , respectively. The HI 3 and HI 4 sera had a 90% coefficient of variation, and this value was very high.

The sera subjected to inactivation and adsorption with RBCs and kaolin, that is, HI 5, HI 6, HI 11, and HI 12, presented lower titers on

average, but no false-positive results were encountered. The mean antibody titers for these sera were 5.9, 5.9, 1.9, and 2.1 \log_2 , respectively, in the positive samples. Hence, when pig serum was subjected to prior treatment, more reliable and accurate results were generated. Moreover, the titer obtained was higher when chicken RBCs were used than when bovine RBCs were used. In the protocol evaluation, with either 4 or 8 HAU, the mean of the titer sera was higher when using 4 HAU, especially when using chicken RBCs. Under the conditions established in the different protocols, HI 5 and HI 6 had better values and repeatability (Table 2).

Regarding the sensitivity and specificity of the HI test, the sera that were not inactivated or adsorbed achieved high sensitivities, of 95% and 94%, using chicken RBCs (HI 1 and HI 2) and only 79% when using bovine RBCs (HI 7 and HI 8). Conversely, the specificity ranged from mid to high, with values of 77% and 98% when using chicken RBCs and values of 98% and 100% when using bovine RBCs.

Sera that were only heat-inactivated (HI 3, 4, 9, and 10) presented a similar sensitivity to those not inactivated. The specificity diminished to values of 65% and 67% when chicken RBCs were used and to 90% when bovine RBCs were used.

Last, sera that were heat-inactivated and adsorbed (HI 5, 6, 11, and 12) presented a lower sensitivity percentage (89%) when using chicken RBCs and sensitivities of 43% and 44% with bovine RBCs, whereas the specificity was higher, reaching 100% using either chicken or bovine RBCs. When chicken RBCs were used, the sensitivity increased, but with bovine RBCs, the specificity increased.

In those tests in which 8 HAU was used, the specificity values were slightly higher than those obtained with 4 HAU. The kappa coefficient was very good for HI tests 5 and 6 and for the serum neutralization test. Conversely, for the IPMA, a value of 0.73 for the kappa coefficient was good (Table 3).

3.2. Serum-neutralization

In the SN test, the average titer of the pig sera was 6.1 \log_2 , very similar to the titer obtained with the HI test using chicken RBCs and when the sera were inactivated and adsorbed (HI 5, 6). However, some of the negative sera returned positive results in the first dilution (1:2). The results of the average titer, standard deviations, and coefficients of variation are provided in Table 2. The sensitivity was high, at 91%; however, the specificity was lower than that of the HI test, which presented a specificity of 100% (HI 5, 6, 8, 11, and 12) (Table 3).

3.3. IPMA

The IPMA showed good sensitivity and excellent specificity; the zero

Table 2

Average titer, standard deviations, and coefficients of variation of the HI, SN and IPMA tests (the titers were transformed into \log_2 values).

Test	Positive controls			Negative controls		
	Titer	SD	CV (%)	Titer	SD	CV (%)
HI 1	6.7	0.37	5.52	0.8	0.75	93.75
HI 2	6.3	0.51	8.09	0.2	0.21	105
HI 3	6.8	0.43	6.32	1.6	1.44	90
HI 4	6.3	0.76	12.06	1.4	1.26	90
HI 5	5.9	0.45	7.62	0	0	0
HI 6	5.9	0.45	7.62	0	0	0
HI 7	4	0.51	12.75	0	0.04	0
HI 8	3.5	0.52	14.85	0	0	0
HI 9	3.2	1.42	44.37	0.4	0.76	0
HI 10	3.4	0.71	20.88	0.3	0.48	16
HI 11	1.9	0.07	3.68	0	0	0
HI 12	2.1	0.37	17.61	0	0	0
SN	6.1	1.19	19.5	0.1	0.1	100
IPMA	5.7	1.1	19.29	0	0	0

SD = Standard deviation. CV = Coefficient of variation.

Table 3
Sensitivity, specificity, kappa coefficient, and predictive values of the HI, SN, and IPMA tests.

Test	Sensitivity (%)	Specificity (%)	Kappa Coef.	PPV	NPV
HI 1	95	77	0.74	0.93	0.84
HI 2	94	98	0.86	0.99	0.83
HI 3	98	65	0.68	0.89	0.92
HI 4	94	67	0.63	0.9	0.83
HI 5	89	100	0.8	1	0.75
HI 6	89	100	0.8	1	0.75
HI 7	79	98	0.65	0.99	0.62
HI 8	79	100	0.65	1	0.62
HI 9	73	90	0.51	0.95	0.53
HI 10	77	90	0.56	0.96	0.57
HI 11	43	100	0.28	1	0.38
HI 12	44	100	0.29	1	0.38
SN	91	96	0.8	0.99	0.77
IPMA	85	100	0.73	1	0.68

PPV = Positive predictive value. NPV = Negative predictive value.

values of the standard deviation and the variation coefficient of the negative controls indicate the reproducibility of the test without false-positive results. The IPMA presented excellent specificity, with values of 100%. The standard deviation, variation coefficients, and average titers are shown in Table 2, and the specificity and sensitivity results are shown in Table 3. Fig. 1 shows an immunoperoxidase reaction.

4. Discussion

BED in pigs was first described in 1980 in central Mexico, where 75% of pig production occurs. To understand the epidemic of this virus in farms at that time, blood samples were taken to determine the disease prevalence. Mexico has 32 states, and investigations were carried out in 27 of the 32 states, where pig sera were obtained. The results showed that 10 of the states had animals with antibodies against BED (Fuentes et al., 1992). This research generated much controversy because some of these states export pork.

The states that export pork are located in northwestern Mexico in an area located 1500 km from the center of the country. Other states where positive serology was present were located in southern Mexico, where pig farms are scarce. The distance between the pig-producing area in the center of Mexico and the states where positive results were obtained in the south of the country is 1700 km.

Live animals are not sold between the center and the northeast and south of the country. There are very strict sanitary controls that make it impossible for live animals to pass into these areas. However, positive serology results were obtained in these areas. The serological test used to obtain these results was HI. This technique was used for a long time for the diagnosis of BED in pigs. This technique uses guinea pig RBCs at a

high concentration (1%), and the entire serological test is performed at 37 °C (Moreno-López et al., 1986; McNeilly et al., 1997). The HI test with these parameters caused many false-positive results; thus, this serological test has detracted from the credibility of diagnoses and related research on BED.

In diagnostics and research related to influenza, when antibodies from chickens, horses, pigs, or dogs are evaluated, the use of hemagglutination inhibition is frequent and shows a high level of reliability. In serological tests for the diagnosis of diseases of chickens caused by viruses that hemagglutinate, nonspecific inhibitors are commonly not removed. Furthermore, the sera are not inactivated at 56 °C, nor are they adsorbed on kaolin and RBCs, as is the case for Newcastle disease or avian influenza virus (OIE, 2019). However, the HI has been considered an unreliable test for BED in pigs because of its propensity to produce false-positive results. Moreover, there is no standardization for this test.

In the first investigations, where piglets showed neurological signs, a paramyxovirus was isolated. This virus has the ability to hemagglutinate red blood cells from different domestic species, such as chickens, mice, guinea pigs, rats, bovines, hamsters, goats, sheep, and even different types of erythrocytes in humans (O, AB, and AB). In this investigation, these RBCs were not evaluated in hemagglutination inhibition tests (Stephano et al., 1988). Currently, many laboratories carry out this test with different types of RBCs (mainly chickens, guinea pigs, and bovines). Different concentrations of RBCs are used, as well as different temperatures (room temperature or 37 °C). With every change in each of these parameters, different results are obtained. The same sample processed in different laboratories can show different results.

McNeilly et al. developed a method that removes hemagglutination inhibitors. This method employs a 10% guinea pig RBC suspension and heparin/MgCl₂, which the authors justify by claiming that the hemagglutination inhibitors for PRV are lipoproteins. They also used a pretreatment of kaolin sera and guinea pig RBCs, with which they obtained false-positive results (McNeilly et al., 1997). In the present study, by pretreating the samples with inactivation at 56 °C for half an hour, 10% chicken RBC suspension and kaolin, it was possible to completely remove nonspecific hemagglutination inhibitors. We suggest that the results of the work by McNelly can be attributed to having used guinea pig RBCs in the HI test; with these RBCs, elution is produced within a few minutes after hemagglutination (McNeilly et al., 1997).

In this investigation, when the sera were not subjected to complete treatment (inactivation at 56 °C, adsorption with RBCs and kaolin), the sensitivity was high and the specificity was low, especially when using chicken RBCs. The test was more sensitive when using chicken RBCs (up to 95%). Using these tests without the complete treatment of the sera caused false-positive results. When the negative sera did not undergo complete treatment, false-positive results were also obtained.

This study revealed that the protocols that offered the highest reproducibility and concordance ($\kappa = 0.80$) were HI 5 and HI 6. These

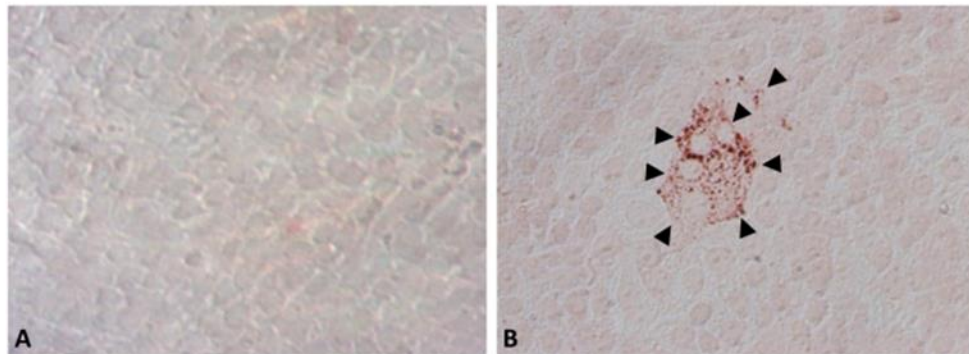


Fig. 1. IPMA negative (A) and positive (B), serum dilution 1:1024, objective 40 X. The black arrowheads indicate intracytoplasmic inclusion bodies.

results confirmed the importance of the inactivation of proteins of the complement system and the removal of nonspecific inhibitors of hemagglutination.

When 4 HAU of the virus was used, the antibody titers were higher than when 8 HAU was used. The negative sera generated positive results when they did not undergo complete pretreatment. These results had very low titers; however, interpretation of these samples containing antibodies is possible.

The HI5 and HI6 tests generated very good sensitivity and specificity values of 89 and 100%, respectively, indicating that they could be widely used as screening tests in disease-endemic areas or even as confirmatory tests.

The highest specificity values were obtained with bovine RBCs. Further treatment of the sera decreased the sensitivity and increased the specificity. Using hemagglutination inhibition with bovine RBCs may cause false-negative results. When chicken RBCs were used, the antibody titers were higher than when bovine RBCs were used. When the sera from pigs positive for PRV were subjected to treatment before the HI test was performed, the antibody titer decreased. The difference in the antibody titer in the HI test can be up to three times higher when chicken RBCs are used instead of bovine RBCs. The sera must be treated at 56 °C, and adsorption must be performed with homologous RBCs and kaolin. If the sera do not receive complete treatment, then negative sera can generate false-positive results.

The antigen used in this study was the PAC-3 strain due to its high hemagglutinating activity, in addition to its cross-antigenicity with some other strains of PRV.

In this work, we propose the use of HI with chicken RBCs and heat-inactivated sera adsorbed with RBCs from the same species and kaolin. The HI technique offers very good sensitivity and specificity values, and this method can even be used as a confirmatory serological test. Sedimentation of chicken RBCs control occurs within 30 min, whereas bovine RBC control occurs at 90 min. The sensitivity of HI is higher when using chicken RBCs; however, with these RBCs, elution can be observed at 60 min. If the HI reading is performed after 60 min, false-positive results can be obtained induced by the elution. When the HI test was performed with bovine RBCs, the elution phenomenon was not observed during the entire day of the test.

For serum neutralization, the κ coefficient values were high; however, some positive results were obtained with negative sera. This conclusion establishes a cutoff point of dilution $\geq 1:4$ for this serological test under these conditions (300 TCID₅₀).

Good levels of sensitivity and specificity were obtained in the SN test, reaching up to 91 and 96%, respectively. The false-positive results that were obtained were as high as 1 log₂.

The IPMA test was very sensitive and specific, and the choice of the cell line was adequate because it supported viral replication; moreover, the immunodetection of intracytoplasmic inclusion bodies was easily observed. This test has several advantages, including the simple preparation of plates and infection of cells and the stability of the staining, which allows the samples to be stored for months. Another advantage offered by this test is the safety of working with an inactivated antigen. The IPMA technique showed sensitivity and specificity values similar to those obtained with serum neutralization. The development of this test would allow its implementation in disease-free areas with a low risk of disseminating the disease due to the use of inactivated antigens.

5. Conclusion

The Animal Health authorities in Mexico have not established a diagnostic test for BED in pigs, nor have they established a campaign for the control and eradication of this disease, although the disease is endemic to the central area of the country. All of the tests carried out have pros and cons. In the case of IPMA, while it has good characteristics, in the laboratories where it is implemented, an inverted microscope

must be available for its interpretation. For the HI test, the equipment is minimal if the antigen is acquired from a central laboratory. In the case of SN, more equipment and greater specialization of the personnel is required to carry it out. The results obtained in this research propose hemagglutination inhibition is a reliable test as long as the established parameters are used. The serum neutralization test is also reliable; however, the laboratory must have cell cultures available, which is uncommon in Mexico. The immunoperoxidase monolayer assay does not use an active virus; hence, it is considered safe and does not represent any risk of disseminating the virus. The parameters obtained in this research can allow the animal health authorities to start the control and monitoring of BED, which should lead to its rapid eradication.

Declaration of competing interest

The authors declare that they have no conflicts of interest.

Acknowledgements

Funding. This study was partially financed by PAPIIT-UNAM (IT201918) and SEP-CONACYT No. CB-2016-01-284863.

References

- Berg, M., Sundqvist, A., Moreno-Lopez, J., Linne, T., 1991. Identification of the porcine paramyxovirus LPMV matrix protein gene: comparative sequence analysis with other paramyxoviruses. *J. Gen. Virol.* 72, 1045–1050. <https://doi.org/10.1099/0022-1317-72-5-1045>.
- Escobar-López, A. C., Rivera-Benitez, J.F., Castillo-Juárez, H., Ramírez-Mendoza, H., Trujillo-Ortega, M.E., Sánchez-Betancourt, J.I., 2012. Identification of antigenic variants of the porcine rubulavirus in sera of field swine and their seroprevalence. *Transbound. Emerg. Dis.* 59, 416–420. <https://doi.org/10.1111/t.1865-1682.2011.01286.x>.
- Fuentes, R.M., Carreon, N.R., Ramirez, M.H., Trujillo, O.M.E., de Fraile, L., 1992. Pilot study about the frequency of blue eye paramyxovirus antibodies in Mexican pigs. *Vet. México* 23, 37–39.
- Hernández, J., Reyes-Leyva, J., Zenteno, R., Ramírez, H., Hernández-Jauregui, P., Zenteno, E., 1998. Immunity to porcine rubulavirus infection in adult swine. *Vet. Immunol. Immunopathol.* 64, 367–381. [https://doi.org/10.1016/S0165-2427\(98\)00169-X](https://doi.org/10.1016/S0165-2427(98)00169-X).
- ICTV, 2019. International Committee on Taxonomy of Viruses.
- Landis, J.R., Koch, G.G., 1977. The measurement of observer agreement for categorical data. *Biometrics* 33, 159. <https://doi.org/10.2307/2529310>.
- McNeilly, F., Walker, I., Allan, G.M., Foster, J.C., Linne, T., Merza, M., Hernandez, P., Kennedy, S., Adair, B., 1997. A comparative study on the use of virus and antibody detection techniques for the diagnosis of La Piedad Michoacan paramyxovirus (LPMV) infection in pigs. *J. Vet. Diagn. Investig.* 9, 3–9. <https://doi.org/10.1177/10406387970090102>.
- Moreno-López, J., Correa-Girón, P., Martínez, A., Ericsson, A., 1986. Characterization of a paramyxovirus isolated from the brain of a piglet in Mexico. *Arch. Virol.* 91, 221–231. <https://doi.org/10.1007/BF01314282>.
- Nordengrahn, A., Svenda, M., Moreno-Lopez, J., Bergvall, A., Hernandez, P., McNeilly, F., Allan, G., Merza, M., 1999. Development of a blocking ELISA for screening antibodies to porcine rubulavirus, La Piedad Michoacan virus. *J. Vet. Diagn. Investig.* 11, 319–323. <https://doi.org/10.1177/104063879901100404>.
- OIE, World Organisation for Animal Health, 2019. Manual of Diagnostic Tests and Vaccines for Terrestrial Animals. <https://www.oie.int/en/international-standard-setting/terrestrial-manual/access-online/>.
- Parikh, R., Mathai, A., Parikh, S., Chandra Sekhar, G., Thomas, R., 2008. Understanding and using sensitivity, specificity and predictive values. *Indian J. Ophthalmol.* 56, 45–50. <https://doi.org/10.4103/0301-4738.41424>.
- Pileri, E., Cortey, M., Rodríguez, F., Sibila, M., Fraile, L., Segalés, J., 2014. Comparison of the immunoperoxidase monolayer assay and three commercial ELISAs for detection of antibodies against porcine circovirus type 2. *Vet. J.* 201, 429–432. <https://doi.org/10.1016/j.tvjl.2014.05.025>.
- Stephano, H.A., Gay, G.M., Ramirez, T.C., 1988. Encephalomyelitis, reproductive failure and corneal opacity (blue eye) in pigs, associated with a paramyxovirus infection. *Vet. Rec.* 10, 2–6.
- Sundqvist, A., Berg, M., Moreno-López, J., Linné, T., 1992. The haemagglutinin-neuraminidase glycoprotein of the porcine paramyxovirus LPMV: comparison with other paramyxoviruses revealed the closest relationship to simian virus 5 and mumps virus. *Arch. Virol.* 122, 331–340. <https://doi.org/10.1007/BF01317194>.
- Thrusfield, M., 2018. Diagnostic testing (Kappa statistics). In: Thrusfield, M., Christley, R. (Eds.), *Veterinary Epidemiology*. John Wiley & Sons Ltd, pp. 450–452.

10.1 Artículo enviado a Plos One

Identification and characterization of Ovine gammaherpesvirus type 2 in Artiodactyla and its isolation in horses from an outbreak of malignant catarrhal fever in Mexico

Tania Lucia Madrigal-Valencia^{1¶}, Manuel Saavedra-Montañez^{1¶}, Armando Pérez-Torres^{2¶}, Jesús Hernández^{3¶}, Joaquim Segalés^{4,5¶}, Yesmín Domínguez Hernández^{6&}, Irma Eugenia Candanosa-Aranda^{6&}, Alfredo Pérez-Guio^{7&},
Humberto Ramírez Mendoza^{1*}

¹ Departamento de Microbiología e Inmunología, Facultad de Medicina Veterinaria y Zootecnia, UNAM, Mexico City, Mexico.

² Departamento de Biología Celular y Tisular. Facultad de Medicina, Universidad Nacional Autónoma de México (UNAM), Mexico City, Mexico.

³ Laboratorio de Inmunología, Centro de Investigación en Alimentación y Desarrollo, A.C. (CIAD), Hermosillo, Sonora, Mexico.

⁴ Unitat Mixta d'Investigació IRTA-UAB en Sanitat Animal, Centre de Recerca en Sanitat Animal (CRESA), Campus de la Universitat Autònoma de Barcelona (UAB), Bellaterra, Barcelona, Catalonia, España.

⁵ Department de Sanitat i Anatomia Animals, Facultat de Veterinària, Campus de la Universitat Autònoma de Barcelona (UAB), Bellaterra, Barcelona, Catalonia, España.

⁶ Centro de Enseñanza, investigación y Extensión en Producción Animal en Altiplano (CEIEPAA), Facultad de Medicina Veterinaria y Zootecnia (FMVZ), Universidad Nacional Autónoma de México (UNAM), Tequisquiapan, Queretaro, Mexico.

⁷ División de Ciencias de la Vida, Campus Irapuato-Salamanca, Universidad de Guanajuato, ExHda El Copal, Irapuato, Guanajuato, Mexico.

*Corresponding author

E-mail: betosram@comunidad.unam.mx (HR)

¶ These authors contributed equally to this work.

& These authors also contributed equally to this work.

Abstract

Ovine gammaherpesvirus 2 (OvHV-2), a member of the genus Macavirus, causes sheep-associated malignant catarrhal fever (SA-MCF), a fatal lymphoproliferative disease affecting a wide variety of ungulates in addition to horses. This study described an outbreak of SA-MCF in Mexico and identified the OvHV-2 virus through viral isolation, immunofluorescence (IF), immunocytochemistry (ICC), immunohistochemistry (IHC), endpoint polymerase chain reaction (PCR), and partial sequencing of the *ORF75* gene. The animals involved in this outbreak showed mucogingival ulcers in the vestibule of the mouth and tongue, hypersalivation, corneal opacity, reduced food consumption, and weight loss of variable severity. These clinical signs and the histopathological findings suggested the diagnosis of SA-MCF. Buffy coat fractions from the anticoagulated blood samples of ill animals were collected and analyzed by PCR. Positive buffy coats were used to inoculate the primary cell cultures of rabbit testis to isolate the virus. Small clusters of refractile cytomegalic cells, characteristic of viral cytopathic effects, were observed between 48 and 72 h post-infection. Furthermore, intranuclear acidophilic inclusion bodies (IBs) were identified in the inoculated primary culture cells, and the cytoplasm showed immunoreactivity with hyperimmune rabbit serum against OvHV-2. Moreover, in the liver histological sections from sick deer, immunoreactive juxtannuclear IBs were identified with the same rabbit hyperimmune serum. The obtained sequences were aligned with the OvHV-2 sequences reported in GenBank and revealed a nucleotide identity higher than 98%. Based on the evidence provided in this study, we conclude that the outbreak of SA-MCF in the municipality of Tequisquiapan in the state of Queretaro, Mexico, was caused by OvHV-2. This is the second study reporting that horses are susceptible to OvHV-2 infection and can develop SA-

MCF. We demonstrated the isolation of OvHV-2 from horses' buffy coat lysate and determined that primary rabbit testis cultures could be a cell culture model for the replication of this virus.

Keywords:

Malignant catarrhal fever, OvHV-2, Mexico, horses, primary cell cultures.

Introduction

Malignant catarrhal fever (MCF) is a severe lymphoproliferative disease in susceptible ungulate species of the Artiodactyla order. MCF can be caused by five viral species of the genus *Macavirus*: ovine herpesvirus-2 (OvHV-2), alcelaphine herpesvirus-1 (AIHV-1), alcelaphine herpesvirus 2 (AIHV-2), caprine herpesvirus 2 (CpHV-2), and an MCF virus (MCFV) in white-tailed deer (*Odocoileus virginianus*) for which domestic goats can be a carrier host (97).

The two most well-studied are OvHV-2 and AIHV-1, and their infections are asymptomatic in sheep and wildebeest reservoir populations, respectively (98). OvHV-2 is responsible for sheep-associated malignant catarrhal fever (SA-MCF) disease in susceptible hosts, such as buffalo (99), cattle (100), deer (101) and rarely in pigs (100) and foals (102). However, rabbits are susceptible to SA-MCF following intranasal nebulization of cell-free OvHV-2 and develop a disease similar to SA-MCF in terms of clinical signs and lesions (103,104).

In OvHV-2, infection with non-adapted host species suggests latent infection and abortive lytic viral replication (105).

Typical SA-MCF, often referred to as the head-and-eye form, is the most common presentation of this condition in cattle (98). Sick animals manifest pyrexia, anorexia, bilateral

corneal opacity, nasal and ocular discharge, ulceration of various mucous membranes, and neurological manifestations in the terminal stages (106). The most common gross pathological changes in SA-MCF-affected animals are erosions of the tracheal and bronchial mucosa, erythema of the turbinate mucosa, congestion, and edema of the lungs, and focal white lesions in the kidney (106). Histopathologically, the hallmark of SA-MCF is lymphoproliferative inflammation with vasculitis involving medium-caliber arteries and veins, which is readily detected in most organs of cattle dying from acute SA-MCF (107). Both clinical presentation and pathological features are of significant diagnostic value (108).

Detection of viral DNA by PCR in buffy coats and tissues, especially at high levels, can support the diagnosis of MCF-causing viruses (MCFV) (109). Several serological assays have been used to detect antibodies against SA-MCF, but all assays use Alcelaphine herpesviruses as antigens, predominantly AIHV-1 because these viruses can be propagated *in vitro* (69). These assays include virus serum neutralization (VN), immunoblotting (IFA), enzyme-linked immunosorbent assay (ELISA), competitive inhibition ELISA (cELISA), immunofluorescence assay (IF), immunoperoxidase assay (IPT), and drug complement fixation test (110–116). However, the VN has very limited use in the detection of antibodies in animals infected with OvHV-2, and polyclonal antibody-based assays (ELISA, IFA, and IPT, among others) can detect antibodies against multiple epitopes of AIHV-1 (117,118). To increase specificity, an ELISA has been developed using an Ov8 recombinant protein from OvHV-2 (119).

For the *in vitro* isolation of MCFV, primary cultures of bovine thyroid (BTh), bovine kidney (BK), bovine embryonic kidney (BEK), and calf testis (CT) cells have been used (62,120,121). On the other hand, Hristov et al. (2016) described the use of primary rabbit

kidney (RK) cell cultures and permanent cell cultures (Madin Darby bovine kidney (MDBK) cell line, embryonic bovine tracheal (EBTR) cell line, green monkey kidney cell line (VERO), and monkey cell line (MA-104)) for the isolation of the OvHV-2 virus. However, they mention that additional investigations are needed to confirm which type of OvHV-2 or AIHV-1 viral isolation they performed (61)

Cases of SA-MCF have been documented in North America, and economic losses to bison producers have been estimated at approximately US\$1 million (122). However, the direct economic losses associated with SA-MCF morbidity and mortality in Brazil were estimated at US\$215,592 and US\$214,368, respectively. If the data were projected nationally, it would result in a projected economic loss of US\$3.5 to US\$4.8 billion for the cattle industry in Brazil (53).

The first case of SA-MCF in Mexico was documented in Mexico City in a 6-year-old Holstein cow in 1969, which presented head and ocular clinical manifestations in addition to perivascular lymphoid infiltrate in various organs. However, the diagnosis was based only on a clinicopathological study (123). More recently, an outbreak of SA-MCF occurred in the municipality of Tequisquiapan in the state of Queretaro, Mexico, affecting many animals that developed a typical head-and-eye clinical presentation.

Only one study has been carried out thus far investigating OvHV-2 in Mexico, as it is considered an exotic disease. Moreover, the economic and epidemiological impact of SA-MCF and the distribution and molecular characterization of the OvHV-2 virus in this country are unknown. Therefore, this study aimed to identify and isolate the OvHV-2 virus causing the second SA-MCF outbreak in Mexico.

Material and Methods

Ethics statements

All experimental procedures involving animals were conducted following the Institutional Subcommittee for the Care and Use of Experimental Animals of the Universidad Nacional Autónoma de México (UNAM) (SICUAE.DC-2020/3-5).

Sampling location

Sampling was performed at the Centro de Enseñanza, Investigación y Extensión en Producción Animal en Altiplano (CEIEPAA), belonging to the UNAM, located in Tequisquiapan, state of Queretaro, Mexico. This farm has an area of 186 ha. It is based on a semi-intensive production system with multiple species: deer (European red), dairy cows (Holstein, Jersey, and crosses), feedlot cattle (Limousin), sheep (Suffolk, Katahdin, and crosses), goats (Alpine Frances, Saanen, Toggenburg, and Boer) and horses (English thoroughbred, quarter horse, appendix, Portuguese, Santa Gertrudis, and Creole) (Fig 1). The species were separated between 1.14 and 2.8 km (124).

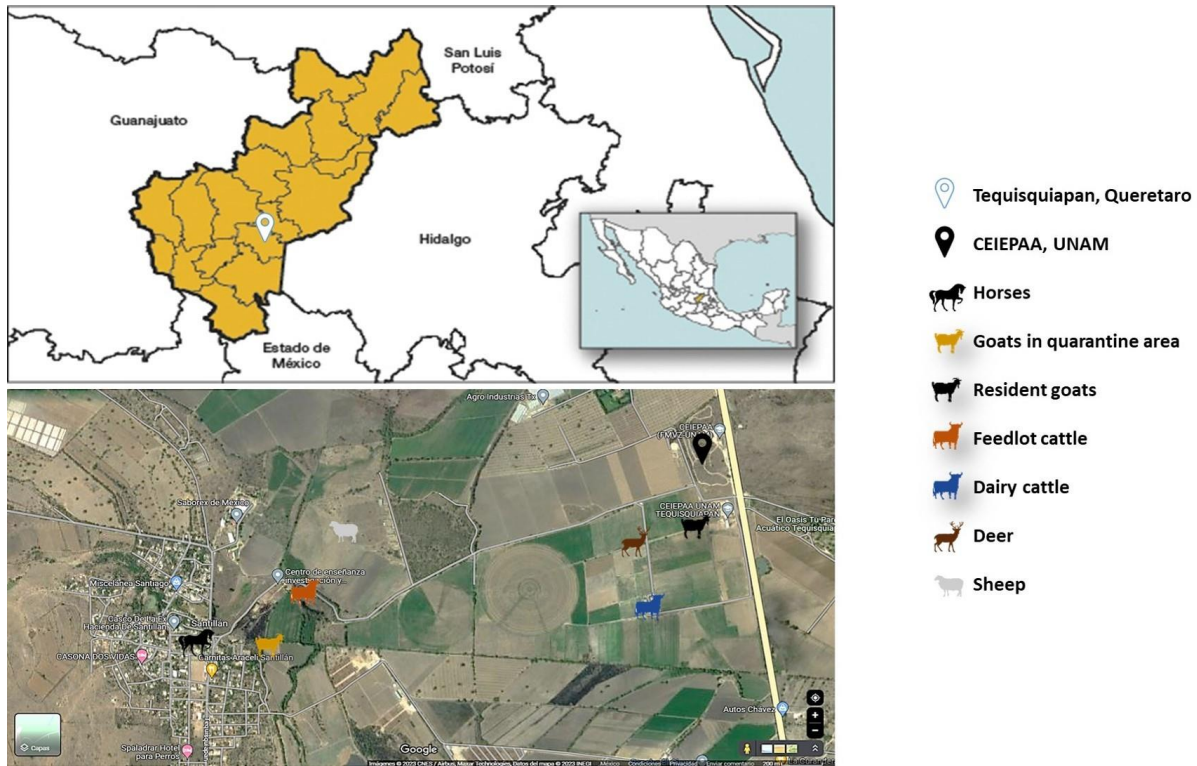


Fig 1. Distribution of animals in the CEIEPAA farm, UNAM. On the upper left, the geographical location of Tequisquiapan, Queretaro (Mexico), is indicated. The species distribution in the area is depicted in the lower section.

The outbreak chronology

From August to December 2018, a vesicular disease occurred that affected all species of animals belonging to the CEIEPAA farm, and the United States-Mexico Commission for the Prevention of Foot-and-Mouth Disease and other Exotic Animal Diseases (CPA) took samples of serum, blood, epithelium of ulcerative lesions of the oral mucosa, deer organs (tongue, brain, submandibular lymph nodes, kidney, and spleen), and nasal swabs to carry out differential diagnoses of vesicular diseases (124). In January 2019, the UNAM performed targeted sampling to isolate the OvHV-2 virus.

Supplementary tests

The serum samples were analyzed with ELISA tests to diagnose foot-and-mouth disease virus (FMDV) and vesicular stomatitis virus (VSV). On the other hand, samples of epithelium, blood, deer organs (tongue, brain, submandibular lymph nodes, kidney, and spleen), and nasal swabs were used to perform different molecular diagnoses: PCR or reverse transcription polymerase chain reaction (RT-PCR) for FMDV, infectious bovine rhinotracheitis virus (IBRV), Indiana and New Jersey VSV, parapoxvirus (PRV), bluetongue virus (BTV), and contagious ecthyma virus (CEV). In addition to viral isolation of VSV (Table 1).

***Post-mortem* evaluation**

Of the 14 deer that died during the 2018 SA-MCF outbreak, 9 deer were assessed *post-mortem* because 5 were in an advanced state of decomposition. The results of the *post-mortem* evaluation were published by Pérez et al. (2022) (124). Our current research presents the results of two of these deer (#172 and #174), which were chosen due to the severity of their clinical signs and lesions. Cornea, lymph nodes, tongue, rumen, liver, lung, and kidney samples were taken and fixed by immersion in 10% buffered formalin solution and routinely processed for paraffin embedding and sectioning using hematoxylin and eosin (H&E) staining for observation and histopathological analysis.

Clinical sample collection and preparation

In January 2019, a new sampling was performed. Nevertheless, this time was aimed at animals that the CPA had previously tested positive for OvHV-2 by PCR, including those that still had ulcerative lesions (11 horses) and some healthy animals. The purpose of this sampling was to isolate OvHV-2. Approximately 30 blood samples from each animal species were obtained in

Vacutainer® tubes. Subsequently, the buffy coats were separated according to the methodology described by English & Andersen (1974) (125), and after identification, they were stored at -196°C until processing for viral isolation and PCR.

Nested endpoint polymerase chain reaction (PCR) for OvHV-2 detection

Nested endpoint PCR was specific for the *ORF75* segment of OvHV-2, which encodes phosphoribosyl-formyl-glycinamide synthase (FGARAT), which participates in purine metabolism and the production of viral tegument proteins (126).

Genetic material was extracted according to the manufacturer's instructions for the High Pure PCR kit (Roche, Basel, Switzerland) (127). Primer pairs designed by Baxter *et al.* (1993) were used, and nested PCR was performed according to the method described by Li *et al.* (1995), with some modifications (126,128). Briefly, in the first and second amplification reactions, 10 µM of each primer set was used, and the reaction volume was adjusted to 25 µL. A PCR Master Mix 5X (Taq-Load) was used. All reactions were performed using a GeneAmp® PCR System 9700 (Applied Biosystems, Waltham, MA, USA). A positive result generated a 238-bp band in the second amplification.

A bovine blood sample that tested positive for OvHV-2 by PCR and partial sequencing (ref. 6191), donated by CPA, was used as a positive control, and nuclease-free water was used as the negative control.

Primary cell cultures

The primary cell culture was prepared using testes from 2-month-old male rabbits, which were humanely euthanized (SICUAE.DC-2020/3-5)]. Testes were washed five times with Hanks balanced salt solution (HBSS, Gibco, Life Technologies) supplemented with penicillin (100

U/mL, Gibco, Life Technologies), streptomycin (100 g/mL, Gibco, Life Technologies) and fungizone (2.5 g/mL, Gibco, Life Technologies). They were then placed in a sterile Petri dish where the tunica albuginea and connective tissue septa from each testis were dissected with sterile scissors. With the help of sterile forceps, manual cuts were made to obtain fragments smaller than 0.5 cm² from both testes. The testes fragments were trypsinized for 1 h at 37°C under constant agitation using 0.25% trypsin-EDTA with phenol red (Gibco, Cat: 25200056) at a 1:5 ratio.

After incubation, the detached cells were filtered through a funnel with sterile gauze, and the filtrate was collected in a centrifuge tube and centrifuged at 800 × g for 10 min. The supernatant was discarded, and the pellet of cells was resuspended in Dulbecco's modified Eagle's medium (DMEM) supplemented with 10% fetal calf serum. Approximately 0.5 × 10⁶ cells/mL were seeded per bottle. Cultures were maintained in 25 cm² flasks (Nunc, Roskilde, Denmark) at 37°C with a 5% CO₂ atmosphere. Cells were monitored daily under an inverted Olympus microscope (IX71) with a 10× objective (Olympus Corporation, Shinjuku City, Tokyo, Japan), and after 2 days, the DMEM supplemented with 10% fetal bovine serum was changed to a similar fresh medium.

Virus isolation

For the isolation of OvHV-2, 25-cm² bottles with 80% cell confluence were used. Each bottle was inoculated with 200 µL of buffy coat lysate (PCR positive for OvHV-2). Lysates were obtained by freezing and thawing the buffy coats from each of the six species naturally infected with OvHV-2 (deer, dairy cattle, feedlot cattle, sheep, goats, and horses). Inoculated cells were propagated in DMEM supplemented with 5% fetal calf serum and incubated at 37°C with a 5%

CO₂ atmosphere. The flasks with the inoculated cells were observed every 24 h for 7 days using an Olympus inverted microscope (IX71) with a 10× objective (Olympus Corporation) to identify the specific cytopathic effect of OvHV-2 (61).

At least four blind passages were performed in all species except horses, in which fourteen blind passages were needed for virus adaptation to cell culture and cell-free virus production. Bottles with inoculated cells were frozen and thawed when cytopathic changes were observed in the monolayers (refractile cytomegalic cell foci, syncytia, or 50% destruction of the monolayer). Then, the culture supernatant was centrifuged at 1200 × g for 10 min, and the final supernatant was divided into small aliquots and stored at -80°C until use. For consecutive passages, fresh monolayers were prepared and inoculated with the virus supernatant mentioned above. When cytopathic changes were observed in the monolayers, the bottles with the inoculated cells were processed as mentioned above. Following the cytopathic changes of the monolayers, culture supernatants from the four blind passages were identified for the *ORF75* segment of the OvHV-2 virus DNA by nested PCR. As a negative control, a 25-cm² bottle with 80% cell confluence was inoculated with 200 µL of buffy coat lysate from OvHV-2-negative horses.

The virus titer was quantified from the cell-free supernatants of the 4th blind passage of all the species and from the 3rd to the 14th blind passages of the horse. Flat-bottomed 96-well plates were used as described by Reed and Muench (75). To analyze the plates under a microscope, they were fixed 72 h post-infection with 4% paraformaldehyde diluted with distilled water and stained with 0.5% crystal violet diluted in 96° alcohol.

To observe intranuclear inclusion bodies (IBs), a 24-well plate at 80% cell confluence was inoculated with 200 μ L of each of the four blind passages described above. The inoculated cells were propagated with DMEM supplemented with 2% fetal calf serum and incubated at 37°C for 24 h in a 5% CO₂ atmosphere. Subsequently, the supernatant was removed, and the cells were fixed with 4% paraformaldehyde. Finally, hematoxylin stain was added for 1 min, washed with distilled water, and stained with eosin stain for 30 s. The bottom of each well was covered with glycerol and a coverslip. The intranuclear IBs were observed under an Olympus inverted microscope (IX71) with a 10 \times objective (Olympus Corporation). As a negative control, a 4-well plate was left at 80% cell confluence and inoculated with 200 μ L of the buffy coat lysate from OvHV-2-negative horses; otherwise, the remaining analytical procedure was identical to that given above.

Viral replication kinetics

The kinetics of viral replication were analyzed from the cell-free supernatants of the 4th, 5th, and 14th passages of the buffy coat lysate from horses. Primary cultures of rabbit testis grown in 96-well flat bottom plates were inoculated and processed according to the technique of Reed and Muench (75). Briefly, primary cultures were inoculated with serial 10-fold dilutions of each of the samples in quadruplicate per dilution. The inoculum was then removed at different time points (24, 48, 72, 96, and 120 h post-infection), and the plates were fixed with 4% paraformaldehyde for 10 min and stained with 0.5% crystal violet. Graphics were prepared using GraphPad Prism 9.5.1 software (GraphPad, USA).

Partial sequencing of the ORF75 gene

Partial sequencing of the *ORF75* gene was performed from the fourth blind passage obtained by inoculating primary cultures with buffy coat lysate from different animal species (deer, dairy cattle, feedlot cattle, sheep, goats, and horses). Furthermore, partial sequencing of the CPA-donated positive control was performed. The seven samples were amplified by endpoint PCR to obtain a 422-bp fragment corresponding to a segment of the *ORF75* gene, and 300 ng of each PCR product was sequenced by bidirectional capillary electrophoresis through Sanger sequencing using external PCR primers as sequencing primers (MCF 556 and MCF 755) (72). Electropherograms from each pair of sequencing reactions were edited and assembled with the Biological Sequence Alignment Editor (BioEdit), v 7.2.0; (76). Sequences were aligned using MEGA 11 software (77).

Phylogenetic analysis

The seven consensus sequences obtained using BioEdit software were compared with partial sequences of the *ORF75* gene reported in GenBank (76). For the phylogenetic analysis, the alleles of high and low similarity for *ORF75* were selected using the BLAST (Basic Local Alignment Search Tool) of the NCBI (National Center for Biotechnology) (78).

Finally, the seven sequences were phylogenetically analyzed with sequences from the genus *Macavirus* (OvHV-2, AlHV-1, and AlHV-2) and human gammaherpesvirus types 4 and 8 (HHV-4 and HVH-8). The substitution model was selected with Jmodeltest, indicating that the Tamura-Nei model was the most appropriate for this data set (80,129). The analysis was performed with MEGA 11 software using the maximum likelihood method with 1,000 replicas (77).

The seven consensus nucleotide sequences of the *ORF75* gene fragment amplified in this work have been submitted to the GenBank public database and have been assigned the following accession numbers: ON375578 (horses), ON375579 (goats), ON375580 (deer), ON375581 (dairy cattle), ON375582 (feedlot cattle), ON375583 (sheep) and ON375584 (CPA positive control).

Hyperimmune serum

To prepare an anti-OvHV-2 hyperimmune serum, we followed a protocol from a previous study by Orós *et al.* (1997), with some modifications. Three 9-week-old New Zealand white rabbits weighing approximately 1.7 kg and negative for OvHV-2 by nested endpoint PCR were used (130).

Rabbits were inoculated intramuscularly with the cell-free supernatant from the fourth blind passage of the horses (Tissue Culture Infectious Dose $10^{4.19}$ TCID₅₀/mL) dissolved in phosphate-buffered saline (PBS) and a 2% Alhydrogel® (w/v) aqueous suspension of aluminum hydroxide gel adjuvant (InvivoGen). The supernatant from the previously mentioned fourth blind passage was inactivated with 0.2% formaldehyde diluted in distilled water.

Rabbits were housed in stainless-steel cages with wire mesh, fed commercial pellets, and had free access to running water. The animals were kept at a temperature of 23-25°C. After an acclimatization period, the rabbits received weekly intramuscular inoculation for 5 weeks. Subsequently, the rabbits were tranquilized (acepromazine 1 mg/kg), and their hearts were bled and then euthanized with an overdose of pentobarbital. The serum obtained was stored at -20°C until its subsequent use in immunofluorescence (IF), immunocytochemistry (ICC), and immunohistochemistry (IHC) techniques.

Immunocytochemistry (ICC) and immunofluorescence (IF) techniques

To perform the ICC and indirect IF analyses, we modified the methodology described by Rossiter (1981). Two 24-well plates were used with a cell confluence of 80%, and the wells were inoculated with 200 μ L of each of the four blind passages obtained previously (131). Subsequently, they were incubated at 37°C for 72 h and fixed with 4% paraformaldehyde diluted in distilled water for 10 min at room temperature. The cells were permeabilized with 0.2% Triton X-100 for 5 min at room temperature. The plates were then washed three times with PBS. For ICC, endogenous peroxidase was inhibited by incubation with 3% hydrogen peroxide diluted in distilled water for 15 min and washed three times with distilled water. To reduce background noise, the two plates were incubated with 2.5% bovine serum albumin diluted in Tris-HCl buffer for 30 min at 37°C. Next, the two plates were incubated with anti-OvHV-2 rabbit hyperimmune serum diluted 1:5 in 0.1% albumin for 24 h at 4°C. After three washes with PBS, peroxidase-conjugated protein A was added to the ICC plate diluted 1:16 in 0.1% albumin and incubated for 1 h at 37°C, followed by three washes with PBS. The chromogen (hydrogen peroxide and 3,3'-diaminobenzidine) was added for 5 min, and the reaction was stopped with distilled water. Cells with positive immunoreactivity to the anti-OvHV-2 hyperimmune serum presented an insoluble brown coloration. The plate used for IF was processed in the same way as for ICC; however, endogenous peroxidase inhibition was omitted, and a fluorescein isothiocyanate (FITC)-conjugated anti-rabbit conjugate (anti-rabbit IgG) diluted 1:20 in 0.1% albumin was used as the conjugate. Cells with positive immunoreactivity to the anti-OvHV-2 hyperimmune serum were determined as those that presented an apple-green fluorescent emission at 520 nm. Immunoreactivity of the plates was

observed using an Olympus epifluorescence inverted microscope (IX71) (Olympus Corporation). Uninoculated primary cell cultures and sera from rabbits negative for SA-MCF were used as negative controls.

Immunohistochemistry

The specificity of the anti-OvHV-2 hyperimmune serum was evaluated in the liver of deer that died naturally during the SA-MCF outbreak at the CEIEPAA farm. This technique was performed as described by Headley *et al.* (2022), with some modifications (132). Liver sections were mounted on positively charged slides (Biocare™), deparaffinized with xylene, rehydrated with 0.1 M Tris-HCl buffer (pH 7.2) and transferred to a glass Coplin staining bottle with citrate buffer (0.1 M [pH 6.0]) for antigen retrieval. The procedure was performed in a pressure cooker for 10 min at 200°C. The slides were then left for 15 min at room temperature (RT) in a Coplin jar containing 0.1 M Tris-HCl buffer (pH 7.2). Subsequently, endogenous peroxidase was inhibited using 3% hydrogen peroxide diluted in distilled water. To reduce non-specific background staining, slides were incubated for 1 h at 37°C in a solution containing 0.1 M Tris-HCl buffer (pH 7.2), 1% dry milk, and 0.01% Triton X-100. This solution was decanted, and the slides were incubated overnight at 4°C with rabbit anti-OvHV-2 hyperimmune serum diluted 1:5 in 0.1 M Tris-HCl buffer (pH 7.2) with bovine serum albumin (BSA) at 0.1%. After three washes with 0.1 M Tris-HCl buffer (pH 7.2), the slides were incubated with a peroxidase-coupled anti-rabbit IgG diluted 1:50 in 0.1 M Tris-HCl buffer (pH 7.2) with 0.1% BSA for 1 hour at RT. After three washes with 0.1 M Tris-HCl buffer (pH 7.2), a mixture of 3% hydrogen peroxide and 3,3'-diaminobenzidine was added to the slides to reveal the binding of anti-OvHV-2 hyperimmune serum in deer hepatocytes. Finally, the slides were counterstained with hematoxylin for 1 min.

Positive immunoreactivity to anti-OvHV-2 hyperimmune serum was observed as an insoluble brown stain in the cytoplasm of the hepatocytes. A deer liver sample slide was used and processed as described above as a negative control, but anti-OvHV-2 rabbit hyperimmune serum was omitted.

Results

The outbreak chronology

On August 29, 2018, the first case of SA-MCF was suspected during the necropsy of a six-month-old goat belonging to the quarantine area that had recently been donated to the farm. The animal showed ulcerative lesions on the tongue and larynx; in addition, vasculitis and perivasculitis in different tissues were observed histopathologically. In September, 6 goats from the quarantine area and 15 Holstein cows had ulcerative lesions on the oral mucosa. SA-MCF is considered an exotic disease with mandatory reporting in Mexico, so on September 2, 2018, the outbreak was reported to the CPA. On September 3, the CPA first sampled the animals with and without clinical signs of all animal species to confirm the diagnosis. One week later, the CPA released the results, and the goats and dairy cows were confirmed to be negative for FMDV and VSV by ELISA and PCR. However, on October 4, 2018, six of the Holstein cows were PCR positive for OvHV-2 and negative for IBRV, PRV, and BTV.

By November, the disease had already spread to deer, feedlot cattle, and sheep. At that time, 21 deer had ulcerative lesions in the oral mucosa, and 5 blood samples and 3 tissues of these animals were PCR positive for OvHV-2 and negative for IBRV, VSV, PRV, FMDV, and CEV. On the other hand, 8 Limousine cattle had ulcerative lesions and were also positive for OvHV-2

by PCR. Finally, 10 sheep showed lesions suggestive of MCF, and on November 21, 2018, they were confirmed as positive for OvHV-2 by PCR.

In December 2018, 27 sheep had slight ulcerative oral cavity lesions and at the end of this month, the virus spread to horses; 14 of them displayed ulcerative lesions on the lips although only 2 were PCR positive for OvHV-2 and negative for VSV by RT-PCR and viral isolation (Table 1). Most of the species recovered in a period of 20 days. However, the disease extended in deer for a few more days due to the severity of the ulcerative lesions in the oral mucosa, which made it impossible for them to eat.

During the outbreak, all animals of the farm received medical treatment based on immunological stimulants, vitamins A, D, and E, and the drinking water was alkalized. In November 2019 and 2020, there were two new outbreaks. Affected animals showed clinical signs similar to those observed in 2018. However, in these two new outbreaks, the most affected species was the horse due to the severity of the ulcers. In addition, in 2020, parturient goats also had ulcerative lesions on the oral mucosa.

Post-mortem evaluation

The animals affected during the outbreak at CEIEPAA showed mucogingival ulcers in the buccal vestibule and tongue, hypersalivation, lower food consumption, weight loss, and corneal opacity (Fig 2). The two deer (#172 and #174) had marked retromandibular lymphadenomegaly, congested and edematous tongue, with ulcers on its dorsal part and the base. In addition, focal ulcers were observed in the rumen pillars, covered by a fibrinous pseudomembrane. The liver was slightly enlarged and congested. The main microscopic lesions observed were vasculitis and perivasculitis with fibrinous necrosis of blood vessels in the tongue and rumen, epithelial

erosion, edema, and neovascularization of the cornea. The retromandibular lymph nodes showed lymphoid hyperplasia. The liver showed multifocal hepatic necrosis and cytoplasmic eosinophilic IB (Fig 3). No *post-mortem* lesions were observed in the kidney or lung.

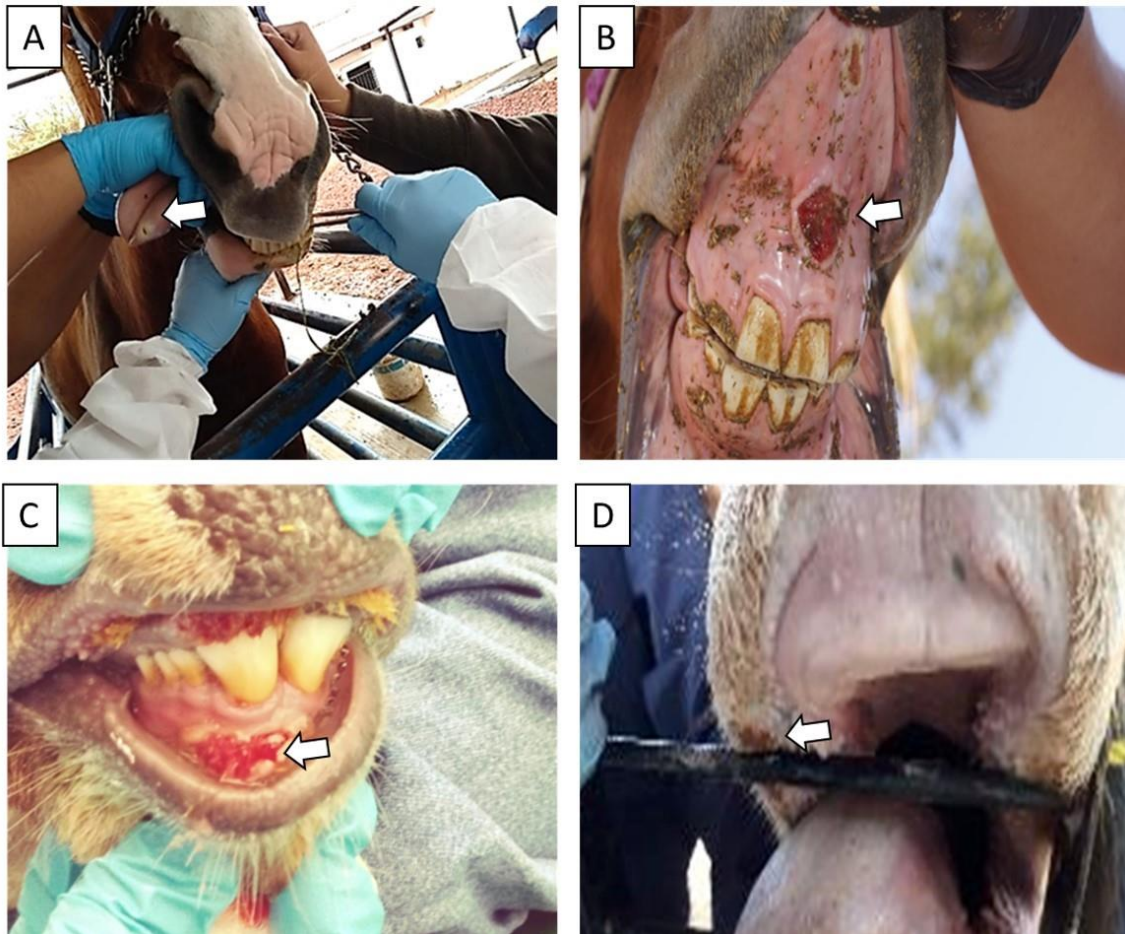


Fig 2. Ulcerative lesions in the oral mucosa of animals that survived the 2018 SA-MCF outbreak and deer that died 5 days after disease onset in CEIEPAA, Tequisquiapan, Queretaro, Mexico. (A) Horse with an ulcer on the apex of the tongue, (B) horse with an ulcer on the mucosa of the gums, (C) deer with ulcers on the mucosa of the upper and lower gums, (D) dairy cattle with an ulcer on the corner of the mouth. White arrows point to ulcers.

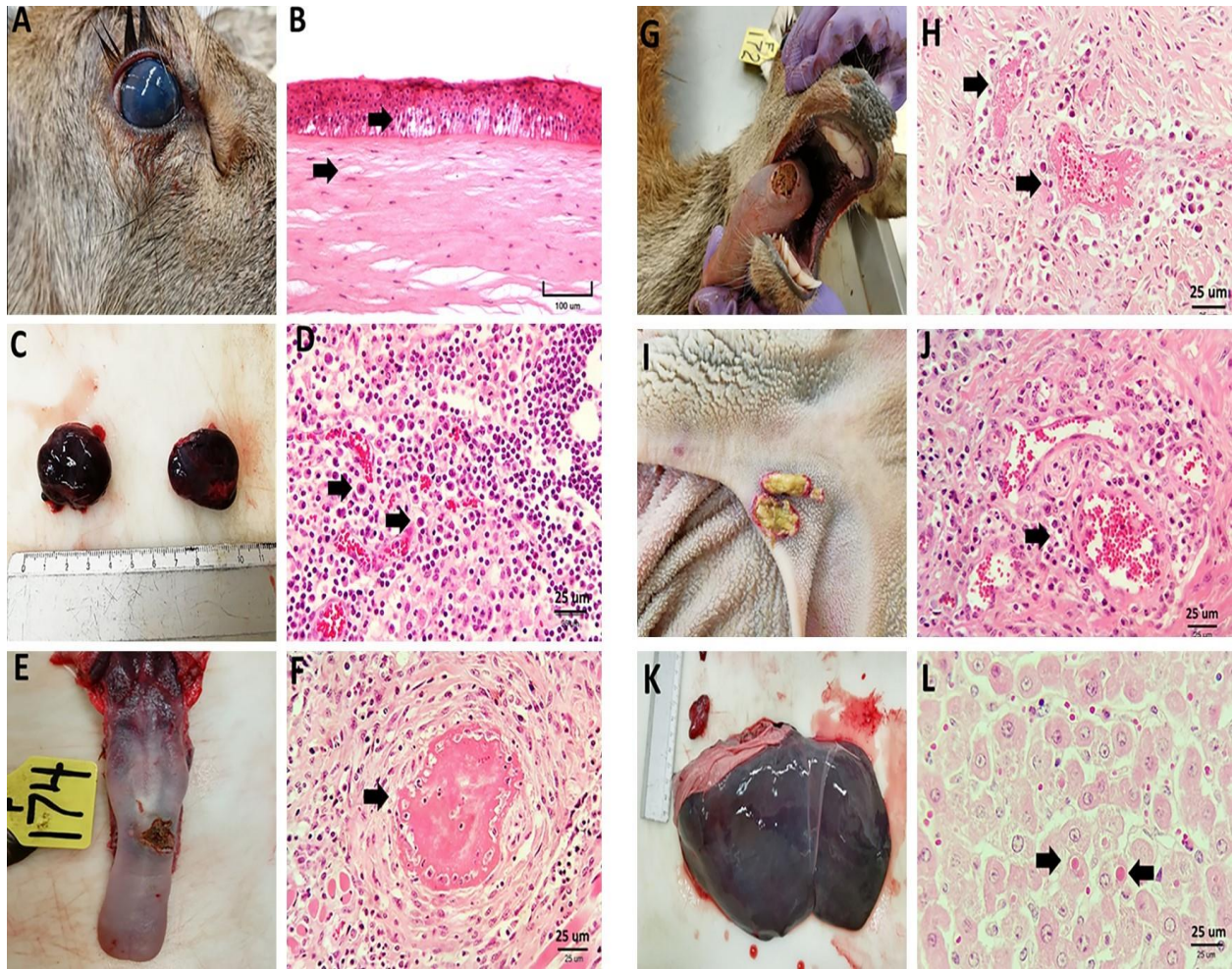


Fig 3. Post-mortem lesions were observed in deer #172 and #174 that died during the 2018 SA-MCF outbreak in CEIEPAA, Tequisquiapan, Queretaro, Mexico. (A) Corneal opacity, (B) cornea with edema and detachment of the corneal epithelium (black arrows), (C) enlarged, congested, and edematous retromandibular lymph nodes, (D) para-follicular region with numerous lymphocytes, plasma cells, and lymphoblasts (black arrows), (E) tongue with loss of epithelium continuity (ulcer) in the dorsal portion, (F) tongue with vasculitis and fibrin thrombus that occludes the lumen and fibrinoid necrosis (black arrow), (G) tongue with an ulcer in the dorsal portion of the tongue, with food encrustation, (H) tongue with thrombosis and infiltrate lymphoplasmacytic and lymphoblastic perivascular inflammation (black arrows), (I) rumen with focal ulcers in the pillar covered by a pseudomembrane, (J) rumen with perivascular inflammation composed of lymphocytes, plasma cells and lymphoblasts (black arrow), (K)

enlarged and congested liver (hepatomegaly), (L) liver with areas of necrosis and cytoplasmic eosinophilic IB (black arrows).

Buffy coat samples

A total of 213 buffy coat samples from the animals with clinical signs compatible with SA-MCF were tested by nested end-point PCR; 86 were positive (40.38%), and 127 were negative (59.62%). The PCR results revealed that resident goats and sheep had the highest percentage of animals positive for OvHV-2, whereas dairy cattle and horses had the lowest number of positive animals (Table 1).

Table 1. Affected species, testing by PCR of other viruses and percentage of positive animals for OvHV-2.

Affected species	*Previous Diagnoses/R esults (PCR)	**Clinical signs	Total, population/ sick/dead	***Total number of animals sampled by CPA, OvHV-2 PCR positive, and percentage of positive	****Sampled animals, OvHV-2 PCR-positive and percentage of positive
Horses	VSV/ (-)	MUMV, UT, LFC, WL	39/14/0	35 [2] (5.71%)	39 [9] (23%)
Feedlot cattle	IBRV, VSV, PRV, FMDV, BTV/ (-)	MUMV, HS, LFC, WL	109/8/0	38 [8] (21.05%)	30 [11] (36%)

Dairy cattle	IBRV, VSV, PRV, FMDV, BTV/ (-)	MUMV, HS, LFC, WL	169/15/0	51 [6] (11.76%)	32 [5] (15%)
Resident goats	IBRV, VSV, PRV, FMDV, BTV/ (-)	-	271/0/0	30 [7] (23.33%)	32 [19] (59%)
Goats in the quarantine area	IBRV, VSV, PRV, FMDV, BTV, CEV/ (-)	MUMV	97/7/0	98 [35] (35.71%)	32 [8] (25%)
Sheep	IBRV, VSV, PRV, FMDV, BTV, CEV/ (-)	MUMV	246/37/0	67 [22] (32.83%)	30 [26] (86%)
Deer	IBRV, VSV, PRV, FMDV, BTV, CEV/ (-)	MUMV, HS, CO, LFC, WL	103/21/14	17 [8] (47.05%)	18 [8] (44%)
Total			1034/65/14	336[88](26.19%)	213[86] (40.3%)

Results of the nested end-point PCR for detecting the OvHV-2 virus in buffy coat samples of different species.

[] = positive to PCR, () = percentage of animals positive to PCR.

*Infectious bovine rhinotracheitis virus (IBRV), vesicular stomatitis virus serotypes Indiana and New Jersey (VSV), parapoxvirus (PRV), foot and mouth disease virus (FMDV), bluetongue virus (BTV), contagious ecthyma virus (CEV).

**mucogingival ulcers in the mouth vestibule (MUMV), ulcers in the tongue (UT), hypersalivation (HS), corneal opacity (CO), lower food consumption (LFC), and weight loss (WL).

*** Total number of animals sampled by CPA from August to December 2018

**** Total number of animals sampled by UNAM during January 2019

Virus isolation in primary cell cultures

The cytopathic effect (CPE) caused by the buffy coat lysate pools, characterized by changes in primary culture morphology, generated small clusters of refractile cytomegalic cells between 48 and 72 h post-infection and was similarly induced with the six buffy coat lysate pools used (Fig 4).

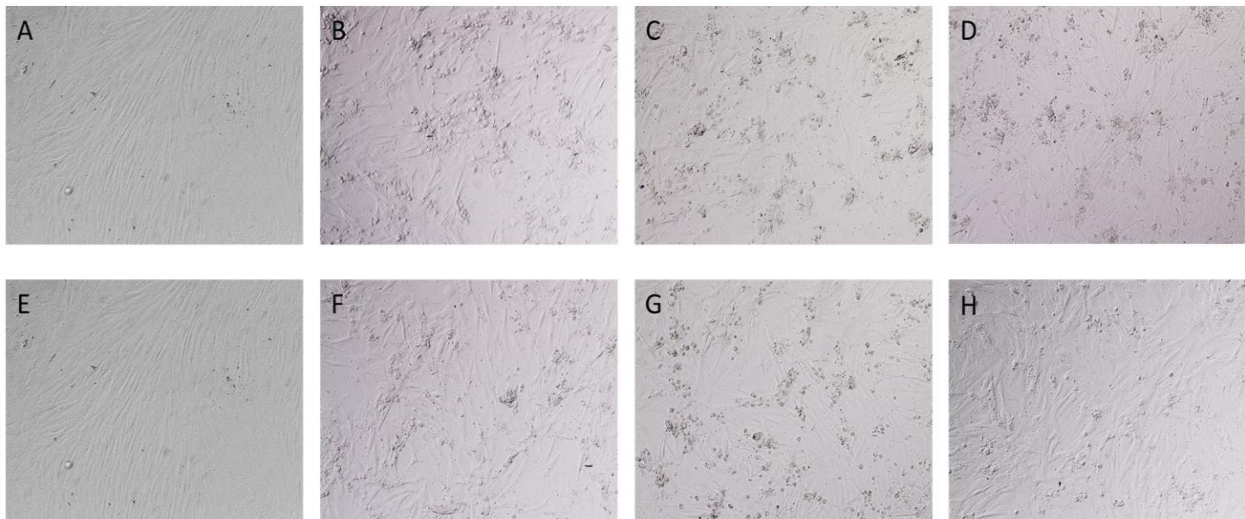


Fig 4. Cytopathic effect in primary cell cultures of rabbit testis cells inoculated with buffy coats of the different animal species affected during the SA-MCF outbreak at 72 h post-infection. (A) Negative controls, (B) fourth blind passage from horses, (C) fourth blind passage from sheep, (D) fourth blind passage from sheep, (E) negative control, (F) fourth blind passage from deer, (G) fourth blind passage from dairy cattle, (H) fourth blind passage from feedlot cattle. Magnification: 100X.

Buffy coat lysates from sheep and goats induced marked CPE with 50% destruction of the monolayer from the first passage to 72 h and 100% between 96 and 120 h post-infection. Similarly, the percentage of CPE increased from the second passage and fourth passage onward for goat and sheep buffy coat lysates, respectively (Table 2). In contrast, primary cell cultures

inoculated with buffy coat lysate pools from horses, dairy cattle, feedlot cattle, and deer showed low CPE, ranging between 20 and 30% in the first and second passages, respectively. In contrast, in the third and fourth passages, monolayer destruction increased to 50% and 90% at 72 h post-infection (Table 2).

Table 2. Cytopathic effect in primary cell cultures.

Affected species	CPE*	CPE*	CPE*	CPE*
	1° passage	2° passage	3° passage	4° passage
Horses	20-30%	20-30%	50%	90-100%
Feedlot cattle	20-30%	20-30%	20-30%	90-100%
Dairy cattle	20-30%	20-30%	90-100%	90-100%
Goats	50%	90-100%	90-100%	90-100%
Sheep	50%	20-30%	20-30%	90-100%
Deer	20-30%	20-30%	50%	90-100%

Percentage of cytopathic effect in primary cell cultures of rabbit testis.

CPE* = Cytopathic effect (percentages reflect the degree of cellular monolayer destruction)

In cell cultures, viral titers obtained from the cell-free supernatants of the 4th blind passage at 72 h post-infection were as follows: horses $10^{4.19}$ TCID₅₀/mL, goats $10^{3.8}$ TCID₅₀/mL, deer $10^{3.3}$ TCID₅₀/mL, dairy cattle $10^{3.5}$ TCID₅₀/mL, feedlot cattle $10^{2.8}$ TCID₅₀/mL and sheep $10^{3.5}$ TCID₅₀/mL.

Viral titers of the cell-free supernatants of the 3rd to 14th passages from the buffy coat lysate from horses were collected at 72 h post-infection in each passage, and the CPE in crystal

violet-stained wells was read (Fig 5). We determined that the viral titer of the 3rd passage was $10^{3.33}$ TCID₅₀/mL, while the viral titers of passages 4, 5, 6, 7, 8, 9, 10, and 11 ranged from 10^4 TCID₅₀/mL to $10^{4.96}$ TCID₅₀/mL, which were very similar. However, an increase in titers was observed in passage 12, 13, and 14 viruses with titers of $10^{5.52}$ TCID₅₀/mL, $10^{6.46}$ TCID₅₀/mL, and $10^{6.67}$ TCID₅₀/mL, respectively.

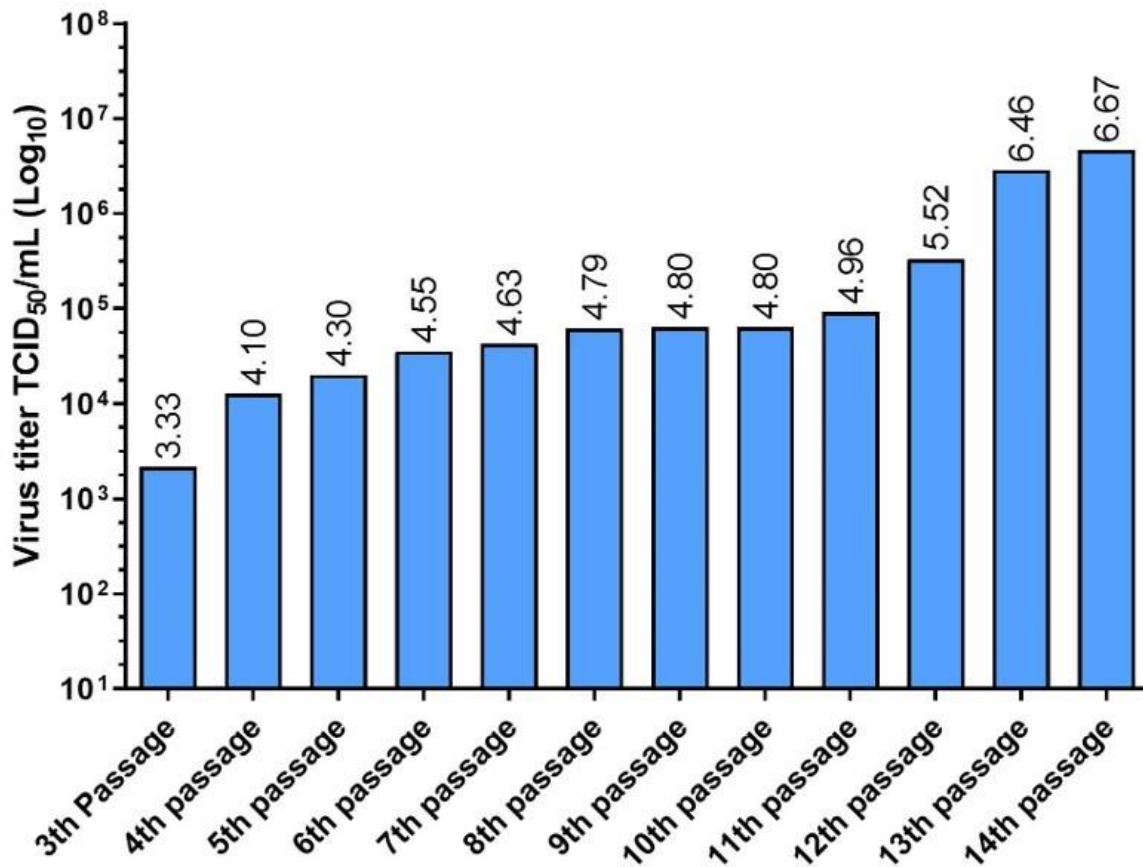


Fig 5. Virus titration of the supernatants from the 3rd to 14th passages of the buffy coat lysate from horses. Continuous passage of the buffy coat lysate from horses in primary rabbit testis cultures led to an increase in viral titer.

Intranuclear acidophilic IBs were observed in primary cell cultures of rabbit testis cells inoculated with the cell-free supernatants of the four blind passages at 24 h post-infection.

However, in the wells containing the cells inoculated with cell-free supernatants of the fourth blind passages from goats and horses, more than five IBs were observed (Fig 6). In contrast, in wells inoculated with cell-free supernatants of the fourth blind passages from dairy cattle, feedlot cattle, sheep, and deer, fewer than three IBs were observed in the entire well.

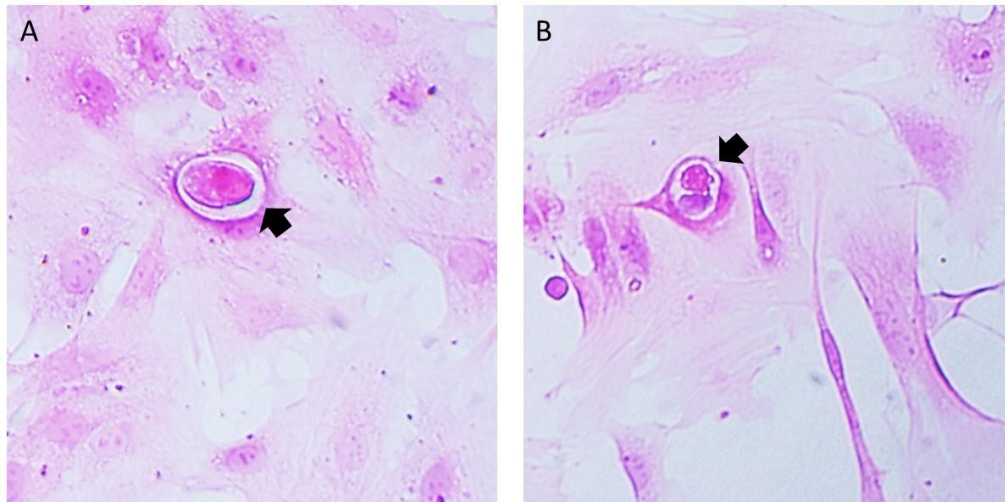


Fig 6. Intranuclear acidophilic IBs were observed at 24 h post-infection. (A) Fourth blind passage from horses, **(B)** fourth blind passage from goats. The black arrows indicate the intranuclear IB. Magnification: 200X. H&E staining.

Nested end-point PCR for OvHV-2 detection

DNA was extracted from the cell-free supernatants of the four blind passages obtained from the infection of the primary cultures with buffy coat lysate pools from the different animal species affected during the SA-MCF outbreak. The cell-free supernatants from horses, goats, and dairy cattle were positive by PCR for OvHV-2 from the first passage. The cell-free supernatants from sheep and deer were positive until the second passage. However, the cell-

free supernatant of feedlot cattle was negative by PCR until the third and fourth passages (Fig 7).

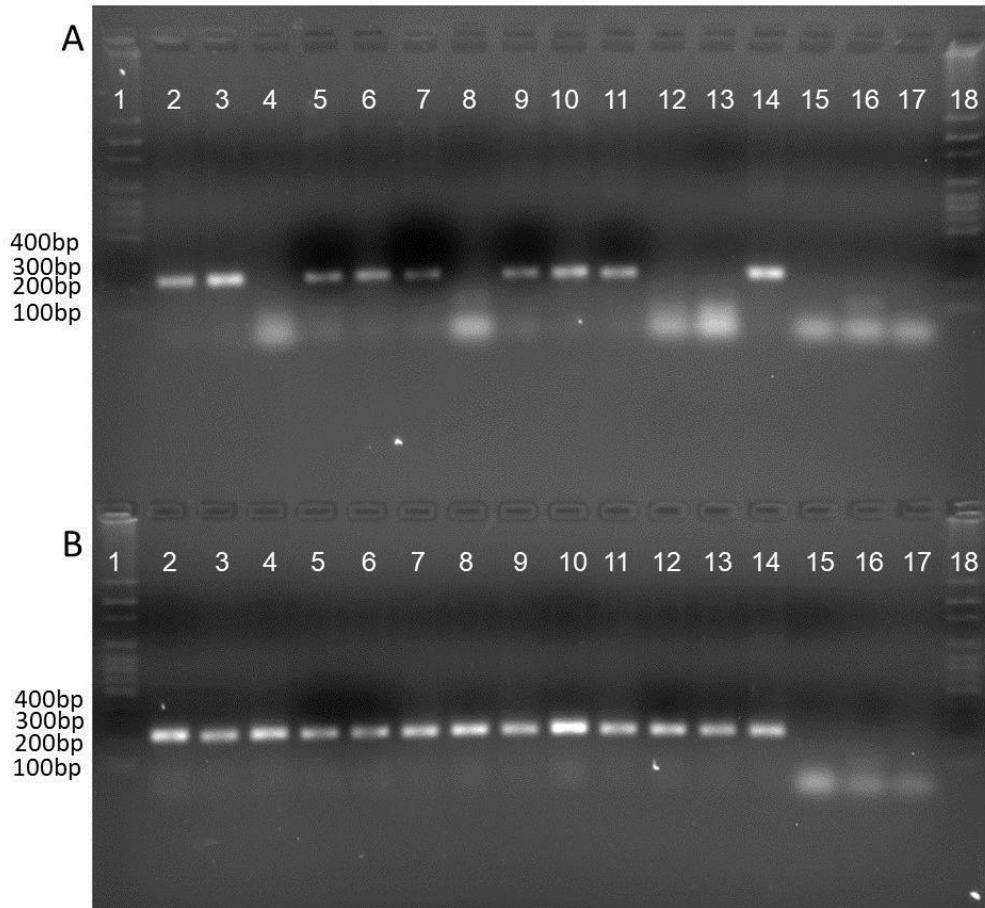


Fig 7. Agarose gel (1.5%) run in TAE 1X buffer. (A) Nested PCR of the first and second passages of primary cell cultures of rabbit testis. (1) Molecular weight marker 1 kb, (2) first blind passage from horses, (3) second blind passage from horses, (4) first blind passage from sheep, (5) second blind passage from sheep, (6) first blind passage from goats, (7) second blind passage from goats, (8) first blind passage from deer, (9) second blind passage from deer, (10) first blind passage from dairy cattle, (11) second blind passage from dairy cattle, (12) first blind passage from feedlot cattle, (13) second blind passage from feedlot cattle, (14) positive control, (15) negative control of amplification (NCA), (16) negative control of extraction (NCE), (17) non-inoculated primary cell cultures (NPCC), (18) molecular weight marker 1 kb. (B) Nested PCR of passages three and four in primary cell cultures of rabbit testis.

(1) Marker of molecular weight of 100 bp, (2) third blind passage from horses, (3) fourth blind passage from horses, (4) third blind passage from sheep, (5) fourth blind passage from sheep, (6) third blind passage from goats, (7) fourth blind passage from goats, (8) third blind passage from deer, (9) fourth blind passage from deer, (10) third blind passage from dairy cattle, (11) fourth blind passage from dairy cattle, (12) third blind passage from feedlot cattle, (13) fourth blind passage from feedlot cattle, (14) positive control, (15) negative control of amplification (NCA), (16) negative control of extraction (CNE), (17) non-inoculated primary cell cultures (NPCC), (18) molecular weight marker 1 kb.

Viral replication kinetics

The growth kinetics study showed that the buffy coat lysate from horses replicated rapidly, and syncytia could be observed starting at 24 h post-infection in the 5th passage and up to 72 h in the 14th passage (Fig 8A).

The 4th and 5th passages achieved similar peak titers of $10^{4.1}$ TCID₅₀/mL and $10^{4.3}$ TCID₅₀/mL at 72 h post-infection, respectively. However, the 14th passage achieved higher peak titers of $10^{6.6}$ TCID₅₀/mL at 72 h post-infection. In addition, at 120 h post-infection, the viral titers decreased (Fig 8C).

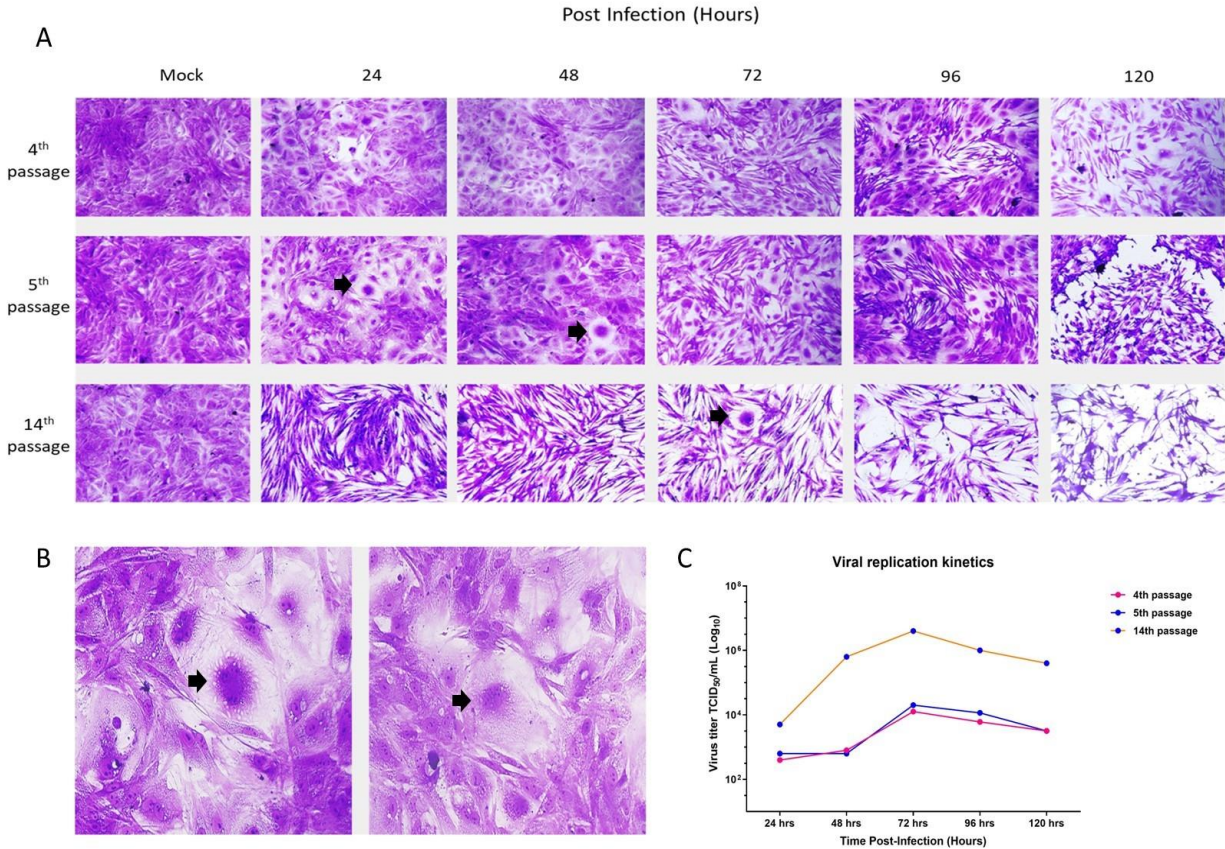


Fig 8. Growth kinetics of the cell-free supernatants from the 4th, 5th, and 14th passages of the buffy coat lysate from horses.

(A) Cells inoculated with supernatant from the 4th passage, upper panel; supernatant from the 5th passage, middle panel; and supernatant from the 14th passage, lower panel. Magnification: 100X. (B) Syncytia were observed in the 5th passage at 24 h and 48 h post-infection (black arrows). Magnification: 200X. (C) Graph of viral titers at 24, 48, 72, 96, and 120 h post-infection corresponding to the 4th, 5th, and 14th passages of the buffy coat lysate from horses, where a maximum replication peak is observed at 72 h post-infection.

Phylogenetic analysis

The alignment of the partial sequences of 422 bp of the *ORF75* gene indicated that the six partial sequences from the cell-free supernatants of the fourth passage from the different species affected by SA-MCF and the positive control of OvHV-2 shared 98%-99% nucleotide identity with other partial *ORF75* sequences obtained from the GenBank database. Regarding the structure of the inferred topology, the analysis indicated that our seven partial sequences present high homology with macaviruses with different OvHV-2 *ORF75* genes, reported in different parts of the world and separated from the clade of rhadinoviruses (human gammaherpesvirus 8) and from lymphocryptovirus (human gammaherpesvirus 4), found in different clades (Fig 9).

On the other hand, the *ORF75* partial sequences of the six cell-free supernatants of the fourth passage compared to the BJ1035 sequence, presented a non-synonymous substitution at position 1213, changing the amino acid (AA) from lysine (K) to threonine (T) (Table 3); however, the partial sequence of the sheep presented a second mutation at position 1314, changing the AA cysteine (C) to glycine (G) (Table 3), and therefore, they were classified as *ORF75*0201* due to the number of substitutions according to Russell's classification *et al.* (2014).

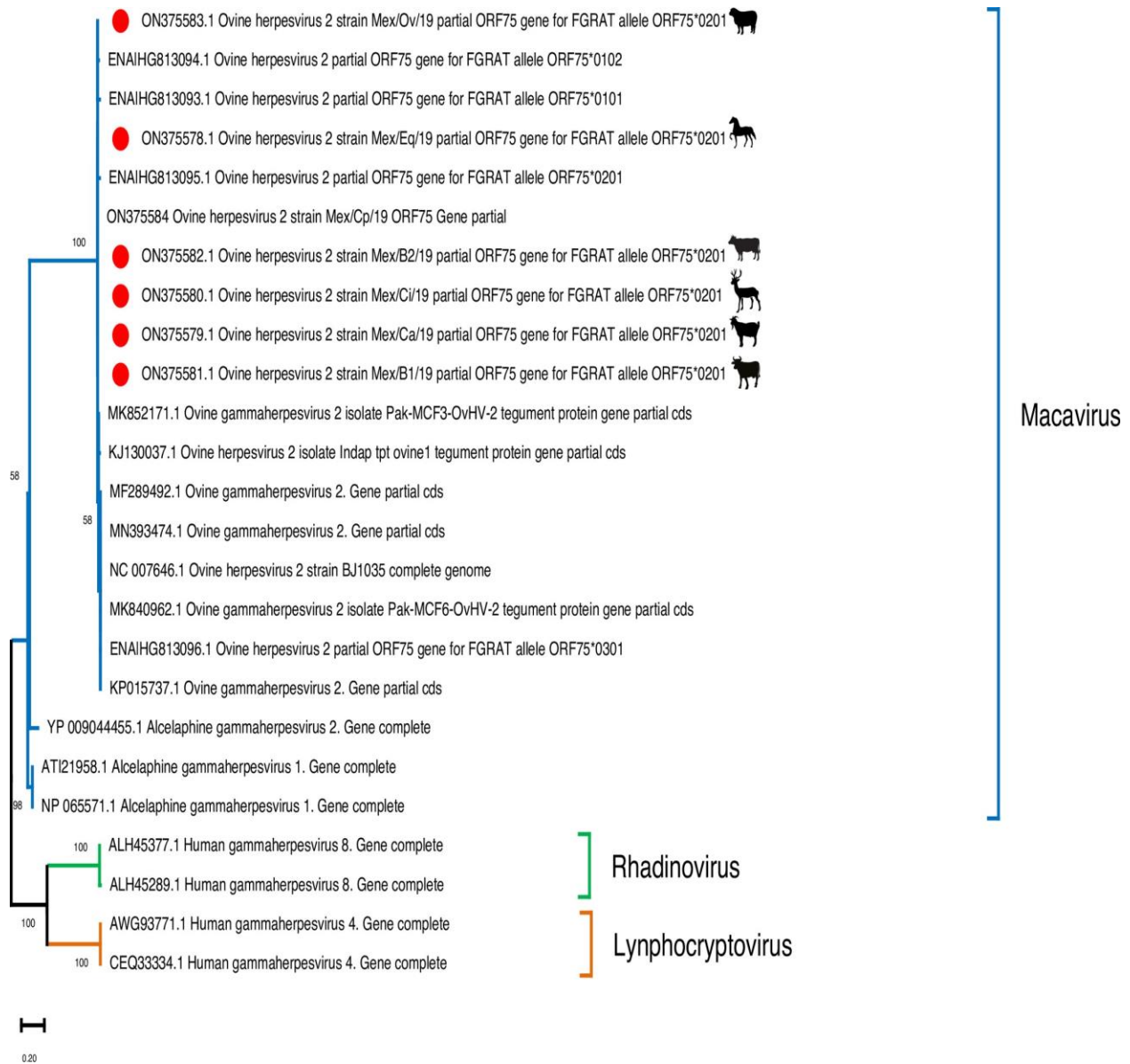


Fig 9. Phylogenetic analysis of partial sequences of the *ORF75* gene. The tree is at scale, and the bar indicates the number of substitutions per site. The Mexican sequences are marked with red circles.

Table 3. Genetic diversity of Mexican *ORF75* sequences compared to the reference gene BJ1035.

GENE <i>ORF75</i>	NT	NT	NT	AA	NT	NT	NT	AA
	[3637]	[3637]	[3637]	[1213]	[3940]	[3941]	[3942]	[1314]
*REF NC_007646.1	A	A	A	LYS	T	G	C	CYS
BJ1035								
ON375578.1	A	C	G	THR	-	-	-	NA
(HORSE)								
ON375579.1	A	C	G	THR	-	-	-	NA
(GOAT)								
ON375580.1	A	C	G	THR	-	-	-	NA
(DEER)								
ON375581.1	A	C	G	THR	-	-	-	NA
(DAIRY COW)								
ON375582.1	A	C	G	THR	-	-	-	NA
(FEEDLOT CATTLE)								
ON375583.1	A	C	G	THR	G	G	C	GLY
(SHEEP)								

*Ref = reference, ()= source isolation, NT = nucleotides, AA= amino acids, [] = position, NA = does not apply.

Immunocytochemistry (ICC) and immunofluorescence (IF) techniques

Positive cytoplasmic immunoreactivity to anti-OvHV-2 rabbit hyperimmune serum was observed in all wells inoculated with cell-free supernatants of the four blind passages from horses, goats, dairy cattle, feedlot cattle, sheep, and deer. However, with the third blind passage of horses and goats, a higher proportion of cells (40% and 50% of the monolayer) with

positive immunoreactivity to rabbit serum was observed (Fig 10). In contrast, wells inoculated with the third and fourth passages of feedlot cattle, dairy cattle, sheep, and deer had a lower proportion of cells (10% of the monolayer), with cytoplasmic immunoreactivity. Apple-green emission at 520 nm by IF and a brown precipitate by ICC were evident.

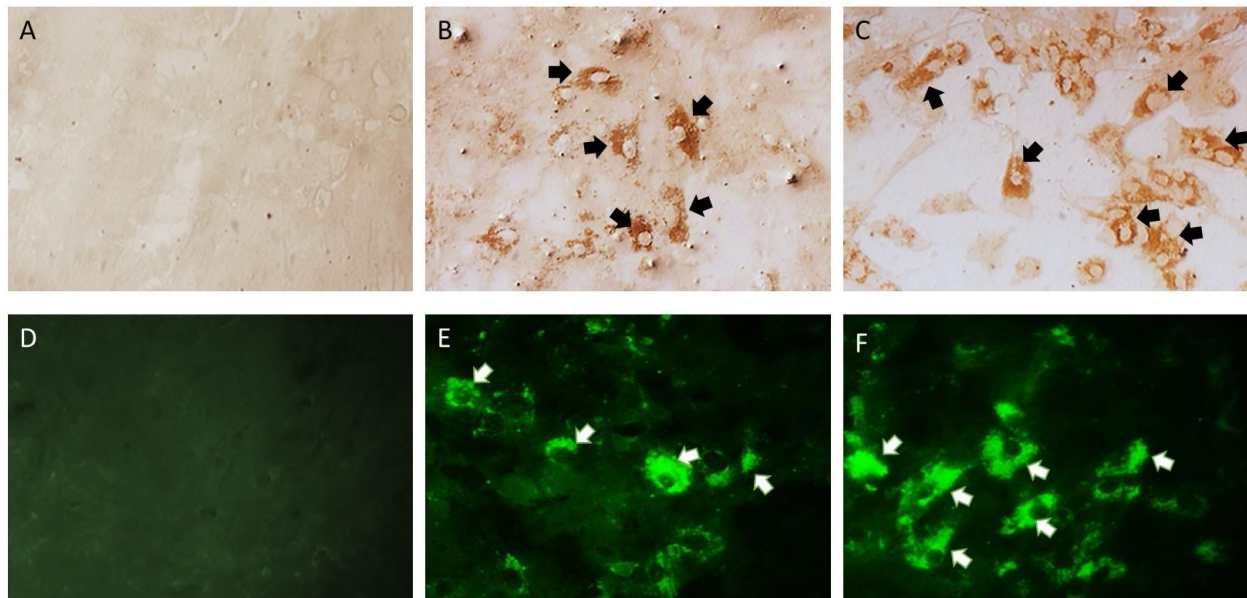


Fig 10. Cytoplasmic immunoreactivity with the ICC and IF techniques in primary cell cultures of rabbit testis cells. (A) ICC negative control, (B) ICC of the third passage from horses, (C) ICC of the third passage from goats, (D) IF negative control, (E) IF of the third passage from horses, (F) IF of the third passage from goats. Arrows indicate the cytoplasmic immunoreactivity appearing as an insoluble brown color for the ICC and a green-apple color for the IF. Magnification: 200X.

Deer liver immunohistochemistry

The cytoplasmic IBs of hepatocytes from the affected deer were immunoreactive to anti-OvHV-2 hyperimmune rabbit serum. In addition, also slight intranuclear immunoreactivity was also observed in hepatocytes (Fig 11).

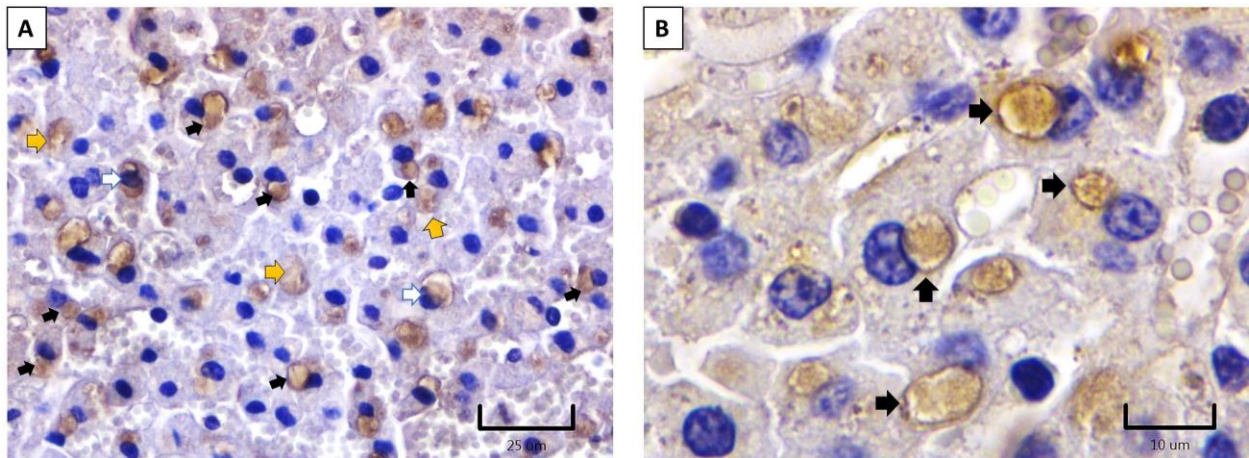


Fig 11. Deer liver immunohistochemistry. (A) and (B) Immunoreactivity to OvHV-2 antigens with rabbit hyperimmune serum in cytoplasmic IBs (black arrows), within the cytoplasm (yellow arrows), and in the nucleus of hepatocytes (white arrows).

Discussion

An outbreak of SA-MCF that occurred in CEIEPAA, located in Tequisquiapan, state of Querétaro, Mexico, is described in the present study. The etiologic agent was identified and characterized as OvHV-2 using different diagnostic techniques, including IF, ICC, CPE, end-point PCR, and partial sequencing of the *ORF75* gene. During the outbreak, many animals of different species were affected, showing typical head-and-eye clinical signs compatible with SA-MCF and corneal opacity (133). The microscopic lesions of vasculitis and perivasculitis in different organs and varying degrees of thrombosis and lymphoid hyperplasia in lymph nodes observed in deer that died during the SA-MCF outbreak are consistent with those reported by Brown *et al.* (1992) in white-tailed deer (88).

This study used buffy coats from affected animals to isolate OvHV-2. This approach is similar to that of a study by Hristov *et al.* (2016), who used bison buffy coats, whole blood, lung, and spleen samples from differently affected animals during an outbreak of SA-MCF (61).

Primary cultures of rabbit testis were used for the *in vitro* isolation of OvHV-2. The use of primary cultures to perform isolations had already been reported previously for AIHV-1 and AIHV-2 (62–64). From the third passage on primary cell cultures of rabbit testis, a marked CPE was observed at 72 h post-infection, consisting of small foci of refractile cytomegalic cells. This CPE was also described by Rossiter *et al.* (1980) during the isolation of AIHV-1 and by Hristov *et al.* (2016) during the isolation of OvHV-2 from camels affected by SA-MCF (61,89).

In the present study, titers of the fourth blind passages from horses, goats, sheep, deer, feedlot cattle, and dairy cattle obtained in primary cell cultures of rabbit testis ranged from log

$10^{2.8}$ to $\log 10^{4.19}$ TCID₅₀/mL. On the other hand, the cell-free supernatant from horses reached its highest peak of $10^{6.6}$ TCID₅₀/mL in passage 14 at 72 h post-infection.

These results indicated that propagation of the OvHV-2 virus in primary rabbit testis cultures led to an increase in viral titers at each passage. This viral titer is similar to that found by Hristov *et al.* (2016) of 10^6 TCID₅₀/mL in Madin-Darby bovine kidney (MDBK) cells after passage 19 (61). This increase in viral titers at higher passages could be because in the first passages, the virus is predominantly cell-associated, and after five passages, there is a period during which the viral genome undergoes rearrangements, leading to viral attenuation and resulting in better cell-free virus yields. However, this has only been shown in AIHV-1 (90). In addition, in primary cultures of rabbit testis inoculated with buffy coats, we identified intranuclear acidophilic IB by H&E staining, which coincides with the results reported by Hristov *et al.* (2016) (61)

OvHV-2 was identified in primary cell cultures from rabbit testis through end-point nested PCR targeting a 238-bp fragment of the *ORF75* gene, with a greater intensity starting in the third and fourth passages in all cell-free supernatants from the different affected species. These results indicate that several blind passages are required to generate better cell-free virus yields and achieve adaptability of the virus to the cell, consistent with the report by Hristov *et al.* (2016) (61).

The buffy coat lysate from horses replicated with similar growth kinetics in the 4th and 5th passages, however, in the 14th passage, it reached a higher titer. Viral replication could be detected starting at 24 h post-infection due to syncyties formation only in the 5th passage and 14th passage. The CPE gradually increased, reaching a maximum at 72 h post-infection and the

decrease in the viral titer at 120 h post-infection could be due to the death of cells. With these results, we can infer that primary cultures of rabbit testis support OvHV-2 replication. Our results agree with those of Hristov *et al.* (2016), in that the bison buffy coat isolate was characterized by small syncytia at 24 h post-infection, and between 60-72 h post-infection there was more than 50% destruction of the monolayer (61)

Furthermore, the definitive diagnosis of OvHV-2 infection was confirmed using partial sequencing of the 422-bp fragment of the *ORF75* gene. Interestingly, the seven sequences from the cell-free supernatants of the fourth passage from different species affected by SA-MCF and the positive control of OvHV-2 shared 98%-99% nucleotide identity among them and with the OvHV-2 sequences reported in different regions of the world. These results align with those reported by Martins *et al.* (2017), who sequenced 13 positive samples of bovines from different areas of Brazil and found 97%-100% similarity with OvHv-2 from several other regions of the world (91)

In the present study, the *ORF75* sequences were classified as *ORF75*0201* for presenting at least one non-synonymous substitution, change from AA cysteine to glycine; this indicates that the infectious agent that affected all animals during the 2018 outbreak with SA-MCF was the same strain as OvHV-2. On the other hand, our results differ from those of Russell *et al.* (2014) because they found that the major allele in 18 samples was *ORF75*0101*, which they found to be similar to the reference sequence BJ1035 (92,93). We can infer that in Mexico, the allele that circulates the most is *ORF75*0201*. However, for genetic characterization and epidemiological studies, we would need to sequence the *ORF50* and *Ov9.5* genes, the latter being the most important for studies of this type (92). In this sense, and with the results

presented above, we could infer goats and sheep as sources of infection (transmission between species) or as potential reservoirs able to transmit to susceptible species (horses, deer, dairy cows, and feedlot cattle) due to their closeness to each other and sharing some of these grasslands.

The cytoplasmic immunoreactivity observed through IF and ICC in primary cell cultures from rabbit testis is equivalent to the intracytoplasmic immunoreactivity observed in multiple tissue samples affected by OvHV-2 using a monoclonal antibody (mAb-15A) targeted at a conserved epitope among all macaviruses (94). In contrast, cytoplasmic acidophilic (eosinophilic) IBs immunoreactive to OvHV-2 using rabbit hyperimmune serum were observed in hepatocytes of deer that died during the SA-MCF outbreak. These results are consistent with those reported by Aluja *et al.* (1969), who described cytoplasmic acidophilic IBs in the neurons of cows infected with SA-MCF (123). Similarly, our results are consistent with those reported by Goss *et al.* (1947), who described these IBs in Purkinje cells and epithelial cells of mucous membranes (134). The cytoplasmic acidophilic IBs observed in the present study could be due to viral multiplication and the overproduction of viral and cellular proteins. These macromolecular aggregates, also called “dense bodies” in transmission electron microscopy, are very common in human cells inoculated with cytomegalovirus. Most of these structures are sequestered in Golgi-derived vesicles, and some dense bodies are located near or in contact with the nuclear envelope, where they appear to be transferred through nuclear pore viral proteins necessary for viral assembly (135). The presence of acidophilic IB, as a manifestation of cytoplasmic accumulation of viral protein, also coincided with that described by Nelson *et al.* (2013), suggesting that cytoplasmic distribution of the capsid protein in OvHV-2 in infected

terminal hosts represents abortive viral replication (136). As a result, it can be speculated that cytoplasmic IBs in deer hepatocytes are formed by the accumulation of viral proteins necessary for virion assembly, in addition to abortive virions and cellular proteins. Further studies are needed to confirm this hypothesis.

Conclusions

The SA-MCF outbreak that affected CEIEPAA animals in Tequisquiapan, Queretaro, Mexico, was caused by the OvHV-2 virus. In addition, it was shown for the first time in Mexico that horses are susceptible to OvHV-2 infection and develop SA-MCF, so it should be considered in the differential diagnosis of vesicular diseases in horses. Considering all results described above, we demonstrate the isolation of OvHV-2 in buffy coat lysate from horses, with the best adaptation to primary cell cultures of rabbit testis and achieving an increase in the viral titer in consecutive passages. Furthermore, we determined that primary rabbit testis cultures could be a good choice of cell culture model for OvHV-2, supporting viral replication kinetics, CPE development, intranuclear IBs, and cytoplasmic immunoreactivity.

We also showed that the Mexican *ORF75* sequences shared 98%-99% nucleotide identity among them and with the OvHV-2 sequences reported in different regions of the world, and the *ORF75*0201* allele affected all animals in the CEIEPAA during the 2018 SA-MCF outbreak.

Acknowledgments

Thanks to PAPIIT-UNAM (IN213321) and T.L. Madrigal-Valencia received a scholarship SEP-CONACYT, ID (968751). Thanks to the Special Cathedra “Dr. José E. Mota” 2019-2020. We would also like to thank the United States-Mexico Commission for the Prevention of Foot-and-Mouth Disease and Other Exotic Animal Diseases (CPA) for their technical support in laboratory testing and positive control. Special thanks to the histotechnologist Verónica Rodríguez Mata.

References

1. Russell GC, Stewart JP, Haig DM. Malignant catarrhal fever: A review. *The Veterinary Journal* [Internet]. 2009 Mar 1 [cited 2023 Mar 2];179(3):324–35. Available from: <https://linkinghub.elsevier.com/retrieve/pii/S1090023307003899>
2. Davison AJ, Eberle R, Ehlers B, Hayward GS, McGeoch DJ, Minson AC, et al. The order Herpesvirales. [cited 2023 Mar 2]; Available from: <http://www.>
3. Current ICTV Taxonomy Release. <https://ictv.global/taxonomy>. 2023.
4. Davison AJ. Herpesvirus systematics. *Vet Microbiol*. 2010 Jun;143(1):52–69.
5. Ensser A, Pflanz R, Fleckenstein B. Primary structure of the alcelaphine herpesvirus 1 genome. *J Virol* [Internet]. 1997 Sep [cited 2023 Mar 2];71(9):6517–25. Available from: <https://journals.asm.org/journal/jvi>
6. Taus NS, Herndon DR, Traul DL, Stewart JP, Ackermann M, Li H, et al. Comparison of ovine herpesvirus 2 genomes isolated from domestic sheep (*Ovis aries*) and a clinically affected cow (*Bos bovis*). *Journal of General Virology* [Internet]. 2007 Jan 1 [cited 2023 Mar 2];88(1):40–5. Available from: <https://www.microbiologyresearch.org/content/journal/jgv/10.1099/vir.0.82285-0>
7. Hart J, Ackermann M, Jayawardane G, Russell G, Haig DM, Reid H, et al. Complete sequence and analysis of the ovine herpesvirus 2 genome. *Journal of General Virology* [Internet]. 2007 Jan 1 [cited 2023 Mar 2];88(1):28–39. Available from: <https://www.microbiologyresearch.org/content/journal/jgv/10.1099/vir.0.82284-0>
8. Li H, O’toole D, Kim O, Oaks JL, Crawford TB. Malignant catarrhal fever-like disease in sheep after intranasal inoculation with ovine herpesvirus-2. *Brief Communications J Vet Diagn Invest*. 2005;17:171–5.

9. PLOWRIGHT W. Malignant Catarrhal Fever in East Africa: I.—Behaviour of the Virus in Free-living Populations of Blue Wildebeest (*Gorgon taurinus taurinus*, Burchell). *Res Vet Sci*. 1965 Jan 1;6(1):56–68.
10. Li H, Taus NS, Jones C, Murphy B, Evermann JF, Crawford TB. A devastating outbreak of malignant catarrhal fever in a bison feedlot. *J Vet Diagn Invest* [Internet]. 2006 [cited 2023 Mar 2];18(1):119–23. Available from: <https://pubmed.ncbi.nlm.nih.gov/16566270/>
11. HOFFMANN D, SOBIRONINGSIH S, CLARKE BC, YOUNG PJ, SENDOW I. Transmission and virological studies of a malignant catarrhal fever syndrome in the Indonesian swamp buffalo (*Bubalus bubalis*). *Aust Vet J* [Internet]. 1984 Apr 1 [cited 2023 Mar 2];61(4):113–6. Available from: <https://onlinelibrary.wiley.com/doi/full/10.1111/j.1751-0813.1984.tb07202.x>
12. Taus NS, Oaks JL, Gailbreath K, Traul DL, O’Toole D, Li H. Experimental aerosol infection of cattle (*Bos taurus*) with ovine herpesvirus 2 using nasal secretions from infected sheep. *Vet Microbiol*. 2006 Aug 25;116(1–3):29–36.
13. O’toole D, Taus NS, Montgomery DL, Oaks JL, Crawford TB, Li H. Intra-nasal Inoculation of American Bison (*Bison bison*) with Ovine Herpesvirus-2 (OvHV-2) Reliably Reproduces Malignant Catarrhal Fever.
14. Costa ÉA, Bomfim MRQ, Da Fonseca FG, Drumond BP, Coelho FM, Vasconcelos AC, et al. Ovine Herpesvirus 2 Infection in Foal, Brazil. *Emerg Infect Dis* [Internet]. 2009 May [cited 2023 Mar 2];15(5):844. Available from: </pmc/articles/PMC2687043/>
15. Gailbreath KL, Taus NS, Cunha CW, Knowles DP, Li H. Experimental infection of rabbits with ovine herpesvirus 2 from sheep nasal secretions. *Vet Microbiol*. 2008 Nov 25;132(1–2):65–73.
16. Li H, Cunha CW, Taus NS. Malignant catarrhal fever: understanding molecular diagnostics in context of epidemiology. *Int J Mol Sci* [Internet]. 2011 Oct [cited 2023 Mar 2];12(10):6881–93. Available from: <https://pubmed.ncbi.nlm.nih.gov/22072925/>
17. Anderson IE, Buxton D, Campbell I, Russell G, Davis WC, Hamilton MJ, et al. Immunohistochemical Study of Experimental Malignant Catarrhal Fever in Rabbits. *J Comp Pathol*. 2007 Feb 1;136(2–3):156–66.
18. Cunha CW, O’Toole D, Taus NS, Knowles DP, Li H. Are rabbits a suitable model to study sheep-associated malignant catarrhal fever in susceptible hosts? *Vet Microbiol* [Internet]. 2013 May 3 [cited 2023 Mar 2];163(3–4):358–63. Available from: <https://linkinghub.elsevier.com/retrieve/pii/S0378113513000485>
19. Buxton D, Reid HW, Finlayson J, Pow I. Pathogenesis of ‘sheep-associated’ malignant catarrhal fever in rabbits. *Res Vet Sci*. 1984 Mar 1;36(2):205–11.
20. Plowright W, Ferris RD, Scott GR. Blue wildebeest and the aetiological agent of bovine malignant catarrhal fever. *Nature* [Internet]. 1960 [cited 2023 Mar 2];188(4757):1167–9. Available from: <https://pubmed.ncbi.nlm.nih.gov/13736396/>

21. Li H, Snowder G, O'Toole D, Crawford TB. Transmission of ovine herpesvirus 2 in lambs. *J Clin Microbiol* [Internet]. 1998 [cited 2023 Mar 2];36(1):223–6. Available from: <https://journals.asm.org/journal/jcm>
22. Hüsey D, Janett F, Albini S, Stäuber N, Thun R, Ackermann M. Analysis of the pathogenetic basis for shedding and transmission of ovine gamma herpesvirus 2. *J Clin Microbiol* [Internet]. 2002 Dec 1 [cited 2023 Mar 2];40(12):4700–4. Available from: <https://journals.asm.org/doi/10.1128/JCM.40.12.4700-4704.2002>
23. Li H, Hua Y, Snowder G, Crawford TB. Levels of ovine herpesvirus 2 DNA in nasal secretions and blood of sheep: implications for transmission. *Vet Microbiol*. 2001 Apr 19;79(4):301–10.
24. Li H, Taus NS, Lewis GS, Kim O, Traul DL, Crawford TB. Shedding of ovine herpesvirus 2 in sheep nasal secretions: The predominant mode for transmission. *J Clin Microbiol* [Internet]. 2004 Dec [cited 2023 Mar 2];42(12):5558–64. Available from: <https://journals.asm.org/doi/10.1128/JCM.42.12.5558-5564.2004>
25. Selman IE, Wiseman A, Wright NG, Murray M. Transmission studies with bovine malignant catarrhal fever. *Vet Rec* [Internet]. 1978 Mar 1 [cited 2023 Mar 2];102(12):252–7. Available from: <https://europepmc.org/article/med/644823>
26. Pierson RE, Storz J, McChesney AE, Thake D. Experimental transmission of malignant catarrhal fever. *Am J Vet Res*. 1974;35(No.4):523–5.
27. Li H, Cunha CW, Davies CJ, Gailbreath KL, Knowles DP, Oaks JL, et al. Ovine herpesvirus 2 replicates initially in the lung of experimentally infected sheep. *Journal of General Virology* [Internet]. 2008 Jul 1 [cited 2023 Mar 2];89(7):1699–708. Available from: <https://www.microbiologyresearch.org/content/journal/jgv/10.1099/vir.0.2008/000554-0>
28. Meier-Trummer CS, Ryf B, Ackermann M. Identification of peripheral blood mononuclear cells targeted by Ovine herpesvirus-2 in sheep. *Vet Microbiol*. 2010 Mar 24;141(3–4):199–207.
29. Cunha CW, Traul DL, Taus NS, Oaks JL, O'Toole D, Davitt CM, et al. Detection of ovine herpesvirus 2 major capsid gene transcripts as an indicator of virus replication in shedding sheep and clinically affected animals. *Virus Res*. 2008 Mar 1;132(1–2):69–75.
30. Taus NS, Schneider DA, Oaks JL, Yan H, Gailbreath KL, Knowles DP, et al. Sheep (*Ovis aries*) airway epithelial cells support ovine herpesvirus 2 lytic replication in vivo. *Vet Microbiol*. 2010 Sep 28;145(1–2):47–53.
31. Cunha CW, Gailbreath KL, O'Toole D, Knowles DP, Schneider DA, White SN, et al. Ovine herpesvirus 2 infection in American bison: virus and host dynamics in the development of sheep-associated malignant catarrhal fever. *Vet Microbiol* [Internet]. 2012 Oct 12 [cited 2023 Mar 2];159(3–4):307–19. Available from: <https://linkinghub.elsevier.com/retrieve/pii/S0378113512002702>
32. Meier-Trummer CS, Tobler K, Hilbe M, Stewart JP, Hart J, Campbell I, et al. Ovine herpesvirus 2 structural proteins in epithelial cells and M-cells of the appendix in rabbits with malignant

- catarrhal fever. *Vet Microbiol* [Internet]. 2009 Jun 12 [cited 2023 Mar 2];137(3–4):235–42. Available from: <https://linkinghub.elsevier.com/retrieve/pii/S0378113509000510>
33. Nelson DD, Taus NS, Schneider DA, Cunha CW, Davis WC, Brown WC, et al. Fibroblasts express OvHV-2 capsid protein in vasculitis lesions of American bison (*Bison bison*) with experimental sheep-associated malignant catarrhal fever. *Vet Microbiol* [Internet]. 2013 Oct 25 [cited 2023 Mar 2];166(3–4):486–92. Available from: <https://linkinghub.elsevier.com/retrieve/pii/S0378113513003830>
 34. OIE. Malignant catarrhal fever. In: *OIE Manual of Diagnostic Tests and Vaccines for Terrestrial Animal*,. Fifth. France; 2004. 570–579 p.
 35. O’toole D, Li H, Sourk C, Montgomery DL, Crawford TB. Malignant catarrhal fever in a bison (*Bison bison*) feedlot, 1993-2000. *J Vet Diagn Invest*. 2002;14:183–93.
 36. Palmer MV, Thacker TC, Madison RJ, Koster LG, Swenson SL, Li H. Active and Latent Ovine Herpesvirus-2 (OvHV-2) Infection in a Herd of Captive White-tailed Deer (*Odocoileus virginianus*). *J Comp Pathol* [Internet]. 2013 Aug 1 [cited 2023 Mar 2];149(2–3):162–6. Available from: <https://linkinghub.elsevier.com/retrieve/pii/S0021997513000194>
 37. Reid HW, Buxton D, McKelvey WA, Milne JA, Appleyard WT. Malignant catarrhal fever in Père David’s deer. *Vet Rec* [Internet]. 1987 [cited 2023 Mar 2];121(12):276–7. Available from: <https://pubmed.ncbi.nlm.nih.gov/3672838/>
 38. Berezowski JA, Appleyard GD, Crawford TB, Haigh J, Li H, Middleton DM, et al. BRIEF COMMUNICATIONS An outbreak of sheep-associated malignant catarrhal fever in bison (*Bison bison*) after exposure to sheep at a public auction sale. *J Vet Diagn Invest*. 2005;17:55–8.
 39. Rech RR, Schild AL, Driemeier D, Garmatz SL, Oliveira FN, Riet-Correa F, et al. Malignant catarrhal fever in cattle in Rio Grande do Sul, Brazil: epidemiology, clinical signs and pathology. *Pesquisa Veterinária Brasileira* [Internet]. 2005 [cited 2023 Mar 2];25(2):97–105. Available from: <http://www.scielo.br/j/pvb/a/snHFypBVPZqwt6QcD8gwMVD/abstract/?lang=en>
 40. Collery P, Foley A. An outbreak of malignant catarrhal fever in cattle in the Republic of Ireland. *Vet Rec* [Internet]. 1996 Jul 6 [cited 2023 Mar 2];139(1):16–7. Available from: <https://pubmed.ncbi.nlm.nih.gov/8819289/>
 41. Frölich K, Li H, Müller-Doblies U. SEROSURVEY FOR ANTIBODIES TO MALIGNANT CATARRHAL FEVER-ASSOCIATED VIRUSES IN FREE-LIVING AND CAPTIVE CERVIDS IN GERMANY. *J Wildl Dis* [Internet]. 1998 Jan 1 [cited 2023 Mar 2];34(4):777–82. Available from: <https://meridian.allenpress.com/jwd/article/34/4/777/122072/SEROSURVEY-FOR-ANTIBODIES-TO-MALIGNANT-CATARRHAL>
 42. Desmecht D, Cassart D, Rollin F, Coignoul F, Tham KM. Molecular and clinicopathological diagnosis of non-wildebeest associated malignant catarrhal fever in Belgium. *Veterinary Record* [Internet]. 1999 Apr 1 [cited 2023 Mar 2];144(14):388–388. Available from: <https://onlinelibrary.wiley.com/doi/full/10.1136/vr.144.14.388>

43. Yus E, Guitián J, Díaz A, Sanjuán ML. Outbreak of malignant catarrhal fever in cattle in Spain. *Vet Rec* [Internet]. 1999 Oct 16 [cited 2023 Mar 2];145(16):466–7. Available from: <https://pubmed.ncbi.nlm.nih.gov/10576285/>
44. Dabak M, Bulut H. Outbreak of malignant catarrhal fever in cattle in Turkey. *Vet Rec* [Internet]. 2003 Feb 22 [cited 2023 Mar 2];152(8):240–1. Available from: <https://pubmed.ncbi.nlm.nih.gov/12625541/>
45. Rossiter PB. Antibodies to malignant catarrhal fever virus in sheep sera. *J Comp Pathol* [Internet]. 1981 [cited 2023 Mar 2];91(2):303–11. Available from: <https://pubmed.ncbi.nlm.nih.gov/7047584/>
46. Wilson PR. Advances in health and welfare of farmed deer in New Zealand. *N Z Vet J* [Internet]. 2002 [cited 2023 Mar 2];50(3 Suppl):105–9. Available from: <https://pubmed.ncbi.nlm.nih.gov/16032253/>
47. Aluja A, Rocha TC De, Velázquez A. Fiebre catarral maligna. *Rev Mex Cienc Pecu.* 1969;
48. Li H, Cunha CW, Taus NS, Knowles DP. Malignant catarrhal fever: inching toward understanding. *Annu Rev Anim Biosci* [Internet]. 2014 [cited 2023 Mar 2];2:209–33. Available from: <https://pubmed.ncbi.nlm.nih.gov/25384141/>
49. Pierson RE, Thake D, McChesney AE, Storz J. An epizootic of malignant catarrhal fever in feedlot cattle. *J Am Vet Med Assoc.* 1973;163(No.4):349–50.
50. Lankester F, Lugelo A, Kazwala R, Keyyu J, Cleaveland S, Yoder J. Correction: The Economic Impact of Malignant Catarrhal Fever on Pastoralist Livelihoods. *PLoS One* [Internet]. 2019 Sep 1 [cited 2023 Mar 2];14(9). Available from: <https://pubmed.ncbi.nlm.nih.gov/31557267/>
51. Schultheiss PC, Collins JK, Spraker TR, DeMartini JC. Epizootic malignant catarrhal fever in three bison herds: differences from cattle and association with ovine herpesvirus-2. *J Vet Diagn Invest* [Internet]. 2000 [cited 2023 Mar 2];12(6):497–502. Available from: <https://pubmed.ncbi.nlm.nih.gov/11108448/>
52. O’Toole D, Li H, Miller D, Williams WR, Crawford TB. Chronic and recovered cases of sheep-associated malignant catarrhal fever in cattle. *Vet Rec* [Internet]. 1997 [cited 2023 Mar 2];140(20):519–24. Available from: <https://pubmed.ncbi.nlm.nih.gov/9178482/>
53. Headley SA, de Oliveira TES, Cunha CW. A review of the epidemiological, clinical, and pathological aspects of malignant catarrhal fever in Brazil. *Braz J Microbiol* [Internet]. 2020 Sep 1 [cited 2023 May 16];51(3):1405–32. Available from: <https://pubmed.ncbi.nlm.nih.gov/32542424/>
54. Li H, McGuire TC, Müller-Doblies UU, Crawford TB. A simpler, more sensitive competitive inhibition enzyme-linked immunosorbent assay for detection of antibody to malignant catarrhal fever viruses. *J Vet Diagn Invest* [Internet]. 2001 [cited 2023 Mar 2];13(4):361–4. Available from: <https://pubmed.ncbi.nlm.nih.gov/11478614/>
55. Powers JG, VanMetre DC, Collins JK, Dinsmore RP, Carman J, Patterson G, et al. Evaluation of ovine herpesvirus type 2 infections, as detected by competitive inhibition ELISA and polymerase chain reaction assay, in dairy cattle without clinical signs of malignant catarrhal fever. *J Am Vet*

- Med Assoc [Internet]. 2005 Aug 15 [cited 2023 Mar 2];227(4):606–11. Available from: <https://pubmed.ncbi.nlm.nih.gov/16117071/>
56. Hüseyin D, Stäubli N, Leutenegger CM, Rieder S, Ackermann M. Quantitative fluorogenic PCR assay for measuring ovine herpesvirus 2 replication in sheep. *Clin Diagn Lab Immunol* [Internet]. 2001 [cited 2023 Jun 12];8(1):123–8. Available from: <https://pubmed.ncbi.nlm.nih.gov/11139205/>
 57. Baxter SIF, Pow I, Bridgen A, Reid HW. PCR detection of the sheep-associated agent of malignant catarrhal fever. *Arch Virol* [Internet]. 1993 Mar [cited 2023 Mar 6];132(1–2):145–59. Available from: <https://link.springer.com/article/10.1007/BF01309849>
 58. Cunha CW, Otto L, Taus NS, Knowles DP, Li H. Development of a multiplex real-time PCR for detection and differentiation of malignant catarrhal fever viruses in clinical samples. *J Clin Microbiol* [Internet]. 2009 Aug [cited 2023 Jun 12];47(8):2586–9. Available from: <https://pubmed.ncbi.nlm.nih.gov/19494077/>
 59. Li H, Snowden G, Crawford TB. Production of malignant catarrhal fever virus-free sheep. *Vet Microbiol* [Internet]. 1999 Mar 1 [cited 2023 Jun 12];65(2):167–72. Available from: <https://pubmed.ncbi.nlm.nih.gov/10078600/>
 60. Traul DL, Taus NS, Oaks JL, O’Toole D, Rurangirwa FR, Baszler T V., et al. Validation of nonnested and real-time PCR for diagnosis of sheep-associated malignant catarrhal fever in clinical samples. *J Vet Diagn Invest* [Internet]. 2007 [cited 2023 Jun 12];19(4):405–8. Available from: <https://pubmed.ncbi.nlm.nih.gov/17609352/>
 61. Hristov M V., Peshev RD. Isolation and identification of malignant catarrhal fever virus in cell cultures. *Bulg J Vet Med*. 2016;19(4):263–73.
 62. Plowright W, Ferris RD, Scott GR. Blue wildebeest and the aetiological agent of bovine malignant catarrhal fever. *Nature* [Internet]. 1960 [cited 2023 May 16];188(4757):1167–9. Available from: <https://pubmed.ncbi.nlm.nih.gov/13736396/>
 63. Plowright W, Ferris RD. The Preparation of Bovine Thyroid Monolayers for use in Virological Investigations. *Res Vet Sci*. 1961 Apr 1;2(2):149–53.
 64. Castro AE, Daley GG, Zimmer MA, Whitenack DL, Jensen J. Malignant catarrhal fever in an Indian gaur and greater kudu: experimental transmission, isolation, and identification of a herpesvirus. *Am J Vet Res* [Internet]. 1982 Jan 1 [cited 2023 May 16];43(1):5–11. Available from: <https://europepmc.org/article/MED/7091816>
 65. Handley JA, Sargan DR, Herring AJ, Reid HW. Identification of a region of the alcelaphine herpesvirus-1 genome associated with virulence for rabbits. *Vet Microbiol* [Internet]. 1995 [cited 2023 Mar 2];47(1–2):167–81. Available from: <https://pubmed.ncbi.nlm.nih.gov/8604548/>
 66. Wright H, Stewart JP, Ireri RG, Campbell I, Pow I, Reid HW, et al. Genome re-arrangements associated with loss of pathogenicity of the γ -herpesvirus alcelaphine herpesvirus-1. *Res Vet Sci* [Internet]. 2003 [cited 2023 Mar 2];75(2):163–8. Available from: <https://pubmed.ncbi.nlm.nih.gov/12893166/>

67. Goss LW, Cole CR, Kissling RE. The Pathology of Malignant Catarrhal Fever (Bovine Epitheliosis): With Special Reference to Cytoplasmic Inclusions. *Am J Pathol* [Internet]. 1947 Sep 1 [cited 2023 May 16];23(5):837–41. Available from: <https://www.ncbi.nlm.nih.gov/pmc/articles/PMC19970964/?tool=EBI>
68. Severi B, Landini MP, Cenacchi G, Zini N, Maraldi NM. Human cytomegalovirus nuclear and cytoplasmic dense bodies. *Arch Virol* [Internet]. 1992 Mar [cited 2023 Mar 2];123(1–2):193–207. Available from: <https://pubmed.ncbi.nlm.nih.gov/1372496/>
69. Li H, Cunha CW, Taus NS. Malignant catarrhal fever: understanding molecular diagnostics in context of epidemiology. *Int J Mol Sci* [Internet]. 2011 Oct [cited 2023 May 16];12(10):6881–93. Available from: <https://pubmed.ncbi.nlm.nih.gov/22072925/>
70. Pérez-Guiot A, Páez-Trejo A, Domínguez-Hernández Y, Carranza-Velázquez J, Hernández-García D, Carrisoza-Urbina I, et al. Pakistan Veterinary Journal Malignant Catarrhal Fever Associated with Ovine Gammaherpesvirus-2 in Domestic Ruminants in Queretaro, Mexico. [cited 2023 Jun 12]; Available from: <http://dx.doi.org/10.29261/pakvetj/2022.076>
71. English D, Andersen BR. Single-step separation of red blood cells. Granulocytes and mononuclear leukocytes on discontinuous density gradients of Ficoll-Hypaque. *J Immunol Methods* [Internet]. 1974 [cited 2023 May 16];5(3):249–52. Available from: <https://pubmed.ncbi.nlm.nih.gov/4427075/>
72. Baxter SIF, Pow I, Bridgen A, Reid HW. PCR detection of the sheep-associated agent of malignant catarrhal fever. *Arch Virol* [Internet]. 1993 Mar [cited 2023 May 16];132(1–2):145–59. Available from: <https://pubmed.ncbi.nlm.nih.gov/8352654/>
73. High Pure PCR Template Preparation Kit Rapidly purify genomic DNA for diverse applications. [cited 2023 Mar 6]; Available from: www.roche-applied-science.com
74. Li H, Shen DT, O'toole D, Knowles DP, Gorham JR, Crawford TB, et al. Investigation of sheep-associated malignant catarrhal fever virus infection in ruminants by PCR and competitive inhibition enzyme-linked immunosorbent assay. *J Clin Microbiol* [Internet]. 1995 [cited 2023 Mar 6];33(8):2048–53. Available from: <https://journals.asm.org/doi/10.1128/jcm.33.8.2048-2053.1995>
75. Reed LJ, Muench H. A simple method of estimating fifty per cent endpoints. *Am J Epidemiol* [Internet]. 1938 May 1 [cited 2023 Mar 6];27(3):493–7. Available from: <https://academic.oup.com/aje/article/27/3/493/99616>
76. Hall T. BIOEDIT: A USER-FRIENDLY BIOLOGICAL SEQUENCE ALIGNMENT EDITOR AND ANALYSIS PROGRAM FOR WINDOWS 95/98/ NT. 1999;
77. Tamura K, Stecher G, Kumar S. MEGA11: Molecular Evolutionary Genetics Analysis Version 11. *Mol Biol Evol* [Internet]. 2021 Jul 1 [cited 2023 May 16];38(7):3022–7. Available from: <https://pubmed.ncbi.nlm.nih.gov/33892491/>

78. Johnson M, Zaretskaya I, Raytselis Y, Merezhuk Y, McGinnis S, Madden TL. NCBI BLAST: a better web interface. *Nucleic Acids Res* [Internet]. 2008 Jul 1 [cited 2023 Mar 6];36(suppl_2):W5–9. Available from: https://academic.oup.com/nar/article/36/suppl_2/W5/2505810
79. Posada D. jModelTest: phylogenetic model averaging. *Mol Biol Evol* [Internet]. 2008 Jul [cited 2023 Jun 18];25(7):1253–6. Available from: <https://pubmed.ncbi.nlm.nih.gov/18397919/>
80. Tamura K, Nei M. Estimation of the number of nucleotide substitutions in the control region of mitochondrial DNA in humans and chimpanzees. *Mol Biol Evol* [Internet]. 1993 May 1 [cited 2023 May 16];10(3):512–26. Available from: <https://academic.oup.com/mbe/article/10/3/512/1016366>
81. Orós J, Poveda JB, Rodríguez JL, Franklin CL, Fernández A. Natural cilia-associated respiratory bacillus infection in rabbits used for elaboration of hyperimmune serum against *Mycoplasma* sp. *Zentralbl Veterinarmed B* [Internet]. 1997 [cited 2023 May 16];44(5):313–7. Available from: <https://pubmed.ncbi.nlm.nih.gov/9270356/>
82. Rossiter PB. Immunofluorescence and immunoperoxidase techniques for detecting antibodies to malignant catarrhal fever in infected cattle. *Trop Anim Health Prod* [Internet]. 1981 [cited 2023 Mar 2];13(4):189–92. Available from: <https://pubmed.ncbi.nlm.nih.gov/7046177/>
83. Headley SA, de Lemos GAA, Dall Agnol AM, Xavier AAC, Depes VCA, Yasumitsu CY, et al. Ovine gammaherpesvirus 2 infections in cattle without typical manifestations of sheep-associated malignant catarrhal fever and concomitantly infected with bovine coronavirus. *Braz J Microbiol* [Internet]. 2022 Mar 1 [cited 2023 May 16];53(1):433–46. Available from: <https://pubmed.ncbi.nlm.nih.gov/34780031/>
84. Fu DA, Campbell-Thompson M. Periodic acid-schiff staining with diastase. *Methods in Molecular Biology* [Internet]. 2017 [cited 2023 Mar 6];1639:145–9. Available from: https://link.springer.com/protocol/10.1007/978-1-4939-7163-3_14
85. Chieco P. The Feulgen reaction 75 years on Identification of innovative microRNA-based biomarkers and anti-cancer strategies for the treatment of hepatocellular carcinoma View project Image Cytometry View project. Article in *Histochemistry and Cell Biology* [Internet]. 1999 [cited 2023 Mar 6]; Available from: <https://www.researchgate.net/publication/12896440>
86. Gailbreath KL, Taus NS, Cunha CW, Knowles DP, Li H. Experimental infection of rabbits with ovine herpesvirus 2 from sheep nasal secretions. *Vet Microbiol*. 2008 Nov 25;132(1–2):65–73.
87. Devan KS, Walther P, von Einem J, Ropinski T, Kestler HA, Read C. Detection of herpesvirus capsids in transmission electron microscopy images using transfer learning. *Histochem Cell Biol* [Internet]. 2019 Feb 5 [cited 2023 Mar 6];151(2):101–14. Available from: <https://link.springer.com/article/10.1007/s00418-018-1759-5>
88. Brown CC, Bloss LL. An epizootic of malignant catarrhal fever in a large captive herd of white-tailed deer (*Odocoileus virginianus*). *J Wildl Dis* [Internet]. 1992 [cited 2023 May 16];28(2):301–5. Available from: <https://pubmed.ncbi.nlm.nih.gov/1602586/>

89. Rossiter PB. A lack of readily demonstrable virus antigens in the tissues of rabbits and cattle infected with malignant catarrhal fever virus. *Br Vet J* [Internet]. 1980 [cited 2023 May 16];136(5):478–83. Available from: <https://pubmed.ncbi.nlm.nih.gov/6784880/>
90. Wright H, Stewart JP, Ileri RG, Campbell I, Pow I, Reid HW, et al. Genome re-arrangements associated with loss of pathogenicity of the γ -herpesvirus alcelaphine herpesvirus-1. *Res Vet Sci* [Internet]. 2003 [cited 2023 May 16];75(2):163–8. Available from: <https://pubmed.ncbi.nlm.nih.gov/12893166/>
91. Martins M de SN, Castro AMMG de, Lima M dos S, Pinto V da SC, Silva TG da, Fava C Del, et al. Malignant Catarrhal Fever in Brazilian cattle presenting with neurological syndrome. *Braz J Microbiol* [Internet]. 2017 Apr 1 [cited 2023 May 16];48(2):366–72. Available from: <https://pubmed.ncbi.nlm.nih.gov/28081979/>
92. Russell GC, Scholes SF, Twomey DF, Courtenay AE, Grant DM, Lamond B, et al. Analysis of the genetic diversity of ovine herpesvirus 2 in samples from livestock with malignant catarrhal fever. *Vet Microbiol* [Internet]. 2014 Aug 6 [cited 2023 May 16];172(1–2):63–71. Available from: <https://pubmed.ncbi.nlm.nih.gov/24846753/>
93. Hart J, Ackermann M, Jayawardane G, Russell G, Haig DM, Reid H, et al. Complete sequence and analysis of the ovine herpesvirus 2 genome. *J Gen Virol* [Internet]. 2007 Jan [cited 2023 May 16];88(Pt 1):28–39. Available from: <https://pubmed.ncbi.nlm.nih.gov/17170433/>
94. Headley SA, de Lemos GAA, Dall Agnol AM, Xavier AAC, Depes VCA, Yasumitsu CY, et al. Ovine gammaherpesvirus 2 infections in cattle without typical manifestations of sheep-associated malignant catarrhal fever and concomitantly infected with bovine coronavirus. *Brazilian Journal of Microbiology* [Internet]. 2022 Mar 1 [cited 2023 Mar 6];53(1):433–46. Available from: <https://link.springer.com/article/10.1007/s42770-021-00653-6>
95. Severi B, Landini MP, Cenacchi G, Zini N, Maraldi NM. Human cytomegalovirus nuclear and cytoplasmic dense bodies. *Arch Virol* [Internet]. 1992 Mar [cited 2023 Mar 6];123(1–2):193–207. Available from: <https://link.springer.com/article/10.1007/BF01317149>
96. Riaz A. Recent Understanding of the Classification and Life Cycle of Herpesviruses: A Review Detection and Molecular Characterization of Mastitis, Mammilitis and Reproductive tract disorders causing Herpesviruses in Dairy Cattles View project Establishing animal gut microbial species catalogue by metagenomic sequencing View project. 2017 [cited 2023 Mar 6]; Available from: <https://www.researchgate.net/publication/320033956>
97. O’Toole D, Li H. The pathology of malignant catarrhal fever, with an emphasis on ovine herpesvirus 2. *Vet Pathol* [Internet]. 2014 Mar [cited 2023 May 16];51(2):437–52. Available from: <https://pubmed.ncbi.nlm.nih.gov/24503439/>
98. Russell GC, Stewart JP, Haig DM. Malignant catarrhal fever: A review. *Veterinary Journal*. 2009 Mar;179(3):324–35.
99. Amoroso MG, Galiero G, Fusco G. Genetic characterization of ovine herpesvirus 2 strains involved in water buffaloes malignant catarrhal fever outbreaks in Southern Italy. *Vet Microbiol*. 2017 Feb 1;199:31–5.

100. Li H, Brooking A, Cunha CW, Highland MA, O'Toole D, Knowles DP, et al. Experimental induction of malignant catarrhal fever in pigs with ovine herpesvirus 2 by intranasal nebulization. *Vet Microbiol* [Internet]. 2012 Oct 12 [cited 2022 Nov 6];159(3–4):485–9. Available from: <https://pubmed.ncbi.nlm.nih.gov/22560763/>
101. Foyle KL, Fuller HE, Higgins RJ, Russell GC, Willoughby K, Rosie WG, et al. Malignant catarrhal fever in sika deer (*Cervus nippon*) in the UK. *Vet Rec* [Internet]. 2009 Oct 10 [cited 2022 Nov 6];165(15):445–7. Available from: <https://pubmed.ncbi.nlm.nih.gov/19820260/>
102. Costa ÉA, Bomfim MRQ, Da Fonseca FG, Drumond BP, Coelho FM, Vasconcelos AC, et al. Ovine Herpesvirus 2 Infection in Foal, Brazil - Volume 15, Number 5—May 2009 - Emerging Infectious Diseases journal - CDC. *Emerg Infect Dis* [Internet]. 2009 May [cited 2022 Oct 26];15(5):844–5. Available from: https://wwwnc.cdc.gov/eid/article/15/5/08-1664_article
103. Gailbreath KL, Taus NS, Cunha CW, Knowles DP, Li H. Experimental infection of rabbits with ovine herpesvirus 2 from sheep nasal secretions. *Vet Microbiol*. 2008 Nov 25;132(1–2):65–73.
104. Li H, Cunha CW, Taus NS. Malignant Catarrhal Fever: Understanding Molecular Diagnostics in Context of Epidemiology. *International Journal of Molecular Sciences* 2011, Vol 12, Pages 6881-6893 [Internet]. 2011 Oct 18 [cited 2022 Oct 26];12(10):6881–93. Available from: <https://www.mdpi.com/1422-0067/12/10/6881/htm>
105. Nelson DD, Taus NS, Schneider DA, Cunha CW, Davis WC, Brown WC, et al. Fibroblasts express OvHV-2 capsid protein in vasculitis lesions of American bison (*Bison bison*) with experimental sheep-associated malignant catarrhal fever. *Vet Microbiol*. 2013 Oct 25;166(3–4):486–92.
106. Sood R KNBS. *Emerging and Re-emerging Infectious Diseases of Livestock*. 2017. 347–362 p.
107. O'Toole D, Li H, Sourk C, Montgomery DL, Crawford TB. Malignant Catarrhal Fever in a Bison (*Bison Bison*) Feedlot, 1993–2000. *J Vet Diagn Invest* [Internet]. 2002 Jun 25 [cited 2022 Oct 26];14(3):183–93. Available from: <https://journals.sagepub.com/doi/10.1177/104063870201400301>
108. O'Toole D, Li H, Sourk C, Montgomery DL, Crawford TB. Malignant catarrhal fever in a bison (*Bison bison*) feedlot, 1993-2000. *J Vet Diagn Invest* [Internet]. 2002 [cited 2023 May 16];14(3):183–93. Available from: <https://pubmed.ncbi.nlm.nih.gov/12033673/>
109. Traul DL, Taus NS, Oaks JL, O'Toole D, Rurangirwa FR, Baszler T V., et al. Validation of nonnested and real-time PCR for diagnosis of sheep-associated malignant catarrhal fever in clinical samples. *J Vet Diagn Invest* [Internet]. 2007 [cited 2023 May 16];19(4):405–8. Available from: <https://pubmed.ncbi.nlm.nih.gov/17609352/>
110. Wan SK, Castro AE, Heuschele WP, Ramsay EC. Enzyme-linked immunosorbent assay for the detection of antibodies to the alcelaphine herpesvirus of malignant catarrhal fever in exotic ruminants. *Am J Vet Res* [Internet]. 1988 Feb 1 [cited 2023 May 16];49(2):164–8. Available from: <https://europepmc.org/article/med/3348526>

111. Rossiter PB. Immunofluorescence and immunoperoxidase techniques for detecting antibodies to malignant catarrhal fever in infected cattle. *Trop Anim Health Prod* [Internet]. 1981 [cited 2023 May 16];13(4):189–92. Available from: <https://pubmed.ncbi.nlm.nih.gov/7046177/>
112. Herring A, Reid H, Inglis N, Pow I. Immunoblotting analysis of the reaction of wildebeest, sheep and cattle sera with the structural antigens of alcelaphine herpesvirus-1 (malignant catarrhal fever virus). *Vet Microbiol* [Internet]. 1989 [cited 2023 May 16];19(3):205–15. Available from: <https://pubmed.ncbi.nlm.nih.gov/2718352/>
113. Sentsui H, Nishimori T, Nagai I, Nishioka N. Detection of sheep-associated malignant catarrhal fever virus antibodies by complement fixation tests. *J Vet Med Sci* [Internet]. 1996 [cited 2023 May 16];58(1):1–5. Available from: <https://pubmed.ncbi.nlm.nih.gov/8645750/>
114. Li H, Shen DT, Knowles DP, Gorham JR, Crawford TB. Competitive inhibition enzyme-linked immunosorbent assay for antibody in sheep and other ruminants to a conserved epitope of malignant catarrhal fever virus. *J Clin Microbiol* [Internet]. 1994 [cited 2023 May 16];32(7):1674–9. Available from: <https://pubmed.ncbi.nlm.nih.gov/7523438/>
115. Mushi EZ, Plowright W. A microtitre technique for the assay of malignant catarrhal fever virus and neutralising antibody. *Res Vet Sci*. 1979 Sep 1;27(2):230–2.
116. Decaro N, Tinelli A, Pratelli A, Martella V, Tempesta M, Buonavoglia C. First two confirmed cases of malignant catarrhal fever in Italy. *New Microbiol* [Internet]. 2003 Oct 1 [cited 2023 May 16];26(4):339–44. Available from: <https://europepmc.org/article/med/14596344>
117. Dubuisson J, Thiry E, Bublot M, Sneyers M, Boulanger D, Guillaume J, et al. Production and characterization of monoclonal antibodies to bovid herpesvirus-4. *Vet Microbiol* [Internet]. 1989 [cited 2023 May 16];19(4):305–15. Available from: <https://pubmed.ncbi.nlm.nih.gov/2546320/>
118. Li D, Shen DT, Davis WC, Knowles DP, Gorham JR, Crawford TB. Identification and characterization of the major proteins of malignant catarrhal fever virus. *J Gen Virol* [Internet]. 1995 [cited 2023 May 16];76 (Pt 1)(1):123–9. Available from: <https://pubmed.ncbi.nlm.nih.gov/7844521/>
119. Alhajri SM, Cunha CW, Knowles DP, Li H, Taus NS. Evaluation of glycoprotein Ov8 as a potential antigen for an OvHV-2-specific diagnostic assay. *PLoS One* [Internet]. 2018 Jul 1 [cited 2023 May 16];13(7). Available from: <https://pubmed.ncbi.nlm.nih.gov/29966004/>
120. Plowright W, Ferris RD. The Preparation of Bovine Thyroid Monolayers for use in Virological Investigations. *Res Vet Sci*. 1961 Apr 1;2(2):149–53.
121. Castro AE, Daley GG, Zimmer MA, Whitenack DL, Jensen J. Malignant catarrhal fever in an Indian gaur and greater kudu: experimental transmission, isolation, and identification of a herpesvirus. *Am J Vet Res* [Internet]. 1982 Jan 1 [cited 2023 Mar 6];43(1):5–11. Available from: <https://europepmc.org/article/med/7091816>
122. Li H, Taus NS, Jones C, Murphy B, Evermann JF, Crawford TB. A devastating outbreak of malignant catarrhal fever in a bison feedlot. *J Vet Diagn Invest* [Internet]. 2006 [cited 2023 May 16];18(1):119–23. Available from: <https://pubmed.ncbi.nlm.nih.gov/16566270/>

123. Aluja A; Rocha T.C; Velázquez A. Fiebre catarral maligna Fiebre catarral maligna. Técnica Pecuaria. 1969;1–8.
124. Pérez-Guiot A, Páez-Trejo A, Domínguez-Hernández Y, Carranza-Velázquez J, Hernández-García D, Carrisoza-Urbina I, et al. Pakistan Veterinary Journal Malignant Catarrhal Fever Associated with Ovine Gammaherpes virus-2 in Domestic Ruminants in Queretaro, Mexico. [cited 2023 May 16]; Available from: <http://dx.doi.org/10.29261/pakvetj/2022.076>
125. English D, Andersen BR. Single-step separation of red blood cells, granulocytes and mononuclear leukocytes on discontinuous density gradients of Ficoll-Hypaque. J Immunol Methods. 1974 Aug 1;5(3):249–52.
126. Baxter SIF, Pow I, Bridgen A, Reid HW. PCR detection of the sheep-associated agent of malignant catarrhal fever. Archives of Virology 1993 132:1 [Internet]. 1993 Mar [cited 2022 Oct 25];132(1):145–59. Available from: <https://link.springer.com/article/10.1007/BF01309849>
127. High Pure PCR Template Preparation Kit. 2020;
128. Li H, Shen DT, O’toole D, Knowles DP, Gorham JR, Crawford TB, et al. Investigation of sheep-associated malignant catarrhal fever virus infection in ruminants by PCR and competitive inhibition enzyme-linked immunosorbent assay. J Clin Microbiol [Internet]. 1995 [cited 2022 Oct 26];33(8):2048–53. Available from: <https://journals.asm.org/doi/10.1128/jcm.33.8.2048-2053.1995>
129. Posada D. jModelTest: Phylogenetic Model Averaging. Mol Biol Evol [Internet]. 2008 Jul 1 [cited 2023 May 16];25(7):1253–6. Available from: <https://academic.oup.com/mbe/article/25/7/1253/1045159>
130. Orós J, Poveda JB, Rodríguez JL, Franklin CL, Fernández A. Natural Cilia-Associated Respiratory Bacillus Infection in Rabbits Used for Elaboration of Hyperimmune Serum Against Mycoplasma sp. Journal of Veterinary Medicine, Series B. 1997;44(5):313–7.
131. Rossiter PB. Immunofluorescence and immunoperoxidase techniques for detecting antibodies to malignant catarrhal fever in infected cattle. Trop Anlm Hlth Prod. 1981;13–189.
132. Headley SA, de Lemos GAA, Dall Agnol AM, Xavier AAC, Depes VCA, Yasumitsu CY, et al. Ovine gammaherpesvirus 2 infections in cattle without typical manifestations of sheep-associated malignant catarrhal fever and concomitantly infected with bovine coronavirus. Brazilian Journal of Microbiology [Internet]. 2022 Mar 1 [cited 2022 Oct 26];53(1):433–46. Available from: <https://link.springer.com/article/10.1007/s42770-021-00653-6>
133. O’Toole D, Li H, Sourk C, Montgomery DL, Crawford TB. Malignant catarrhal fever in a bison (Bison bison) feedlot, 1993-2000. J Vet Diagn Invest [Internet]. 2002 [cited 2023 May 16];14(3):183–93. Available from: <https://pubmed.ncbi.nlm.nih.gov/12033673/>
134. Goss LW, Cole CR, Kissling RE. The Pathology of Malignant Catarrhal Fever (Bovine Epitheliosis): With Special Reference to Cytoplasmic Inclusions*. Am J Pathol [Internet]. 1947 Sep 1 [cited 2022 Oct 26];23(5):837. Available from: <https://www.ncbi.nlm.nih.gov/pmc/articles/PMC1934312/>

135. Severi B, Landini MP, Cenacchi G, Zini N, Maraldi NM. Human cytomegalovirus nuclear and cytoplasmic dense bodies. *Arch Virol* [Internet]. 1992 Mar [cited 2023 May 16];123(1–2):193–207. Available from: <https://pubmed.ncbi.nlm.nih.gov/1372496/>
136. Nelson DD, Taus NS, Schneider DA, Cunha CW, Davis WC, Brown WC, et al. Fibroblasts express OvHV-2 capsid protein in vasculitis lesions of American bison (*Bison bison*) with experimental sheep-associated malignant catarrhal fever. *Vet Microbiol* [Internet]. 2013 Oct 25 [cited 2023 May 16];166(3–4):486–92. Available from: <https://pubmed.ncbi.nlm.nih.gov/23953727/>

